A METHOD FOR ESTIMATING PERFORMANCE OF SINGLE ROTOR HELICOPTERS

A THESIS

Presented to

the Faculty of the Graduate Division

by

Story C. Stevens

In Partial Fulfillment

of the Requirements for the Degree

Master of Science in Aeronautical Engineering

Georgia Institute of Technology

December, 1958

"In presenting the dissertation as a partial fulfillment of the requirements for an advanced degree from the Georgia Institute of Technology, I agree that the Library of the Institution shall make it available for inspection and circulation in accordance with its regulations governing materials of this type. I agree that permission to copy from, or to publish from, this dissertation may be granted by the professor under whose direction it was written, or, in his absence, by the Dean of the Graduate Division when such copying or publication is solely for scholarly purposes and does not involve potential financial gain. It is understood that any copying from, or publication of, this dissertation which involves potential financial gain will not be allowed without written permission.

_____

_____

4A
12R

A METHOD FOR ESTIMATING PERFORMANCE OF SINGLE ROTOR HELICOPTERS

Approved:

Walter Castles, Jr.

Robin B. Gray

Thomas W. Jackson

Date Approved by Chairman: 8 Dec. 1958

ACKNOWLEDGEMENTS

The author wishes to express his most sincere appreciation to Professor Walter Castles, Jr., for suggesting the method of approach and for his invaluable assistance and guidance throughout the preparation of this thesis.

The author wishes to extend his gratitude to Doctor Robin B. Gray and Doctor Thomas W. Jackson for their suggestions and for their review of the work.

The author also wishes to thank Captain Robert Morrison and Howard L. Durham, Jr., for programming the equations for the IBM 650 Computer.

TABLE OF CONTENTS

LIST OF FIGURES

LIST OF SYMBOLS

a	Mean value of the slope of the lift curve for blade element of 0.75 R (per radian)
a_o	Rotor coning angle
a_1	Lateral component of the cyclic pitch angle measured with respect to the tip-path plane
A_o	Mean blade angle, positive above tip-path plane
b	Number of blades in rotor
b_1	Longitudinal component of the cyclic pitch angle measured with respect to the tip-path plane
c	Blade chord at radius r
$\bar{c}$	Mean blade chord, $\dfrac{\int_o^R c r^2 dr}{\int_o^R r^2 dr}$
c_{d_o}	Section profile drag coefficient
c_l	Section lift coefficient
c_{l_m}	Section maximum lift coefficient
c_o	Extended blade root chord at r = 0 (for linear taper)
c_t	Blade chord at tip
c. t.	Refers to counter torque rotor
$\bar{C}_L$	Mean lift coefficient
C_Q	Rotor torque coefficient
$\Delta C_{Q_{a_o}}$	Increment to C_Q from terms involving a_o
$\Delta C_{Q_{DP_c}}$	Increment to C_Q from constant profile drag

$\Delta C_{Q_{DP_v}}$	Increment to C_Q from variable profile drag
ΔC_{Q_L}	Increment to C_Q from lift
ΔC_{Q_S}	Increment to C_Q from tip stall on retreating blade
C_T	Rotor thrust coefficient, $\left(\frac{T}{\rho \pi \Omega^2 R^4}\right)$
C_X	Rotor X-force coefficient, $\left(\frac{F_x}{\frac{1}{2}\rho \pi \Omega^2 R^4}\right)$
$\Delta C_{X_{DP_c}}$	Increment to C_X from constant profile drag
$\Delta C_{X_{DP_v}}$	Increment to C_X from variable profile drag
ΔC_{X_L}	Increment to C_X from lift
C_Y	Rotor Y-force coefficient, $\left(\frac{F_y}{\frac{1}{2}\rho \pi \Omega^2 R^4}\right)$
D_F	Fuselage drag
F_X	Component of rotor resultant force acting along X-axis
F_Y	Component of rotor resultant force acting along Y-axis
ΔF_{XY}	Inplane component of force acting to the rear on a blade element at non-dimensional radius x
HP	Horsepower
I_1	Mass moment of inertia of blade about flapping hinge
ℓ	Perpendicular distance from the main rotor shaft to the counter-torque rotor hub
L_F	Fuselage lift
m	Mass of blade element
M	Free stream Mach number at the three-quarter blade radius

M_{CF}	Mean centrifugal restoring moment
M_T	Mean thrust moment
M_X	Rotor rolling moment
M_Y	Rotor pitching moment
MPH	Miles per hour
Q	Rotor torque, positive in direction of rotation
r	Radius of blade element $\propto dr$
R	Radius of blade tip
t	Maximum blade thickness at radius r
T	Rotor thrust, component of rotor resultant force along Z-axis
U	Component of resultant velocity at blade element that is normal to blade axis
ν_a	Axial velocity ratio, $\left(\frac{V \sin \alpha_v}{\Omega R}\right)$
ν_i	Non-dimensional induced velocity, $\left(\frac{V_i}{\Omega R}\right)$
V_i	Induced velocity
w	Slope of the longitudinal variation of non-dimensional induced velocity
W	Gross weight of helicopter
λ	Non-dimensional blade radius, $\left(\frac{r}{R}\right)$
$\bar{\lambda}$	Mean thrust moment center
λ^*	Mean thrust center
γ	Slope of the lateral variation of non-dimensional induced velocity
α_r	Blade-element angle of attack measured from line of zero lift

α_s	Blade-element angle of attack at stall
α_v	Angle of attack of tip-path plane measured in the XZ-plane between flight path velocity vector and tip-path plane, positive below tip-path plane
γ	Increment of blade circulation
Γ	Circulation of blade element at radius r and azimuth angle ψ
δ_0	Value of c_{d_0} at $c_\ell = 0$
ε	Constant for second term of an even power series for c_{d_0} $(c_{d_0} = \delta_0 + \varepsilon c_\ell^2)$
η	Efficiency of power and drive system of helicopter
$\Delta\theta_t$	Blade twist from the three-quarter radius to the blade tip, positive for increased blade angle at the tip
θ_v	Pitch angle of blade-element at radius r and azimuth angle ψ, measured between zero-lift chord line and tip-path plane, positive above tip-path plane $(A_0 - a_1 \sin\psi + b_1 \cos\psi)$
μ_v	Inplane velocity ratio at tip-path plane, $\left(\frac{V\cos\alpha_v}{\Omega R}\right)$
ρ	Mass density of air
σ	Rotor solidity, $\left(\frac{b\bar{c}}{\pi R}\right)$
σ_t	Rotor solidity based on tip chord
ϕ_v	Angle between flight path and horizontal, positive below horizontal
χ	Wake angle
ψ	Azimuth angle of blade axis measured about Z-axis from X-axis
Ω	Mean angular velocity of rotor blade about Z-axis

SUMMARY

Equations are derived for determining the performance of single rotor helicopters. Charts were constructed from these theoretical equations for relatively rapid estimation of rotor performance for various flight conditions.

The equations are based upon a triangular distribution of induced velocity along the blade radii and a simplified circulation distribution derived from two dimensional blade-element theory. The equations are general within the limitations imposed by the approximations employed in determining the profile drag terms. The blade-element lift coefficient is assumed to be proportional to the sine of the blade-element angle of attack. The blade-element profile drag coefficient is represented by the first two terms of an even power series in the blade-element lift coefficient. Separate terms are developed for tip stall. Effects of compressibility on the blades are neglected and the effect of blade twist is not considered.

Charts relating certain variables with functions from the performance equations were constructed in order to reduce the time and labor involved in the calculation of the rotor in-plane force coefficient and the rotor torque coefficient. The charts cover ranges of the in-plane velocity ratio from 0 to 0.5, the thrust coefficient from 0.002 to 0.02, the

mean angle of attack of blade elements from 0.05 to 0.13, and the axial velocity ratio from -0.10 to 0.04. It is felt that these values will cover current and future helicopter performance. Points for plotting the curves for the charts were determined utilizing an IBM 650 computer. The charts in conjunction with the equations afford a method for the relatively rapid estimation of the rotor horsepower required by a helicopter flying at a given airspeed and at a given rate of climb or descent. The method of applying the charts in calculating the rotor torque coefficient is illustrated in a sample problem.

A comparison of the results given by the performance equations with the full scale helicopter test data of NACA TN 1266 and with the hovering data from the test tower rotor of NACA TN 4357 shows good agreement.

CHAPTER I

INTRODUCTION

There have been numerous methods presented for computing helicopter rotor performance based upon various simplifying assumptions. Approximations such as assuming a uniform distribution of induced velocity or that the resultant rotor force acts along the axis of zero feathering are employed to simplify equations and reduce the amount of labor involved. Use of more exact blade-element equations, such as those developed by Castles and New (1)*, is quite lengthy.

Employment of any performance equations can normally be facilitated by presentation of the equations or pertinent functions in the form of charts. In many cases it would be extremely difficult to reduce the equations to a form suitable for such a presentation owing to the complexity and the number of dependent variables. Gessow and Tapscot (2) have developed charts for estimating helicopter performance in forward flight. The method and charts, developed from equations presented by Gessow and Crim (3) and, with some modification, Bailey and Gustafon (4), afford a quick method of estimating rotor performance in forward flight; however, it is difficult

---

*Numbers in parenthesis refer to items in the bibliography.

to interpolate with consistency when using the charts, due to their small scale. Also the assumption made in (2) that the resultant rotor force acts along the axis of zero feathering introduces considerable error, particularly for partial power and power off conditions.

It is the purpose of this paper to develop performance equations based upon a triangular distribution of induced velocity along the blade radii and a simplified circulation distribution derived from blade-element theory. This approach affords results which appear to be in good agreement with available flight test data. Charts were constructed to reduce the labor involved in performance calculations. The charts relate fundamental variables with functions from the performance equations. Values of the parameters employed in chart construction cover current and probably most future single rotor helicopter designs.

The equations are perfectly general within the limitations imposed by the approximations employed in determining the profile drag terms. Separate terms are developed for tip effect and tip stall. Functions obtained from the charts retain the same generality with the exception of one minor approximation that does not affect the degree of accuracy afforded by the charts.

The development of the equations was based upon methods first presented by Castles (1).

CHAPTER II

ANALYSIS

Equation for Induced Velocity.--It is apparent from the experimental data presented by Heyson (5) that a triangular distribution of induced velocity along the blade radii is a better approximation to the actual case than a uniform distribution.

If a nonuniform radial distribution of circulation along the blade is considered, $\Gamma = f(r)$, the circulation at any radius on a blade is equal to the algebraic sum of all the circulation shed from the blade trailing edge outboard of that radius. Each incremental radial change in blade circulation results in the shedding of a vortex filament of strength equal to the increment $d\Gamma$. The resulting vortex helices may be approximated by an infinite number of vortex rings of infinitesimal strength, lying in planes parallel to the tip-path plane and extending down the wake to infinity. This approximate vortex distribution is equivalent to an infinite number of vortex sheets of uniform finite strength per unit length $d\Gamma/dZ$ measured in the Z direction (see Fig. 1). These sheets form an infinite number of coaxial straight elliptic cylinders. Vortex theory demonstrates that for a right circular cylindrical wake the induced velocities

at radius r are a function only of the circulation shed from trailing edges of blade elements at radii greater than r. The algebraic sum of the strength of these outer vortex filaments is equal to the blade circulation at r. Thus a triangular circulation distribution along the blade radius will result in a triangular induced velocity distribution.

For an elliptic vortex cylinder at some wake angle χ, (Fig. 1), Coleman (6) shows that the longitudinal distribution of the normal component of the induced velocity in the plane of rotation is antisymetric about the lateral axis. Castles and Durham (7) demonstrate that the value of the normal component of the induced velocity for such a wake is constant on the lateral rotor diameter. Thus the mean theoretical value of the normal component of induced velocity occurs on the lateral axis. For the elliptic vortex cylinder, the normal component of induced velocity in the plane of rotation is not zero outside the wake as in the case of the right circular cylinder; however, the induced velocity distribution along the lateral axis due to a triangular circulation distribution is still very nearly triangular, since the normal component of induced velocity outside each cylinder is small compared to the induced velocity within the wakes. It is noted by Heyson (5) from plots of calculated values of the induced velocity along the lateral axis that for a triangular disk loading, i.e. triangular circulation distribution along the blade radii, the deviation from a triangular induced

velocity distribution on the lateral axis is negligible, and the induced velocity is plotted as being triangular.

For each of the straight elliptic vortex cylinders Coleman (6) shows that the induced velocity, V_i , at the center of the plane of rotation is given by

$$V_{i_\alpha} = \frac{1}{2}\left(\frac{d\Gamma}{d\ell}\right)_\alpha \tag{1}$$

$$\text{where } \frac{d\Gamma}{d\ell} = \frac{d\Gamma}{dZ}\cos\chi$$

The subscript α denotes any one of the infinite number of straight elliptic vortex cylinders comprising the wake and located at a nondimensional radius α . The average value $\left(\frac{d\Gamma}{d\ell}\right)_\alpha$ of the wake vortex sheet strength per unit length measured along the wake is equal to the blade circulation at nondimensional radius α , Γ_α , times the number of turns of the wake helices in a unit length of wake.

The time, t , for a unit length of wake to be formed is approximately

$$t = \frac{1}{\frac{d\ell}{dt}} \tag{2}$$

where $\frac{dl}{dt}$ = wake sheet velocity

$$= \sqrt{(V\sin\alpha_v - V_{i_{.75R}})^2 + (V\cos\alpha_v)^2}$$

and V = Velocity along flight path.

α_v = Angle of attack of tip-path plane measured in the XZ plane between flight path velocity vector and tip-path plane, positive below tip-path plane. (Fig. 2)

$V_{i_{.75R}}$ = Value of the induced velocity at the three-quarter radius, the approximate mean thrust center.

The number of turns, n , of the rotor in unit time is

$$n = \frac{\Omega}{2\pi} \tag{3}$$

where Ω = mean angular velocity of rotor blade axis about Z axis (radians per second).

Thus the time average value of the wake sheet strength at non-dimensional radius x is

$$\left(\frac{d\Gamma}{dl}\right)_x = \frac{b\Gamma_x\Omega}{2\pi\sqrt{(V\sin\alpha_v - V_{i_{.75R}})^2 + (V\cos\alpha_v)^2}} \tag{4}$$

where b = number of blades in the rotor.

Substituting Equation 4 into 1 gives

$$V_{i_x} = \frac{b\,\Gamma_x\,\Omega}{4\pi\sqrt{(V\sin\alpha_v - V_{i_{.75R}})^2 + (V\cos\alpha_v)^2}} \qquad (5)$$

Since a triangular distribution of circulation along the blade radii is the simplest reasonably good approximation to the actual blade circulation distribution, it will be used to derive an expression for the induced velocity in terms of known parameters. Castles (1) demonstrates that such a circulation may be expressed as

$$\Gamma_x = \frac{3\pi\Omega R^2 C_T}{b(1-\mu_v^2)}\left(1 - \frac{4}{3}\mu_v \sin\psi\right)x \qquad (6)$$

where R = radius of the blade tip

C_T = rotor thrust coefficient $\left(\frac{T}{\rho\pi\Omega^2 R^4}\right)$

μ_v = in-plane velocity ratio at tip-path plane $\left(\frac{V\cos\alpha_v}{\Omega R}\right)$

(See Fig. 2). This equation follows from thrust and rolling moment equilibrium. Substitution of Equation 6 into 5 and nondimensionalizing gives the expression for the nondimensional induced velocity, ν_{i_x}, at any radius, x, and azimuth angle ψ :

$$\bar{v}_{i_x} = \frac{3 C_T \left(1 - \frac{4}{3}\mu_v \sin\psi\right) x}{4\left(1-\mu_v^2\right)\sqrt{\left(\bar{v}_a - \bar{v}_{i_{.75R}}\right)^2 + \mu_v^2}} \qquad (7)$$

where $\bar{v}_{i_x} = \dfrac{V i_x}{\Omega R}$

$$\bar{v}_a = \frac{V}{\Omega R} \sin\alpha_v$$

Equation for Blade Circulation.--Two-dimensional thin airfoil theory demonstrates that the local blade circulation is related to the lift on the blade element by

$$dL = \rho U \Gamma \, dr \qquad (8)$$

where U = Component of resultant velocity at the blade element that is normal to the blade axis.

but

$$dL = \frac{1}{2} \rho U^2 c c_\ell \, dr \qquad (9)$$

where c = blade chord at radius r

c_ℓ = section lift coefficient

therefore

$$\Gamma = \frac{1}{2} U c c_\ell \qquad (10)$$

As shown in (1), approximating the lift coefficient as

$$c_\ell = a \sin \alpha_r \tag{11}$$

where a = mean value of the slope of the lift curve for blade element at 0.75R (per radian)

$$= \frac{a'}{\sqrt{1 - M^2}}$$ (Prandtl-Glauert Mach number correction)

and

a' = mean value of the low Mach number lift-curve slope from two-dimensional wind-tunnel tests

M = free stream Mach number at the three-quarter blade radius

α_r = blade-element angle of attack measured from line of zero lift

is applicable for blade-element rotor theory over the unstalled range of blade-element angles of attack. Equation 11 also permits the elimination of small angle approximations for the inflow angle, ϕ_v , in the subsequent double angle expansion.

Noting that $\alpha_r = \theta_v + \phi_v$ (See Fig. 3), Equation 11 may be written as

$$c_\ell = a \sin (\theta_v + \phi_v) \tag{12}$$
$$= a (\sin \theta_v \cos \phi_v + \cos \theta_v \sin \phi_v)$$

where for an untwisted blade $\theta_v = A_0 - a_1 \sin\psi + b_1 \cos\psi$

and A_0 = mean blade pitch angle (radians)

a_1 = lateral component of cyclic-pitch angle (radians)

b_1 = longitudinal component of cyclic-pitch angle (radians)

The approximation is made that the cosine of the blade coning angle, a_0, is unity and that the resultant induced velocity is everywhere normal to the tip-path plane, the component of velocity, $U\cos\phi$, at r, ψ, that is perpendicular to the blade axis and parallel to the tangential velocity vector Ωr is

$$U\cos\phi_v = \Omega R(x + \mu_v \sin\psi) \tag{13}$$

The component of velocity, $U\sin\psi$, at r, ψ, that is perpendicular to both the blade axis and the tangential velocity vector Ωr is very nearly

$$U\sin\phi_v = \Omega R[\nu_a - \nu_{ix} + \gamma x \sin\psi + (wx - a_0\mu_v)\cos\psi] \tag{14}$$

where γ = slope of the lateral variation of nondimensional induced velocity

μ_T = slope of the longitudinal variation of nondimensional induced velocity

a_0 = rotor coning angle (radians).

The equation for the slope of the lateral variation of nondimensional induced velocity, γ, can be obtained from Equation 7. Consider the value of the induced velocity at the three-quarter radius, the approximate blade mean thrust center. The principal variation in the nondimensional induced velocity, given by Equation 7, for the three-quarters radius position is $-\nu_i \mu_v \sin\psi$. If the lateral variation of induced velocity is approximated by a linear variation between a magnitude of $-\nu_i \mu_v$ at $\psi = 90^\circ$ and $+\nu_i \mu_v$ at $\psi = 270^\circ$, where ν_i is the average value of the nondimensional induced velocity given by

$$\nu_i = \frac{\frac{3}{4} C_T}{(1-\mu_v^2)\sqrt{(\nu_a - \frac{3}{4}\nu_i)^2 + \mu_v^2}} \qquad (15)$$

then the slope of the lateral variation is

$$\gamma = 2\nu_i \mu_v \qquad (16)$$

Again taking the mean value of the induced velocity at the three-quarter radius, it can be shown (1) that the slope of the longitudinal variation of the nondimensional induced velocity, w , is given by

$$w = -\nu_i \left[(1 - 1.8\mu_v^2) \sqrt{1 + \left(\frac{\nu_a - \frac{3}{4}\nu_i}{\mu_v} \right)^2} - \sqrt{\left(\frac{\nu_a - \frac{3}{4}\nu_i}{\mu_v} \right)^2} \right] \qquad (17)$$

Substitution of Equations 12, 13, and 14 into Equation 10 gives

$$\frac{2\Gamma}{ac\Omega R} = (x + \mu_v \sin\psi)\sin\theta + (\nu_a - \nu_i x + \gamma x \sin\psi + [wx - a_0 \mu_v]\cos\psi)\cos\theta \qquad (18)$$

Then taking $\sin\theta \approx \theta = A_0 - a_1 \sin\psi + b_1 \cos\psi$ and $\cos\theta \approx 1$, and neglecting the $\gamma x \sin\psi$ term since it is very small (of the order of C_T), Equation 18 for the nondimensional blade circulation reduces to

$$\begin{aligned} \frac{2\Gamma}{ac\Omega R} = {} & \nu_a + (A_0 - \nu_i)x - \tfrac{1}{2} a_1 \mu_v \\ & + \sin\psi\,(-a_1 x + A_0 \mu_v) \\ & + \cos\psi\,(b_1 x + wx - a_0 \mu_v) \\ & + \sin 2\psi\,(\tfrac{1}{2} b_1 \mu_v) \\ & + \cos 2\psi\,(\tfrac{1}{2} a_1 \mu_v) \end{aligned} \qquad (19)$$

Neglecting the second harmonic sine term which has no effect on the integrated force coefficients, Equation 19 may be written as

$$\frac{2\Gamma}{a c \Omega R} = \gamma_0 + \gamma_1 \alpha + (\gamma_2 + \gamma_3 \alpha) \sin\psi + (\gamma_4 + \gamma_5)\cos\psi + \gamma_6 \cos 2\psi \qquad (20)$$

where

$$\gamma_0 = \nu_a - \tfrac{1}{2} a_1 \mu_v$$

$$\gamma_1 = A_0 - \nu_i$$

$$\gamma_2 = A_0 \mu_v$$

$$\gamma_3 = -a_1$$

$$\gamma_4 = -a_0 \mu_v$$

$$\gamma_5 = b_1 + w$$

$$\gamma_6 = \tfrac{1}{2} a_1 \mu_v = -\tfrac{1}{2} \gamma_3 \mu_v$$

The equation is further simplified for the subsequent developments by neglecting the small terms γ_2 , and $-\frac{1}{2} a_1 \mu_v$, the second term of γ_0 . The omission of the γ_2 term has the effect of preserving the proper signs in the reverse flow region. The omission of the latter term has very little

effect on the final result since it is compensated for by other terms in satisfying rolling moment equilibrium. Thus the circulation becomes

$$\Gamma = \frac{a c \Omega R}{2} \left(\gamma_0 + \left[\gamma_1 + \gamma_3 \sin\psi \right] \alpha + \left[\gamma_4 + \gamma_5 \alpha \right] \cos\psi - \tfrac{1}{2} \gamma_3 \mu_v \cos 2\psi \right) \tag{21}$$

The mean rotor thrust, T , is given by

$$T = \frac{b}{2\pi} \int_0^{2\pi} \int_0^R \rho U \cos\phi_v \, \Gamma \, d\psi \, dr \tag{22}$$

Define a mean blade chord $\bar{c}$ as

$$\bar{c} = \frac{\int_0^R c r^2 dr}{\int_0^R r^2 dr} \tag{23}$$

and a rotor solidity, σ , as

$$\sigma = \frac{b \bar{c}}{\pi R} \tag{24}$$

It follows from substitution of Equations 13, 21, 23 and 24 into 22 that the mean rotor thrust is

$$T = \frac{\rho \sigma a \pi \Omega^2 R^4}{2} \left(\frac{\gamma_0}{2} + \frac{\gamma_1}{3} + \frac{\gamma_3 \mu_v}{4} \right) \tag{25}$$

The expression for the rotor thrust coefficient (see Equation 6) is

$$C_T = \frac{T}{\rho \pi \Omega^2 R^4} \tag{26}$$

Substitution of Equation 25 into the above equation gives

$$C_T = \frac{\sigma a}{2} \left(\frac{\gamma_0}{2} + \frac{\gamma_1}{3} + \frac{\gamma_3 \mu_v}{4} \right) \tag{27}$$

The rolling moment, M_X , and pitching moment, M_Y , are very nearly equal to zero for an articulated rotor with small offset flapping hinge in unaccelerated flight, and equal to zero when the flapping hinge axis lies on the axis of rotation. Thus

$$M_X = \frac{\rho b}{2\pi} \int_0^{2\pi} \int_0^R U \cos \phi_v \, \Gamma r \sin \psi \, d\psi \, dr = 0 \tag{28}$$

Substitution of respective terms from Equations 13 and 21 and integration gives γ_3 in terms of γ_1 as

$$\gamma_3 = -\frac{8}{2+\mu_v^2}\left(\frac{\mu_v \gamma_1}{3} + \frac{\nu_a \mu_v}{2}\right) \tag{29}$$

By substituting Equation 29 into 27 and noting that $\gamma_0 = \nu_a$, an expression for γ_1 is obtained.

$$\gamma_1 = \frac{6 C_T}{\sigma a}\left(\frac{2+\mu_v^2}{2-\mu_v^2}\right) - \frac{3}{2}\nu_a \tag{30}$$

Similarly from Equation 29 and 30, γ_3 becomes

$$\gamma_3 = -\frac{16 C_T \mu_v}{\sigma a (2-\mu_v^2)} \tag{31}$$

Equating the pitching moment to zero gives

$$M_Y = \frac{\rho b}{2\pi}\int_0^{2\pi}\int_0^R U(\cos\phi)\, r \cos\psi \, d\psi \, dr = 0 \tag{32}$$

Substitution of Equations 13 and 21 into the above equation and subsequent integration gives γ_5 in terms of γ_4 as

$$\gamma_5 = -\frac{4}{3}\gamma_4 \tag{33}$$

Since γ_4 is equal to $-a_o \mu_v$ then

$$\gamma_5 = \frac{4}{3} a_o \mu_v \tag{34}$$

Substitution of the values for γ_1 , γ_2 , etc. into the blade circulation equation, Equation 20, gives

$$\begin{aligned} \Gamma = \frac{3\pi \Omega R^2 C_T}{b} \Bigg\{ & \frac{\nu_a \sigma a}{6 C_T} \\ & + \left[\left(\frac{2+\mu_v^2}{2-\mu_v^2} - \frac{\nu_a \sigma a}{4 C_T} \right) - \left(\frac{8 \mu_v}{3[2-\mu_v^2]} \right) \sin\psi \right] x \\ & + \frac{a_o \mu_v \sigma a}{6 C_T} \left(\frac{4}{3} x - 1 \right) \cos\psi \\ & + \left(\frac{4 \mu_v^2}{3[2-\mu_v^2]} \right) \cos 2\psi \Bigg\} \end{aligned} \tag{35}$$

Define a mean angle of attack of blade-elements as

$$\overline{\alpha} = \frac{6 C_T}{\sigma a} \tag{36}$$

Substitution of this expression into Equation 35 gives the final expression for the blade circulation as

$$\Gamma = \frac{3\pi\Omega R^2 C_T}{b}\left\{\frac{\nu_a}{\bar{\alpha}} + \kappa\left[\left(\frac{1+\frac{1}{2}\mu_v^2}{1-\frac{1}{2}\mu_v^2} - \frac{3\nu_a}{2\bar{\alpha}}\right) - \left(\frac{4\mu_v}{3\left[1-\frac{1}{2}\mu_v^2\right]}\right)\sin\psi\right] + \frac{a_0\mu_v}{\bar{\alpha}}\left(\frac{4}{3}\kappa - 1\right)\cos\psi + \left(\frac{2\mu_v^2}{3\left[1-\frac{1}{2}\mu_v^2\right]}\right)\cos 2\psi\right\} \tag{37}$$

Equation for the Blade Coning Angle.--A sufficiently accurate value of the blade coning angle, a_0 , for performance analysis may be obtained by equating the mean centrifugal restoring moment about the blade root to the mean thrust moment about the blade root. Neglecting the gravity moment introduces no significant error since it is only about three per cent of the centrifugal moment. The mean centrifugal moment, M_{CF} , can be written as

$$M_{CF} = -\int_0^R m r^2 \Omega^2 \cos\beta \sin\beta \, dr \tag{38}$$

The flapping angle, β , measured with respect to the tip-path plane is equal to the coning angle, a_0 , plus second and higher harmonic terms which may be neglected. Thus for small angles and noting that the mass moment of inertia of the blade about the flapping hinge, I_1 , is given by

$$I_1 = \int_0^R m r^2 dr \tag{39}$$

the centrifugal moment may be expressed as

$$M_{CF} = -I_1 a_0 \Omega^2 \tag{40}$$

The mean thrust moment, M_T , is given by

$$M_T = \frac{\rho}{2\pi} \int_0^{2\pi} \int_0^R \Omega R (x + \mu_v \sin\psi) \Gamma r \, d\psi \, dr \tag{41}$$

Equating the summation of moments about the flapping hinge equal to zero, substituting the expression for Γ given by Equation 37 and integrating gives

$$a_0 = \frac{\rho \pi R^5 C_T}{4 I_1 b} \left[\frac{3\left(1 - \frac{7}{18}\mu_v^2\right)}{\left(1 - \frac{1}{2}\mu_v^2\right)} - \frac{\nu_a}{2\alpha} \right] \tag{42}$$

Equation for the Mean Blade Angle.--Again considering two dimensional thin airfoil theory and noting that for a perfect fluid the section lift coefficient, κ_ℓ , is

$$\kappa_\ell = 2\pi \alpha_r \tag{43}$$

then the local blade circulation is related to the blade angle of attack and velocity by

$$\frac{2\Gamma}{\bar{c} U} = 2\pi \alpha_r \tag{44}$$

The local blade angle, θ_v , (see Fig. 3) is

$$\theta_v = \alpha_r - \phi_v \tag{45}$$

Evaluation of the mean blade angle, A_0 , at the blade mean thrust center, $\overset{\star}{x}$, gives approximately

$$\underset{mean}{\theta_v} = A_0 = \frac{1}{2\pi}\int_0^{2\pi} (\alpha_r)_{\overset{\star}{x}}\, d\psi - \frac{1}{2\pi}\int_0^{2\pi} (\phi_v)_{\overset{\star}{x}}\, d\psi \tag{46}$$

Take ϕ as a small angle, then $\phi \approx \tan\phi$. It follows from Equations 44 and 46 that

$$A_0 = \frac{1}{2\pi}\int_0^{2\pi} \left(\frac{\Gamma}{\pi \bar{c} U}\right)_{\overset{\star}{x}} d\psi - \frac{1}{2\pi}\int_0^{2\pi} (\tan\phi)_{\overset{\star}{x}}\, d\psi \tag{47}$$

Substituting the values from Equations 13, 14, 16 and 37 into Equation 47 and taking Cos $\phi_v \approx 1$ and

$$\tau_{\overset{*}{x}} = \bar{\tau} = \frac{\sigma \pi R}{b} \tag{48}$$

and integrating gives

$$A_0 = \frac{3C_T}{\sigma\pi}\left[\frac{\nu_a\left(1-\frac{3}{2}\overset{*}{x}\right)}{\alpha\sqrt{\overset{*}{x}^2-\mu_v^2}} + \frac{\overset{*}{x}\left(1+\frac{1}{2}\mu_v^2\right)}{\sqrt{\overset{*}{x}^2-\mu_v^2}\left(1-\frac{1}{2}\mu_v^2\right)}\right.$$

$$\left. + \frac{2\mu_v^2}{3\left(1-\frac{1}{2}\mu_v^2\right)\sqrt{\overset{*}{x}^2-\mu_v^2}}\right] \tag{49}$$

$$+ \frac{\overset{*}{x}\nu_i - \nu_a}{\sqrt{\overset{*}{x}^2-\mu_v^2}} + 2\overset{*}{x}\nu_i\left(\frac{\overset{*}{x}}{\sqrt{\overset{*}{x}^2-\mu_v^2}} - 1\right)$$

<u>Equation for the Mean Thrust Center</u>.--The non-dimensional mean thrust center, $\overset{*}{x}$, may be determined by dividing the mean thrust moment by the mean thrust. Thus it follows from Equations 26, 41 and 42 that

$$\overset{*}{x} = \frac{\frac{\rho\pi\Omega^2R^5C_T}{4}\left[\frac{3\left(1-\frac{7}{18}\mu_v^2\right)}{\left(1-\frac{1}{2}\mu_v^2\right)} - \frac{\nu_a}{2\alpha}\right]}{R\left(\rho\pi\Omega^2R^4C_T\right)} \tag{50}$$

or

$$\bar{\alpha}^* = \frac{1}{4}\left[\frac{3\left(1-\frac{7}{18}\mu_v^2\right)}{\left(1-\frac{1}{2}\mu_v^2\right)} - \frac{\sigma a}{2\bar{\alpha}}\right] \tag{51}$$

Equation 51 is applicable to constant chord blades. For blades with taper, the mean thrust center, $\bar{\alpha}^*$, may be obtained by multiplying the result from Equation 51 by

$$\left(\frac{1-\frac{4}{5}t}{1-\frac{3}{4}t}\right) \tag{52}$$

where $t = 1 - \frac{c_t}{c_o}$

and c_t = tip chord

c_o = extended blade root chord at $r = 0$ (for linear taper).

Equation for a_1, the Lateral Component of the Cyclic Pitch Measured with Respect to the Tip-path Plane.--The change in blade angle may be written as

$$\Delta\theta = -a_1 \sin\psi + b_1 \cos\psi \tag{53}$$

The magnitude of the lateral component of the cyclic pitch, a_1, can be determined from the difference in the blade angle of attack, α_r, and the inflow angle, ϕ_v, at the blade thrust moment centers on the retreating and

advancing blades at $\psi = \frac{\pi}{2}$ and $\psi = \frac{3\pi}{2}$. See Figure 3.

As was shown in Equation 44, the blade angle of attack may be expressed as

$$\alpha_r = \frac{\Gamma}{\pi \bar{x} U} \tag{54}$$

Substituting the mean blade moment center, $\bar{x}$, Γ from Equation 37, and taking the difference between α_r at $\psi = \frac{3\pi}{2}$ and $\psi = \frac{\pi}{2}$ gives

$$\Delta \alpha_r = -\frac{2C_T \mu_v}{\sigma \pi} \left[\frac{\frac{4\bar{x}^2 + 3\bar{x} - \frac{1}{2}\mu_v^2}{(1 - \frac{1}{2}\mu_v^2)} + \frac{3\nu_a}{\bar{x}}\left(1 - \frac{3}{2}\bar{x}\right)}{\left(\bar{x}^2 - \mu_v^2\right)} \right] \tag{55}$$

It follows from Equations 13 and 14 that the inflow angle, ϕ_v , is given by

$$\phi_v \approx \tan \phi_v = \frac{\nu_a - \nu_i x + \gamma x \sin\psi + (\omega x - a_0 \mu_v)\cos\psi}{x + \mu_v \sin\psi} \tag{56}$$

Substituting $x = \bar{x}$, and taking the difference between ϕ_v at $\psi = \frac{3\pi}{2}$ and $\psi = \frac{\pi}{2}$ gives

$$\Delta \phi_v = 2 \left[\frac{\gamma x^2 + \mu_v(\bar{x}\nu_i - \nu_a)}{(\bar{x}^2 - \mu_v^2)} \right] \tag{57}$$

Since

$$a_1 = -\frac{1}{2}\left(\Delta\alpha_r - \Delta\phi_v\right) \tag{58}$$

then

$$a_1 = \frac{C_T \mu_v}{\sigma\pi}\left[\frac{4\bar{x}^2 + 3\bar{x} - \frac{1}{2}\mu_v^2}{\left(1 - \frac{1}{2}\mu_v^2\right)} + \frac{3\nu_a}{\alpha}\left(1 - \frac{3\bar{x}}{2}\right)}{\left(\bar{x}^2 - \mu_v^2\right)}\right] \tag{59}$$

$$+ \frac{\gamma\bar{x}^2 + \mu_v\left(\bar{x}\nu_i - \nu_a\right)}{\left(\bar{x}^2 - \mu_v^2\right)}$$

Equation for the Mean Thrust Moment Center.--The non-dimensional mean thrust moment center, $\bar{x}$, may be determined by dividing the mean thrust second moment by the mean thrust moment as given by Equation 51.

$$\bar{x} = \frac{\frac{\rho}{2\pi}\int_0^{2\pi}\int_0^R \Omega R\left(x + \mu_v \sin\psi\right) r\, r^2\, d\psi\, dr}{R\left[\frac{\rho\pi\Omega^2 R^5 C_T}{4}\left(\frac{3\left[1 - \frac{7}{18}\mu_v^2\right]}{1 - \frac{1}{2}\mu_v^2} - \frac{\nu_a}{2\alpha}\right)\right]} \tag{60}$$

Substitution of the expression for the blade circulation from Equation 37 and subsequent integration gives

$$\bar{x} = \frac{\frac{4}{5}\bar{\alpha}\left(1 - \frac{11}{18}\mu_v^2\right) - \frac{1}{5}\nu_a\left(1 - \frac{1}{2}\mu_v^2\right)}{\bar{\alpha}\left(1 - \frac{7}{18}\mu_v^2\right) - \frac{1}{6}\nu_a\left(1 - \frac{1}{2}\mu_v^2\right)} \tag{61}$$

Equation 61 is applicable to constant chord blades. For blades with taper, the mean thrust moment center, $\bar{x}$, may be obtained by multiplying the result from Equation 61 by

$$\left(\frac{1 - \frac{5}{6}t}{1 - \frac{4}{5}t}\right) \tag{62}$$

<u>Equation for b_1 , the Longitudinal Component of the Cyclic Pitch Measured with Respect to the Tip-path Plane</u>.--As in Equation 53, the change in blade angle may be expressed as

$$\Delta\theta = -a_1 \sin\psi + b_1 \cos\psi$$

The magnitude of the longitudinal component of the cyclic pitch, b_1 , can be determined from the difference in the blade angle of attack, α_r , and the inflow angle, ϕ_v , at the blade thrust moment centers at the $\psi = 0$ and $\psi = \pi$ blade positions. Again the blade angle of attack is expressed as in Equation 54 as

$$\alpha_r = \frac{\Gamma}{\pi\bar{c}\,U}$$

Substituting the mean blade moment center $\bar{x}$, Γ from Equation 37, and taking the difference between α_r at $\psi = 0$ and $\psi = \pi$ gives

$$\Delta \alpha_r = - \frac{2 a_0 \mu_v}{\bar{\alpha}} \left(\frac{4}{3} - \frac{1}{\bar{x}} \right) \tag{63}$$

Substituting $x = \bar{x}$, and taking the difference between the inflow angle, ϕ_v , given by Equation 56, at $\psi = 0$ and $\psi = \pi$ gives

$$\Delta \phi_v = - 2 \left(- w + \frac{a_0 \mu_v}{\bar{x}} \right) \tag{64}$$

Since

$$b_1 = - \frac{1}{2} \left(\Delta \alpha_r - \Delta \phi_v \right) \tag{65}$$

then

$$b_1 = \frac{a_0 \mu_v}{\bar{\alpha}} \left(\frac{4}{3} - \frac{1}{\bar{x}} \right) - w + \frac{a_0 \mu_v}{\bar{x}} \tag{66}$$

Equation for the Rotor X-Force.--A sufficiently accurate expression for the profile drag coefficient, c_{d_0} , over the unstalled range is given by the first two terms of an

even power series in the blade-element lift coefficient, c_ℓ , i.e.

$$c_{d_o} = \delta_o + \mathcal{E} c_\ell^2 \tag{67}$$

where $\delta_o = c_{d_o}$ for a given airfoil at $c_\ell = 0$

and $\mathcal{E}$ may be evaluated from the value of c_{d_o} at say $c_\ell = 0.8$

Typical values of δ_o and $\mathcal{E}$ are

$$\delta_o = \mathcal{E} = 0.008 \tag{68}$$

Using the above expression for the profile drag coefficient, the inplane component of force, ΔF_{XY} , acting to the rear chordwise on a blade-element at non-dimensional radius, x , and azimuth angle, ψ , (see Fig. 2) is

$$\Delta F_{XY} = -\rho \Gamma (U \sin\phi)\, dr + \tfrac{1}{2} \rho U^2 c (\delta_o + \mathcal{E} c_\ell^2) \cos\phi_v \, dr \tag{69}$$

The inplane component of this force acting toward the X or downwind position is

$$\Delta F_{xy}(\sin\psi) = \left[-\rho\Gamma(U\sin\phi_v) + \frac{1}{2}\rho U^2 c\left(\delta_0 + \varepsilon\alpha_e^2\right)\cos\phi\right]\sin\psi\, dr \tag{70}$$

The rotor X-force is

$$F_x = \frac{b}{2\pi}\int_0^{2\pi}\int_0^R \Delta F_{xy}\ \sin\psi\, d\psi\, dr \tag{71}$$

Define a rotor X-force coefficient as

$$C_x = \frac{F_x}{\frac{1}{2}\rho\pi\Omega^2 R^4} \tag{72}$$

It follows upon substitution of appropriate values from Equations 13, 14, 24, 37 and 70 into 72 that

$$C_x = \frac{-6C_T}{2\pi}\int_0^{2\pi}\int_0^1 \left\{\left[\frac{\nu_a}{\bar{\alpha}} + \left[\left(\frac{1+\frac{1}{2}\mu_v^2}{1-\frac{1}{2}\mu_v^2} - \frac{3\nu_a}{2\bar{\alpha}}\right) - \left(\frac{4\mu_v}{3\left[1-\frac{1}{2}\mu_v^2\right]}\right)\sin\psi\right]x + \frac{a_0\mu_v}{\bar{\alpha}}\left(\frac{4}{3}x - 1\right)\cos\psi + \left(\frac{2\mu_v^2}{3\left[1-\frac{1}{2}\mu_v^2\right]}\right)\cos 2\psi\right]\left[\nu_a - \nu_i x + \gamma x\sin\psi\right] \tag{73}$$

$$+ (\omega x - a_0 \mu_v)\cos\psi \Big]^2 \Big\} \sin\psi \, d\psi \, dx$$

$$+ \frac{\delta_0 \sigma}{2\pi} \int_0^{2\pi}\int_0^1 \frac{(x + \mu_v \sin\psi)^2}{\cos\phi} \sin\psi \, d\psi \, dx$$

$$+ \frac{36\, \varepsilon C_T^2}{\sigma 2\pi} \int_0^{2\pi}\int_0^1 \left\{ \frac{\nu_a}{\alpha} + \left[\left(\frac{1 + \frac{1}{2}\mu_v^2}{1 - \frac{1}{2}\mu_v^2} - \frac{3\nu_a}{2\alpha} \right) - \left(\frac{4\mu_v}{3\left[1 - \frac{1}{2}\mu_v^2\right]} \right) \sin\psi \right] x \right.$$

$$\left. + \frac{a_0 \mu_v}{\alpha} \left(\frac{4}{3} x - 1 \right) \cos\psi + \left(\frac{2\mu_v^2}{3\left[1 - \frac{1}{2}\mu_v^2\right]} \right) \cos 2\psi \right\}^2$$

$$\cos\phi \, \sin\psi \, d\psi \, dx$$

Since the effect of $\cos\phi$ in the denominator of the second integral in the above expression is small, an approximate average value can be used. At the three-quarter radius point and at $\psi = 0$

$$\cos\phi_v = \frac{U \cos\phi_v}{\sqrt{(U\cos\phi_v)^2 + (U\sin\phi_v)^2}} \qquad (74)$$

$$\approx \frac{\frac{3}{4}}{\sqrt{\left(\frac{3}{4}\right)^2 + \left(\nu_a - \nu_i x\right)^2}}$$

Expansion of the above equation by the binomial theorem and neglecting small terms gives

$$\frac{1}{\cos \phi_v} \approx 1 + \frac{8}{9}\left(\nu_a - \nu_i \chi\right)^2 \tag{75}$$

Let $\cos \phi_v = 1$ in the third integral, then the expression for rotor X-force coefficient, C_X, integrates to

$$C_X = \frac{C_T}{1 - \frac{1}{2}\mu_v^2}\left[2\mu_v\left(\nu_a - \frac{2}{3}\nu_i\right) - \gamma\right] + \frac{\delta_0 \sigma \mu_v}{2}\left[1 + \frac{16}{9}\left(\frac{\nu_a^2}{2} - \frac{2}{3}\nu_i \nu_a + \frac{\nu_i^2}{4}\right)\right] - \frac{16 \varepsilon C_T^2 \mu_v}{\sigma\left(1 - \frac{1}{2}\mu_v^2\right)^2} \tag{76}$$

This equation does not include the radial component of the blade skin friction drag and the additional profile drag of the blade elements within the reverse flow region. These are small below $\mu_v = 0.3$, but may be of significant value for larger values of μ_v.

The increment to C_X due to the radial component of skin friction drag is approximately

$$\Delta C_X = \frac{1}{\frac{1}{2}\rho\pi\Omega^2R^4}\,\frac{2}{\pi}\int_0^{\frac{\pi}{2}}\int_0^R \frac{1}{2}\rho b c \delta_0 \left(V\cos\alpha_v\cos\psi\right)^2 (\cos\psi)\,d\psi\,dr \tag{77}$$

Integration is over the first quadrant because of the false change in direction of the force at $\psi = \frac{\pi}{2}$. The average force on a blade is the same in all four quadrants.

Integration gives

$$\Delta C_X = \frac{4}{3\pi}\,\delta_0\,\sigma\,\mu_v^2 \tag{78}$$

The profile drag coefficient of a 0015 airfoil at angles of attack near 180° was found from wind tunnel tests (8) to be of the order of $4\delta_0$ at an IAS of 80 miles per hour at a Reynolds number of 1,230,000 (based on $\alpha = 0$). It can probably be assumed that a value of $4\delta_0$ is a good engineering approximation for the blade-element profile drag coefficient within the reverse flow region of present day helicopter rotors.

Thus

$$\Delta C_X = -\frac{1}{\frac{1}{2}\rho\pi\Omega^2R^4}\,\frac{1}{\pi}\int_{\pi}^{2\pi}\int_0^{-\mu_v R\sin\psi} \frac{1}{2}\rho b c (5\delta_0) \left(U\cos\phi_v\right)^2 \sin\psi\,d\psi\,dr \tag{79}$$

where $5\delta_0$ includes the reverse flow drag plus δ_0 to cancel the profile drag considered in Equation 70, which neglected reverse flow. Integration gives

$$\Delta C_X = \frac{5}{8}\,\delta_0\,\sigma\,\mu_V^{\,3} \tag{80}$$

Thus for flight ranges in excess of $\mu_V = 0.3$, the following equation, which includes the above corrections, should give more accurate results.

$$\begin{aligned} C_X = {} & \frac{C_T}{(1-\frac{1}{2}\mu_V^2)}\left[2\mu_V\left(\nu_a - \frac{2}{3}\nu_i\right) - \gamma\right] \\ & + \frac{\delta_0\,\sigma\,\mu_V}{2}\left[1 + \frac{16}{9}\left(\frac{\nu_a}{2}^2 - \frac{2}{3}\nu_a\nu_i + \frac{\nu_i}{4}\right)\right] \\ & - \frac{16\,\varepsilon\,C_T^{\,2}\,\mu_V}{\sigma\left(1-\frac{1}{2}\mu_V^2\right)^2} \\ & + \frac{4}{3\pi}\,\delta_0\,\sigma\,\mu_V^{\,2} \\ & + \frac{5}{8}\,\delta_0\,\sigma\,\mu_V^{\,3} \end{aligned} \tag{81}$$

<u>Equation for the Rotor Y-Force</u>.--The inplane component of force acting in the Y direction is

$$-\Delta F_{XY}(\cos\psi) = \left[\rho\Gamma\left(U\sin\phi_V\right) - \frac{1}{2}\rho U^2 c\left(\delta_0 + \varepsilon C_\ell^{\,2}\right)\left(\cos\phi_V\right)\right]\cos\psi\; dr \tag{82}$$

The inplane velocity distribution and blade circulation are nearly symmetrical force and aft. Thus the side force due to blade profile drag is essentially zero. Reducing the above equation gives

$$F_Y = \frac{b}{2\pi} \int_0^{2\pi} \int_0^R \rho \Gamma (U \sin\phi) \cos\psi \, d\psi \, dr \tag{83}$$

Substituting values for Γ from Equation 37, and $U \sin\psi$ from Equation 14, and again using a force coefficient

$$C_Y = \frac{F_Y}{\frac{1}{2} \rho \pi \Omega^2 R^4} \tag{84}$$

gives

$$C_Y = \frac{6 C_T}{2\pi} \int_0^{2\pi} \int_0^1 \left\{ \left[\frac{\nu_a}{\alpha} + \left[\left(\frac{1 + \frac{1}{2}\mu_v^2}{1 - \frac{1}{2}\mu_v^2} - \frac{3\nu_a}{2\alpha} \right) - \left(\frac{4\mu_v}{3[1 - \frac{1}{2}\mu_v^2]} \right) \sin\psi \right] x + \frac{a_0 \mu_v}{2} \left(\frac{4}{3} x - 1 \right) \cos\psi + \left(\frac{2\mu_v^2}{3[1 - \frac{1}{2}\mu_v^2]} \right) \cos 2\psi \right] \left[\nu_a - \nu_i x + y x \sin\psi + (\omega x - a_0 \mu_v) \cos\psi \right] \right\} \cos\psi \, d\psi \, dx \tag{85}$$

Subsequent integration gives

$$C_Y = \frac{a_0 \mu_v \sigma a}{2}\left(\frac{\nu_i}{18} - \frac{7}{16}\nu_a\right) + \frac{C_T w (1+\mu_v^2)}{(1-\frac{1}{2}\mu_v^2)} - \frac{\frac{3}{2} a_0 \mu_v C_T (1+\frac{7}{6}\mu_v^2)}{(1-\frac{1}{2}\mu_v^2)} \tag{86}$$

Equation for the Rotor Torque.--The rotor torque, Q, necessary to drive the rotor is equal to the total moment due to the inplane components of force on the blade-elements, plus the torque due to the three-dimensional tip drag. When tip stall occurs an additional torque increment, ΔQ_s, must be considered in the total.

The torque from the inplane components of force on the blade elements is given by

$$Q = \frac{b}{2\pi}\int_0^{2\pi}\int_0^R \Delta F_{XY}\, r\, d\psi\, dr \tag{87}$$

The skin drag of the tip (see Ref. 9) may be expressed as

$$D = 0.085\left(\frac{t}{c}\right)^2 \frac{1}{2}\rho\left(U\cos\phi\right)^2 c_t^{\,2} \tag{88}$$

where $\frac{t}{c}$ = thickness ratio at the blade tip

c_t = tip chord

Define a rotor torque coefficient, C_Q, as

$$C_Q = \frac{Q}{\rho \pi \Omega^2 R^5} \tag{89}$$

It follows from Equations 70, 37, 13, 14, 23, 24, 87 and 88 that the expression for the rotor torque coefficient becomes

$$C_Q = \frac{-3C_T}{2\pi} \int_0^{2\pi} \int_0^1 \left\{ \left[\frac{\nu_a}{\bar{\alpha}} + \left[\left(\frac{1+\frac{1}{2}\mu_v^2}{1-\frac{1}{2}\mu_v^2} - \frac{3\nu_a}{2\bar{\alpha}} \right) \right. \right. \right. \tag{90}$$

$$\left. - \left(\frac{4\mu_v}{3\left[1-\frac{1}{2}\mu_v^2\right]} \right) \sin\psi \right] x$$

$$\left. + \frac{a_0 \mu_v}{\bar{\alpha}} \left(\frac{4}{3} x - 1 \right) \cos\psi + \left(\frac{2\mu_v^2}{3\left[1-\frac{1}{2}\mu_v^2\right]} \right) \cos 2\psi \right]$$

$$\left. \left[\nu_a - \nu_i x + \gamma x \sin\psi + (\omega x - a_0 \mu_v) \cos\psi \right] \right\} x \, d\psi \, dx$$

$$+ \frac{\delta_0 \sigma}{4\pi} \int_0^{2\pi} \int_0^1 \frac{(x + \mu_v \sin\psi)^2}{\cos\phi_v} x \, d\psi \, dx$$

$$+ \frac{9\varepsilon C_T^2}{\sigma\pi} \int_0^{2\pi} \int_0^1 \left\{ \frac{\nu_a}{\bar{\alpha}} + \left[\left(\frac{1+\frac{1}{2}\mu_v^2}{1-\frac{1}{2}\mu_v^2} - \frac{3\nu_a}{2\bar{\alpha}} \right) \right. \right.$$

$$-\left(\frac{4\mu_v}{3[1-\frac{1}{2}\mu_v^2]}\right)\sin\psi\Big]x$$

$$+\frac{a_0\mu_v}{\alpha}\left(\frac{4}{3}x-1\right)\cos\psi$$

$$+\left(\frac{2\mu_v^2}{3[1-\frac{1}{2}\mu_v^2]}\right)\cos 2\psi\Bigg\}^2\cos\phi_v\, x\, d\psi\, dx$$

$$+0.085\left(\frac{t}{c}\right)^2\frac{\sigma_t^2\pi}{2b(2\pi)}\int_0^{2\pi}(1+\mu_v\sin\psi)^2\,d\psi$$

$$+\Delta C_{Q_S}$$

where σ_t = tip solidity $= \dfrac{bc_t}{\pi R}$

The tip stall increment of torque coefficient, ΔC_{Q_S}, occurs at large values of μ_v due to tip stall on the retreating blade. The small negative increment to C_Q of the profile drag on the blade elements within the reverse flow region is neglected in the above equation.

Define a mean blade lift coefficient, $\bar{C}_L$, as

$$\bar{C}_L = \frac{6C_T}{\sigma} \tag{91}$$

Substitution of this expression and Equation 16 into the equation for the rotor torque coefficient, the use of Equation 75 for the $\cos\phi_v$ term in the second integral and $\cos\phi_v = 1$ in the third integral, and subsequent integration gives

$$C_Q = C_T\left(\frac{3}{4}\nu_i - \nu_a\right)\left(\frac{1+\frac{1}{2}\mu_v^2}{1-\frac{1}{2}\mu_v^2}\right) - \frac{\nu_a \nu_i \sigma a}{48} \tag{92}$$

$$+ \frac{\mu_v^2 \nu_i C_T}{(1-\frac{1}{2}\mu_v^2)} - \frac{q_0^2 \mu_v^2 \sigma a}{72}$$

$$+ \frac{\delta_0 \sigma}{2}\left(\frac{1}{4} + \frac{\mu_v^2}{4} + \frac{8}{9}\left[\frac{\nu_a^2}{4} - \frac{2}{5}\nu_a\nu_i - \frac{\nu_i^2}{6}\right]\right)$$

$$+ 3\varepsilon\bar{C}_L C_T\left(\left[\frac{\nu_a}{4\bar{\alpha}}\right]^2 - \frac{\nu_a}{12\bar{\alpha}}\left[\frac{1+\frac{1}{2}\mu_v^2}{1-\frac{1}{2}\mu_v^2}\right]\right.$$

$$\left. + \frac{[1+\frac{25}{18}\mu_v^2][1+\frac{1}{2}\mu_v^2]}{4[1-\frac{1}{2}\mu_v^2]^2} + \left[\frac{a_0 \mu_v}{6\bar{\alpha}}\right]^2\right)$$

$$+ 0.085\left(\frac{t}{c}\right)^2 \frac{\sigma_t^2 \pi}{2b}\left(1+\frac{1}{2}\mu_v^2\right)$$

$$+ \Delta C_{Q_S}$$

The value of the increment ΔC_{Q_S}, to the rotor torque coefficient can be approximately determined by considering the blade angle of attack, α_r, on the retreating blade at non-dimensional radius x and azimuth angle $\psi = \frac{3\pi}{2}$.

$$\alpha_r = \theta_v + \phi_v = A_0 + a_1 + \Delta\theta_t + \frac{\nu_a - \varkappa(\nu_i + \gamma)}{\varkappa - \mu_v} \qquad (93)$$

where $\Delta\theta_t$ = blade twist from $\varkappa = 0.75$ to $\varkappa = 1$ positive for increased blade angle at the blade tip.

Let c_{ℓ_m} denote the blade maximum lift coefficient which normally is of the order of $c_{\ell_m} = 1.2$. Then the local angle of attack at which a given blade element stalls is

$$\alpha_s = \frac{c_{\ell_m}}{2\pi} = A_0 + a_1 + \Delta\theta_t + \frac{\nu_a - \varkappa_s(\nu_i + \gamma)}{\varkappa_s - \mu_v} \qquad (94)$$

It follows from Equation 94 that the non-dimensional radius, $\varkappa_s$, outboard of which the blade is stalled is

$$\varkappa_s = \frac{\nu_a + \mu_v\left(\frac{c_{\ell_m}}{2\pi} - A_0 - a_1 - \Delta\theta_t\right)}{\gamma + \nu_i + \left(\frac{c_{\ell_m}}{2\pi} - A_0 - a_1 - \Delta\theta_t\right)} \qquad (95)$$

The onset of tip stall on the retreating blade will occur when $\varkappa_s = 1$. Thus setting $\varkappa_s = 1$ in Equation 95 and solving for μ_v gives

$$(\mu_v)_s = \frac{\gamma + \nu_i - \nu_a + \left(\frac{c_{\ell_m}}{2\pi} - A_0 - a_1 - \Delta\theta_t\right)}{\left(\frac{c_{\ell_m}}{2\pi} - A_0 - a_1 - \Delta\theta_t\right)} \qquad (96)$$

The portion of the rotor disk within which the tip blade elements of the retreating blade will be stalled is

very nearly a segment of minimum radius μ_s . The area of this segment may be approximated by the inscribed triangles since μ_s is never very much smaller than unity.

$$\text{Area of stall} = (1-\mu_s)\sqrt{1-\mu_s^2} \tag{97}$$

The incremental torque of a stalled blade-element at $\psi = \frac{3\pi}{2}$ and $\mu_s = 1$ is

$$\Delta Q = \frac{1}{2}\rho\Omega^2 R^3 (1-\mu_v)^2 \Delta c_{d_0} c_t \, dr \tag{98}$$

where Δc_{d_0} = average increase in profile drag coefficient for several degrees beyond the angle of attack for stall (the order of $\Delta c_{d_0} = 0.08$)

Consider that on the average the blade area within the stall region is approximately equal to the total area of the blades outboard of μ_s , i.e.

$$\text{Area of blades outboard of } \mu_s = bc\,R(1-\mu_s) \tag{99}$$

times the ratio of the area of the stall segment (given by Equation 97) to the rotor area in the annulus outboard of μ_s given by

$$\text{Area in annulus} = \pi(1-\mu_s^2)R^2 \tag{100}$$

Thus

$$\Delta Q_{total} = \frac{1}{2}\rho\Omega^2 R^4 (1-\mu_v)^2 \Delta c_{d_o} b c_t (1-x_s)\sqrt{\frac{1-x_s}{1+x_s}} \qquad (101)$$

or

$$\Delta C_{Q_s} = \frac{\Delta c_{d_o}}{2\pi}\sigma_t (1-\mu_v)^2 (1-x_s)\sqrt{\frac{1-x_s}{1+x_s}} \qquad (102)$$

If x_s is less than μ_v the stall point is within the reverse flow region, and if x_s is greater than μ_v no outer blade-elements are stalled. It would be convenient to develop an expression for the section lift coefficient in terms of ν_a, μ_v and $\bar{\alpha}$ so that a simpler calculation might be effected to determine the stall region. From Equation 10,

$$c_\ell = \frac{2\Gamma}{cU}$$

Substitutions from Equation 24 and 13, assuming $\cos\phi_v \approx 1$ gives

$$c_\ell = \frac{2\Gamma b}{\pi\sigma\Omega R^2 (x + \mu_v \sin\psi)} \qquad (103)$$

For incipient tip stall $x = 1$, $\psi = \frac{3\pi}{2}$ and $c_\ell = c_{\ell_m}$. Thus substitution of Equation 37 with $x_s = 1$ and $\psi = \frac{3\pi}{2}$

into the above equation gives

$$c_{l_{tip}} = \frac{\bar{\alpha}_t a}{1-\mu_v}\left[\frac{1+\frac{4}{3}\mu_v - \frac{1}{6}\mu_v^2}{1-\frac{1}{2}\mu_v^2} - \frac{\nu_a}{2\bar{\alpha}_t}\right] \qquad (104)$$

$$\text{where} \quad \bar{\alpha}_t = \frac{6C_T}{\sigma_t a}$$

Determination of the Longitudinal Tilt of the Tip-path Plane, θ_y, and the Rotor Angle of Attack α_v.--The forces acting on the rotor hub for the general case of steady inclined flight where the flight path is at an angle, ϕ_c, to the horizontal (positive for descent) and the tip-path plane is at an angle, θ_y, to the horizontal (positive for rearward inclination) are shown in Figure 4.

In helicopter calculations the fuselage lift, L_F, can usually be neglected. Also the lateral tilt of the tip-path plane has a negligible effect. It follows from the geometry of the forces shown in Figure 4, neglecting fuselage lift, that

$$\tan\theta_y = -\frac{D_F\cos\phi_c + F_x\cos\theta_y}{W - D_p\sin\phi_c + F_x\sin\theta_y} \qquad (105)$$

where D_F = fuselage drag

W = gross weight of helicopter

Since the X-force is small compared to the parasite drag for power-on flight conditions, a sufficiently exact solution of Equation 105 may be obtained on the second reiteration using as a first approximation

$$\tan \theta_y \approx - \frac{D_F \cos \phi_c}{W - D_F \sin \phi_c} \tag{106}$$

Knowing the flight path inclination and the longitudinal tilt of the tip-path plane, the rotor angle of attack can be determined.

$$\alpha_v = \phi_c + \theta_y \tag{107}$$

Determination of the Rotor Thrust Coefficient, C_T.--Since the longitudinal tilt of the tip-path plane is always a small angle for steady state flight, an equation for the rotor thrust may be determined by equating to zero the summation of forces acting on the rotor in the vertical direction. Again referring to Figure 4 and neglecting fuselage lift, an expression for the thrust force, T, is

$$T = \frac{W - D_F \sin \phi_c + F_x \sin \theta_y}{\cos \theta_y} \tag{108}$$

Substitution of the above equation into the equation for the

rotor thrust coefficient given by Equation 26 gives

$$C_T = \frac{W - D_F \sin \phi_c + F_x \sin \theta_y}{\rho \pi \Omega^2 R^4 \cos \theta_y} \tag{109}$$

CHAPTER III

APPLICATION

Performance Charts.--The calculation of values of the rotor X-force coefficient from Equation 76 and the rotor torque coefficient from Equation 92 can be simplified by means of charts that relate certain variables with functions from the equation. Such charts are presented in Figures 5 to 10. The charts cover ranges of μ_v from 0 to 0.5, C_T from 0.002 to 0.02, $\bar{\alpha}$ from 0.05 to 0.13, and ν_a from -0.10 to 0.04. Some five thousand points for the charts were determined utilizing an IBM 650 computer. It is necessary to separate certain functions in order to limit each chart to a function of two variables. The breakdown of the equations follows.

The rotor X-force coefficient from Equation 76 is written as

$$C_X = \Delta C_{X_L} + \Delta C_{X_{DP_c}} + \Delta C_{X_{DP_v}} \tag{110}$$

where ΔC_{X_L} = increment of X-force due to lift

$\Delta C_{X_{DP_c}}$ = increment of X-force due to the constant part of the profile drag

$\Delta C_{X_{DP_V}}$ = increment of X-force due to the variable part of the profile drag

Figures 5(a) to 5(h) are a plot of $\frac{\Delta C_{X_L}}{C_T}$ versus C_T for various values of C_T , μ_V and $\bar{\nu}_a$.

$$\frac{\Delta C_{X_L}}{C_T} = \frac{2\mu_V}{1-\frac{1}{2}\mu_V^2}\left(\bar{\nu}_a - \frac{5}{3}\bar{\nu}_i\right) \tag{111}$$

The induced velocity, $\bar{\nu}_i$, is computed from Equation 15. Figures 6(a) to 6(h) are a plot of $\frac{\Delta C_{X_{DP_C}}}{\delta_0 \sigma}$ versus C_T .

$$\frac{\Delta C_{X_{DP_C}}}{\delta_0 \sigma} = \frac{\mu_V}{2}\left[1 + \frac{16}{9}\left(\frac{\bar{\nu}_a^2}{2} - \frac{2}{3}\bar{\nu}_i\bar{\nu}_a + \frac{\bar{\nu}_i^2}{4}\right)\right] \tag{112}$$

Thus knowing C_T , δ_0 , σ , μ_V and $\bar{\nu}_a$, ΔC_{X_L} and $\Delta C_{X_{DP_C}}$ can be rapidly determined from these curves.

The value of α_V for determining $\bar{\nu}_a$ and the value of C_T must be determined by iteration as indicated in the development of Equations 105 through 107.

The value of $\Delta C_{X_{DP_V}}$ is determined from

$$\Delta C_{X_{DP_V}} = -\frac{16\,\xi\,C_T^2\,\mu_V}{\sigma\left(1-\frac{1}{2}\mu_V^2\right)^2} \tag{113}$$

The rotor torque coefficient from Equation 92 is written as

$$C_Q = \Delta C_{Q_L} + \Delta C_{Q_{DP_c}} + \Delta C_{Q_{DP_v}} + \Delta C_{Q_{a_o}} \qquad (114)$$

$$+ \Delta C_{Q_t} + \Delta C_{Q_s}$$

where ΔC_{Q_L} = increment of torque coefficient due to lift (less term involving a_o)

$\Delta C_{Q_{DP_c}}$ = increment of torque coefficient due to the constant part of the profile drag

$\Delta C_{Q_{DP_v}}$ = increment of torque coefficient due to the variable part of the profile drag (less term involving a_o)

$\Delta C_{Q_{a_o}}$ = increment of torque coefficient due to terms involving a_o

ΔC_{Q_t} = increment of torque coefficient due to tip drag

ΔC_{Q_s} = increment of torque coefficient due to tip stall

Figures 7(a) to 7(i) are a plot of $\frac{\Delta C_{Q_L}}{C_T}$ versus C_T .

$$\frac{\Delta C_{Q_L}}{C_T} = \left(\frac{3}{4}\nu_i - \nu_a\right)\left(\frac{1 + \frac{1}{2}\mu_v^2}{1 - \frac{1}{2}\mu_v^2}\right) \qquad (115)$$

$$-\left(\frac{\nu_a \nu_i}{0.8}\right) + \left(\frac{\mu_v^2 \nu_i}{1 - \frac{1}{2}\mu_v^2}\right)$$

The approximation that $\frac{6C_T}{\sigma a} \approx 0.1$ is made in obtaining the relatively small second term in the above equation, i.e.

$$\frac{-\nu_i \nu_a \sigma a}{48 C_T} \approx \frac{-\nu_a \nu_i}{0.8}$$

Again the value of the induced velocity in the equations is computed from Equation 15. Figures 8(a) to 8(i) are a plot of $\frac{\Delta C_{Q_{DP_c}}}{\delta_0 \sigma}$ versus C_T .

$$\frac{\Delta C_{Q_{DP_c}}}{\delta_0 \sigma} = \frac{1}{8} + \frac{\mu_v^2}{8} + \frac{4}{9}\left(\frac{\nu_a^2}{4} - \frac{2}{5}\nu_a\nu_i + \frac{\nu_i^2}{6}\right) \quad (116)$$

Figures 9(a) to 9(i) are a plot of $\frac{\Delta C_{Q_{DP_v}}}{C_T}\Big/\varepsilon \bar{C}_L$ versus $\bar{\alpha}$.

$$\frac{\frac{\Delta C_{Q_{DP_v}}}{C_T}}{\varepsilon \bar{C}_L} = \frac{3}{16}\left(\frac{\nu_a}{\bar{\alpha}}\right)^2 - \frac{\nu_a}{4\bar{\alpha}}\left(\frac{1+\frac{1}{2}\mu_v^2}{1-\frac{1}{2}\mu_v^2}\right) + \frac{\left(1+\frac{25}{18}\mu_v^2\right)\left(1+\frac{1}{2}\mu_v^2\right)}{\frac{4}{3}\left(1-\frac{1}{2}\mu_v^2\right)^2} \quad (117)$$

Thus ΔC_{Q_L} , $\Delta C_{Q_{DP_c}}$ and $\Delta C_{Q_{DP_v}}$ can be determined knowing C_T , $\bar{\alpha}$, $\bar{C}_L$, δ_0 , ε , σ , ν_a and μ_v . $\Delta C_{Q_{a_0}}$ is calculated from

$$\Delta C_{Q_{a_0}} = \frac{a_0^2 \mu_v^2 \sigma a}{72}\left(\varepsilon a - 1\right) \quad (118)$$

The value of a_0 in the above equation is read from the appropriate curve from Figures 10(a) to 10(f), which are plots

of $\frac{a_o}{C_T}\left[\frac{I_1 b}{\rho \pi R^5}\right]$ versus $\bar{\alpha}$.

$$\frac{a_o}{C_T}\left[\frac{I_1 b}{\rho \pi R^5}\right] = \frac{3}{4}\left(\frac{1-\frac{7}{18}\mu_V^2}{1-\frac{1}{2}\mu_V^2}\right) - \frac{\nu_a}{8\bar{\alpha}} \qquad (119)$$

ΔC_{Q_t} is calculated from

$$\Delta C_{Q_t} = 0.085\left(\frac{t}{c}\right)^2 \frac{\sigma_t^2 \pi}{2b}\left(1+\frac{1}{2}\mu_V^2\right) \qquad (120)$$

This term is usually small and can be neglected for low solidity rotors. ΔC_{Q_s} is determined from Equation 102.

Power Required.--Knowing the value of the rotor torque for a certain flight condition, the power required for the main rotor may be readily calculated from

$$\text{Rotor HP required} = \frac{\Omega Q}{550} \qquad (121)$$

In addition to the main rotor, the counter-torque rotor power, along with power for accessories, and power losses, must be included in the determination of the total helicopter engine power.

$$\text{Engine HP required} = \frac{\Omega Q + (\Omega Q)_{c.t.}}{550\,\eta} \qquad (122)$$

where η = efficiency of power and drive system to account for engine cooling power, power lost due to gear and bearing friction and power to drive accessories.

$(\Omega Q)_{c.t.}$ = product of the counter-torque rotor torque and the counter-torque mean angular velocity

The counter-torque rotor torque may be calculated utilizing the equation for the main rotor torque. Parameters used are for the counter-torque rotor. The counter-torque rotor thrust $T_{c.t.}$ is

$$T_{c.t.} = \frac{Q}{\ell} \tag{123}$$

where Q = main rotor torque

ℓ = perpendicular distance from the main rotor shaft to the counter-torque rotor hub

Thus the thrust coefficient of the counter-torque rotor is

$$C_{T_{c.t}} = \left(\frac{R}{\ell}\right)\left(\frac{R}{R_{c.t.}}\right)^4\left(\frac{\Omega}{\Omega_{c.t.}}\right)C_Q \tag{124}$$

It follows that for a given counter-torque rotor geometry and gear ratio and main rotor torque coefficient the counter-torque thrust coefficient may be computed from Equation 124 and the counter-torque rotor torque coefficient then found from Equation 92.

Sample Rotor Performance Calculation Utilizing Performance Charts.--The equations and methods developed herein are most readily applicable for determination of the rotor torque or

engine power required by a helicopter flying at a given airspeed and at a given rate of climb (or climb angle). The method of computing rotor torque will be illustrated by a sample problem: Calculate the rotor torque coefficient for a helicopter traveling at 76 feet per second and climbing at a rate of 8.75 feet per second. The following additional data are known:

W = 2560 pounds

ΩR = 443 feet per second

C_T = 0.00546

σ = 0.06

f = 25.4 square feet parasite area

I_1 = 160 slugs - square feet

ρ = 0.0023 slugs per cubic foot

R = 19 feet

b = 3 blades

r_t = 0.822 feet

$\frac{t}{c}$ = 0.12

Values are from experimental data for run number eleven given in (10).

(1) Calculate $\phi_c = \tan^{-1} \frac{-8.75}{76} = -6.51^\circ$

(2) Calculate $D_f = \frac{1}{2}\rho V^2 f = \frac{1}{2}(.0023)(76)^2(25.4) = 169$

(3) From Equation 106 $\tan \theta_y = -0.0653$ or $\theta_y = -3.75^\circ$

(4) From Equation 107 $\alpha_v = -6.51 - 3.75 = -10.26^\circ$

(5) Calculate $\nu_a = \frac{V \sin \alpha_v}{\Omega R} = \frac{(76)(-0.178)}{443} = -0.0312$

(6) Calculate $\mu_v = \frac{V \cos \alpha_v}{\Omega R} = 0.169$

(7) Calculate C_X

(a) From Figure 5(c) and 5(d) $\frac{\Delta C_{X_L}}{C_T} =$ -0.022 and -0.0285 respectively. Interpolation gives $\frac{\Delta C_{X_L}}{C_T} = -0.0245$ or $\Delta C_{X_L} = -0.000134$

(b) From Figure 6(c) and 6(d) $\frac{\Delta C_{X_{DP_C}}}{\delta_0 \sigma} =$ 0.07516 and 0.10017 respectively. Interpolation gives $\frac{\Delta C_{X_{DP_C}}}{\delta_0 \sigma} = 0.08466$ Assume $\delta_0 = 0.008$ then $\Delta C_{X_{DP_C}} =$ 0.0000406

(c) Assume $\epsilon = 0.008$ then from Equation 113 $\Delta C_{X_{DP_v}} = -0.0000111$

(d) From Equation 110, $C_X = -0.000104$ and from Equation 72, $F_X = -26.8$ pounds

(8) A recheck of θ_y using Equation 105 gives $\tan \theta_y = -0.0556$ or $\theta_y = -3.19^\circ$

(9) Calculate a new value of ν_a from Equation 107, $\alpha_v = -6.51 - 3.19 = -9.7^\circ$, and $\nu_a =$ 0.0288

(10) Repeating steps (6) through (9) gives

$\mu_v = 0.169$

$\Delta C_{x_L} = -0.0001265$

$\Delta C_{x_{DP_c}} = 0.0000406$

$\Delta C_{x_{DP_v}} = -0.0000111$

$C_x = -0.000097$

$F_x = -25$ pounds

$\theta_y = -3.23°$

$\alpha_v = -9.74°$

$\nu_a = -0.029$

Reiteration would not appreciably change the above values; therefore, a $\mu_v = 0.169$ and a $\nu_a = -0.029$ will be used to calculate the rotor torque.

(11) Assume $a = 2\pi$ and calculate $\bar{\alpha} = \frac{6C_T}{\sigma a} = \frac{(6)(0.00546)}{(0.06)\,2\pi} = 0.0868$ and $\bar{C_L} = \frac{6C_T}{\sigma} = 0.546$

(12) Calculate C_Q

(a) Interpolation of appropriate charts gives

$\Delta C_{Q_L} = 0.000269$ from charts 7(d) and 7(e)

$\Delta C_{Q_{DP_c}} = 0.000062$ from charts 8(d) and 8(e)

$\Delta C_{Q_{DP_v}} = 0.000022$ from charts 9(d) and 9(e)

$\frac{a_o}{C_T}\left[\frac{I_1 b}{\rho \pi R^5}\right] = 0.794$ from charts 10(b) and 10(c)

or $a_o = 0.161$ radians

(b) From Equation 118, $\Delta C_{Q_{a_o}} = -0.000003$

(c) From Equation 120 $\Delta C_{q_t} = 0.000001$

(d) A check of Equation 95 indicates $\Delta C_{q_s} = 0$

(e) From Equation 114, $C_q = 0.000351$

This value compares favorably with the experimental value of $C_q = 0.000359$. The blade-element analysis presented in (1) gives a value of $C_q = 0.000328$ for the same run. Calculation of the rotor torque coefficient from circulation equations based on a uniform induced velocity distribution, (1), gives a value of $C_q = 0.000322$.

Comparison of Results with Experimental Data.--A comparison of the parameters for run number eleven calculated from the equations developed herein and from the blade-element analysis of (1), with the experimental values from (10) is shown in the following tabulation:

Parameter	Experimental	Present Theory	Blade-element Theory
α_v	-9.97°	-9.74°	-9.55°
A_o	10.00°	9.4°	9.5°
a_1	4.23°	3.73°	3.81°
b_1	3.56°	3.86°	2.88°
a_o	9.15°	9.22°	8.42°
C_x	- - -	-0.000097	-0.000095
C_q	0.000359	0.000351	0.000322

The rotor blades used in the flight tests were quite flexible permitting more dynamic twist than is encountered in rotor

blades of current design. This dynamic twist was not considered in the calculation of the thrust center and thrust moment center for use in obtaining values of A_o, a_1 and b_1, shown in the present theory column above. For this flight condition, dynamic twist moves the thrust center and thrust moment center inboard of the location determined from Equation 51, 52, 61 and 62. A correction for the twist would result in closer agreement with experimental data.

Comparison of rotor torque coefficients for other runs tabulated in (1) and (10) are shown below.

Run	Flight	MPH	Experimental	Present Theory	Blade-element Theory
2	level	71.7	0.000342	0.000347	0.000328
4	level	58.6	0.000244	0.000246	0.000218
7	level	43.7	0.000202	0.000224	0.000205
8	level	43.1	0.000187	0.000198	- - -
9	level	42.7	0.000287	0.000286	- - -
11	climb	51.8	0.000359	0.000351	0.000322
15	auto-rotation 1260 ft./min.	37.7	-0.000008	-0.000008	-0.000016

Run number two is the only flight listed above in which tip stall was encountered. The calculated values for this run include a correction for tip stall. Δc_{d_o} was assumed equal to 0.08 for both the present theory and the blade-element theory for run number two. For this run, Equation 104 gives $c_{\ell_{tip}} = 1.415$. This value is in excess

of the assumed $\alpha_{\ell_m} = 1.2$ indicating tip stall. An $\alpha_s = 0.682$ was calculated from Equation 95. Tuft pictures in (11) indicate stall around $\alpha_s = 0.7$. Analysis of the low speed level runs, numbers seven, eight and nine, indicate the possibility of experimental error in determining the data for run seven.

Rotor torque coefficients for hovering flight calculated utilizing the charts and equations herein are compared below with data measured from a helicopter rotor mounted on a test stand and presented in (12). Data is for a Reynolds number of 2.82×10^6.

	Experimental	Present Theory
$\bar{C}_L$	C_Q	C_Q
0.395	0.000080	0.000087
0.591	0.000179	0.000184
0.677	0.000112	0.000120

The rotor torque coefficients calculated from the present theory are based on δ_0 equals $\mathcal{E}$ equals 0.008. Values of the rotor torque coefficient calculated from the theory herein are higher than the experimental as they probably should be since the rotor tested on the tower was operating in some slight ground effect.

CHAPTER IV

CONCLUSIONS

1. The equations developed in this study, which are based upon a triangular distribution of induced velocity along the blade radii and a simplified circulation distribution and force equilibrium, appear to afford good agreement with experimental data for both hovering and forward flight.

2. The use of the charts for obtaining certain parameters in conjunction with the equations affords a relatively rapid determination of the rotor torque coefficient for a given flight condition.

3. The use of a separate term for the axial component of the flight path velocity permits the choice of a specific flight condition for helicopter performance estimation.

4. Since the equations are in closed form and relatively brief, it appears that they may be useful in the determination of the optimum values of the rotor parameters for a given flight mission.

APPENDIX

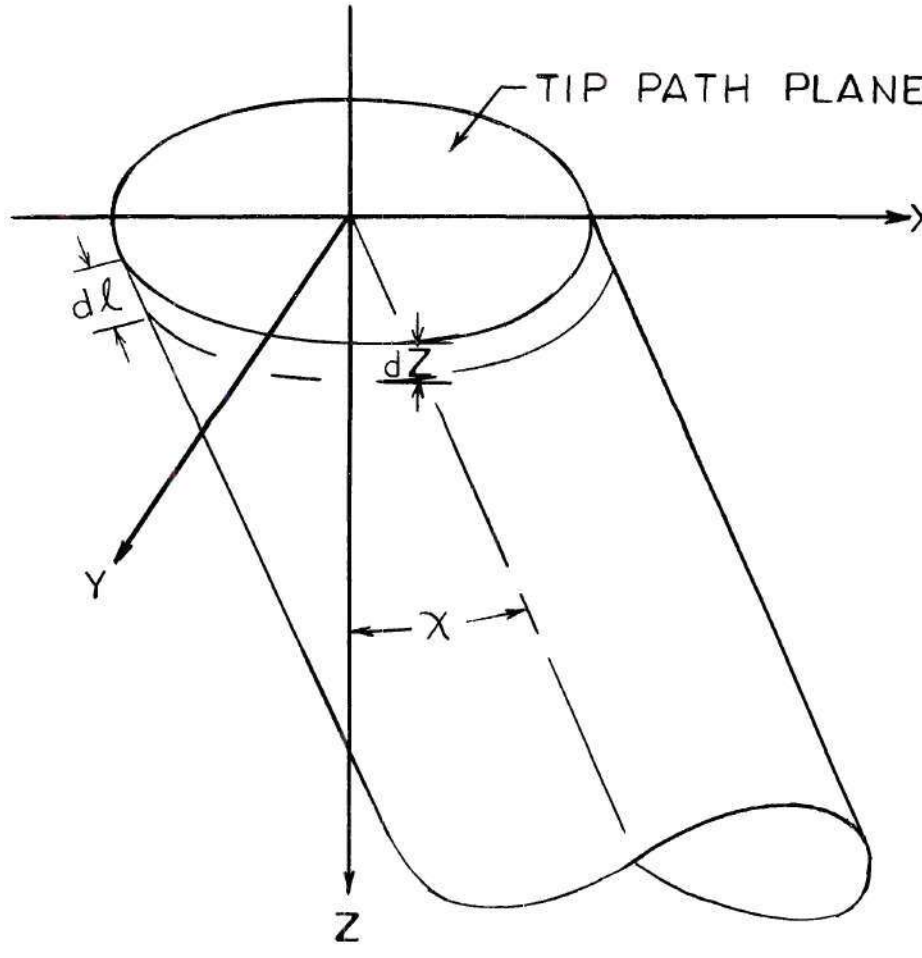

Figure 1. Geometry of Wake

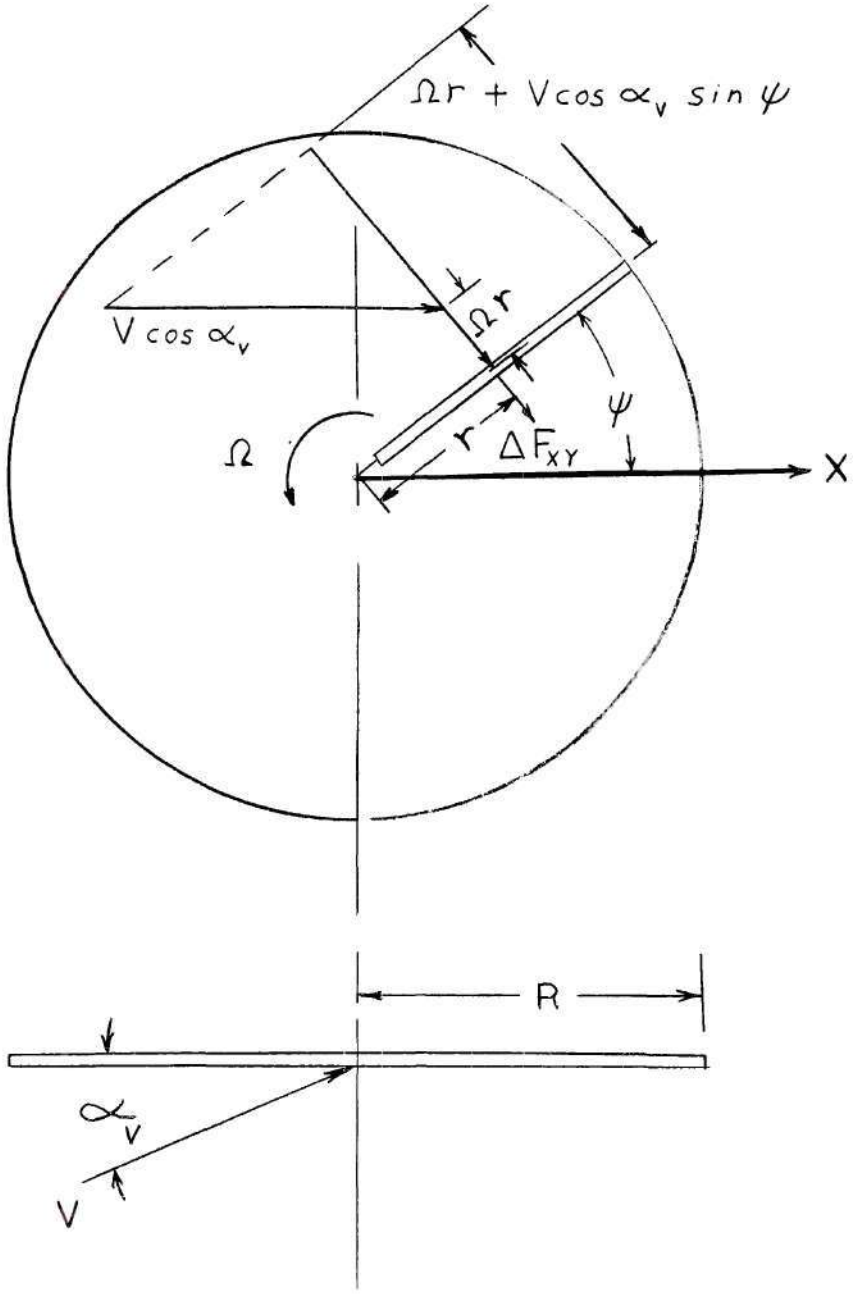

Figure 2. Velocity Components at Blade Element

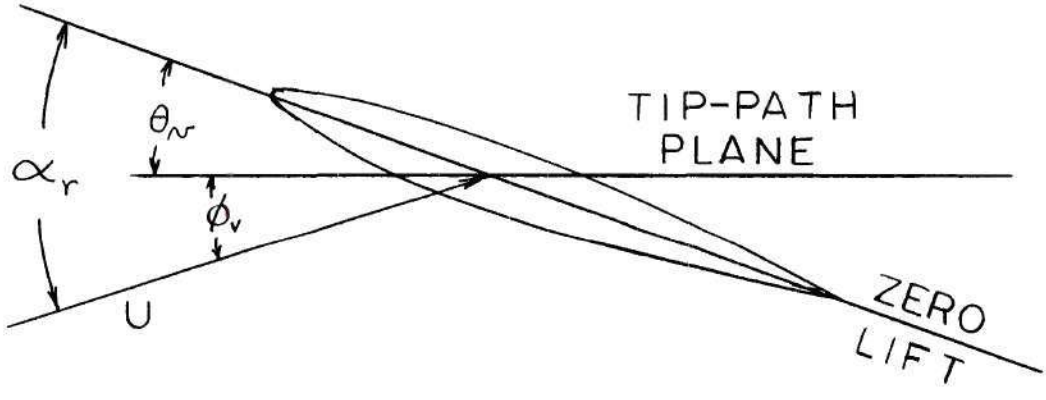

Figure 3. Geometry of Blade Element

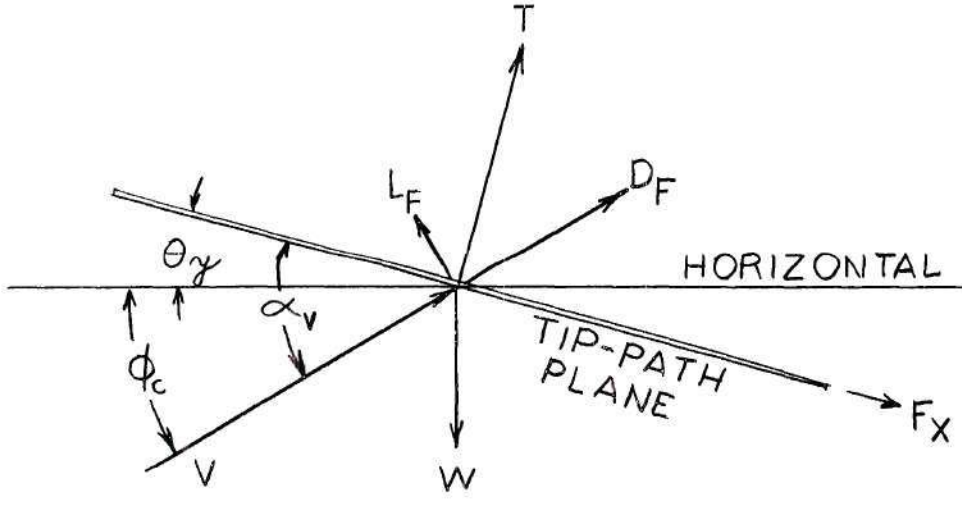

Figure 4. Forces on Rotor Hub

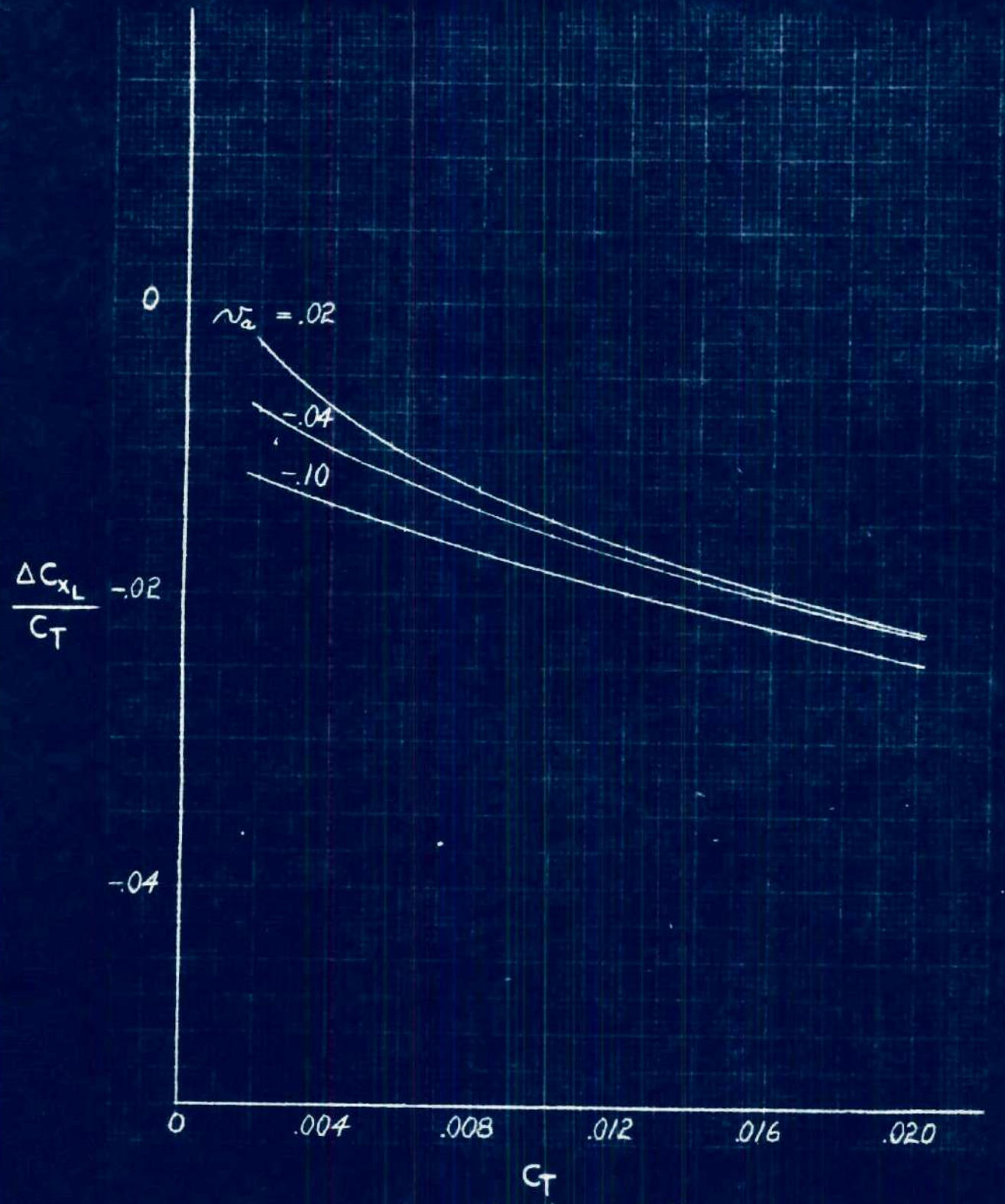

Figure 5 (a), $\mu = 0.05$
Rotor X-Force Due to Lift

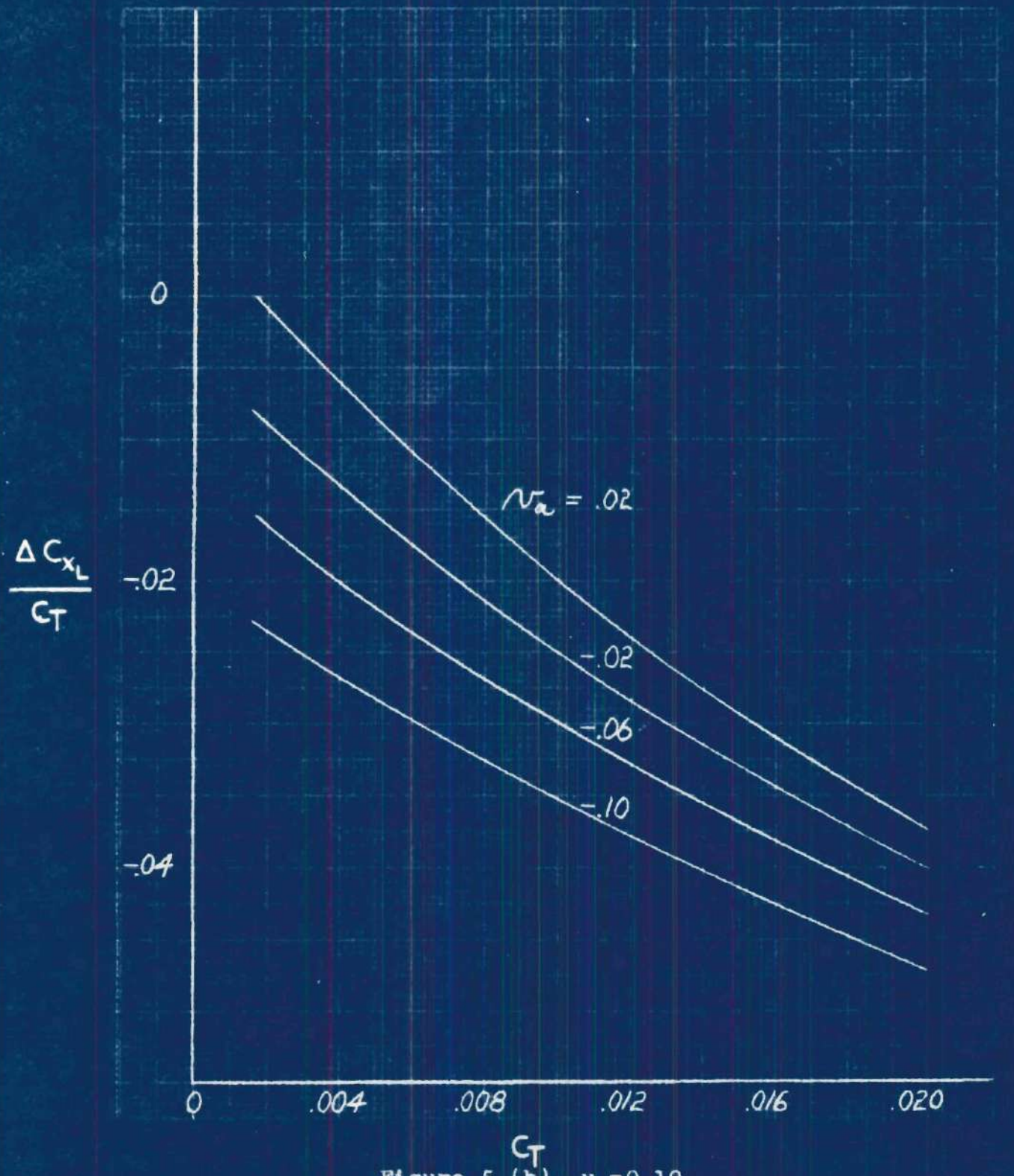

Figure 5 (b), μ_v=0.10

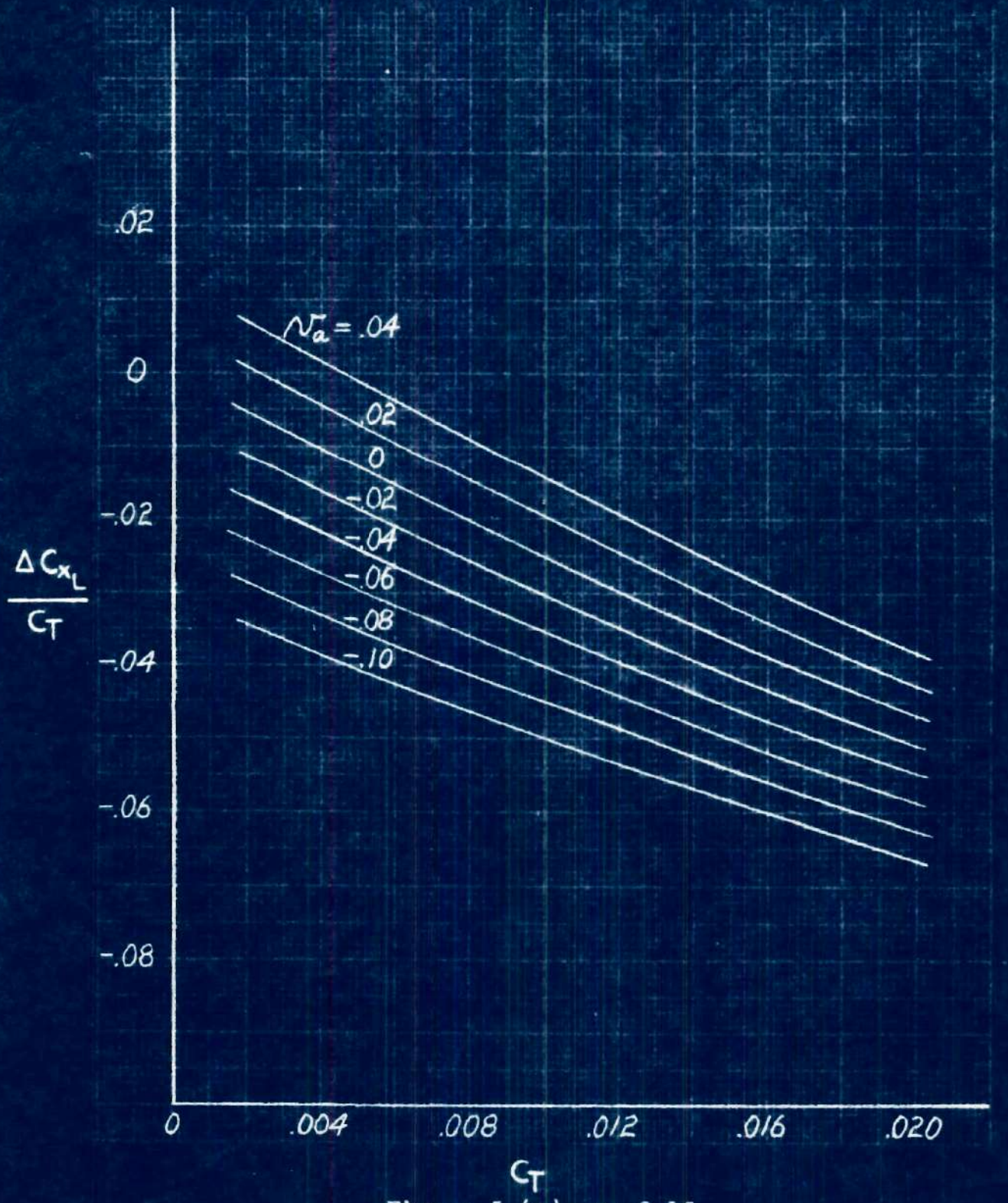

Figure 5 (c), μ_v=0.15

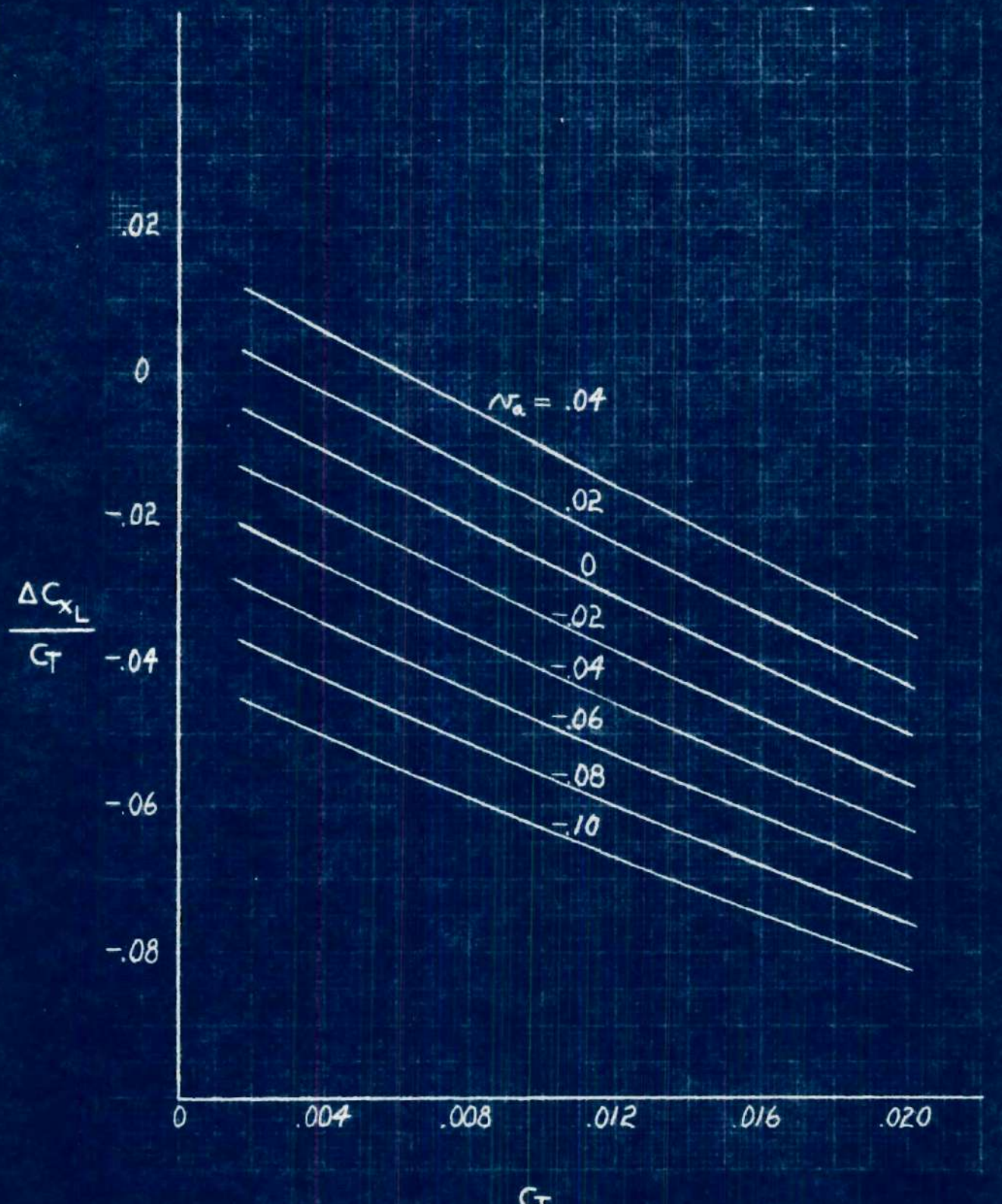

Figure 5 (d), $\mu_v = 0.20$

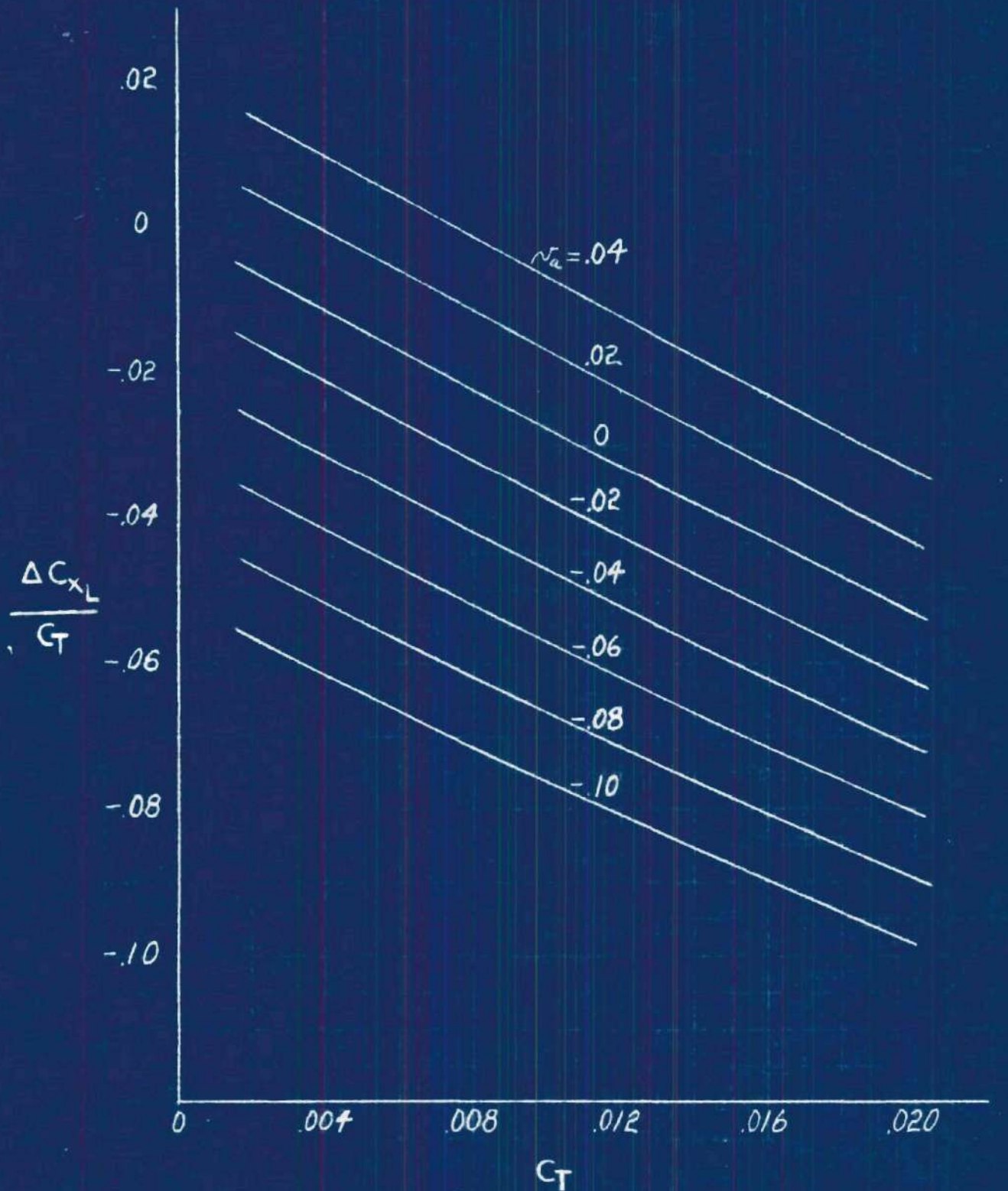

Figure 5 (e) $\mu_v = 0.25$

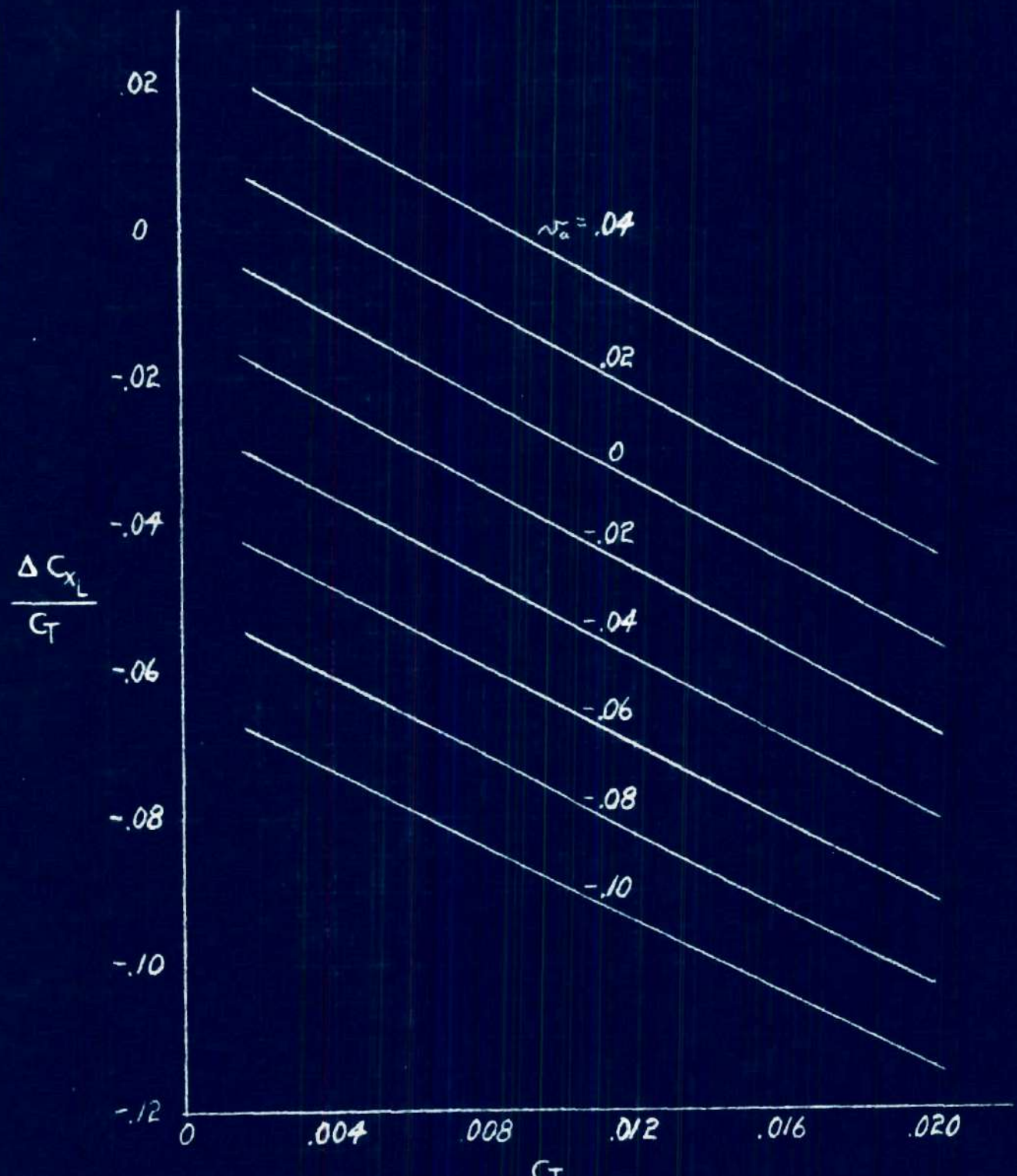

Figure 5 (f), $\mu_v = 0.30$

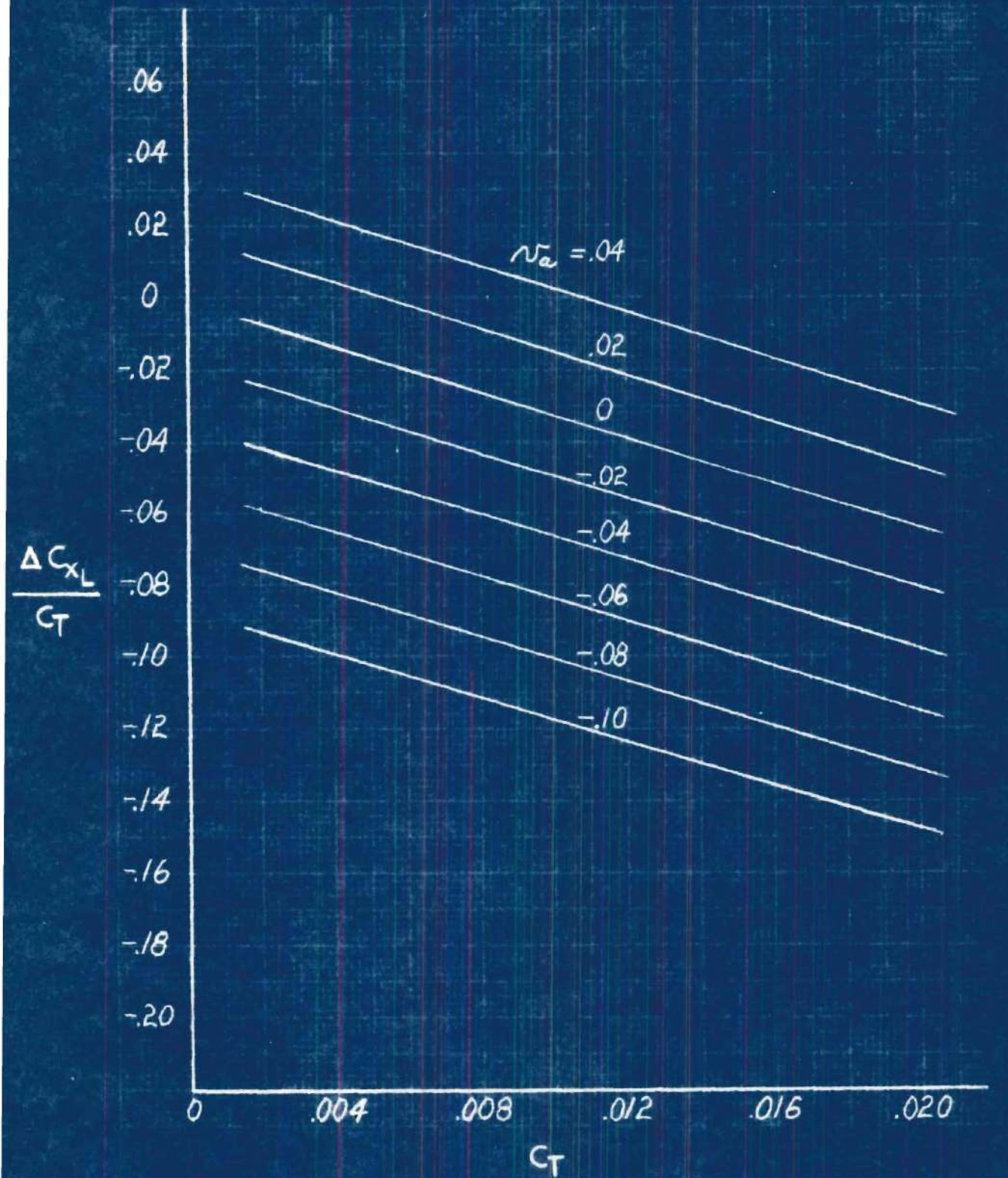

Figure 5 (g), μ_v=0.40

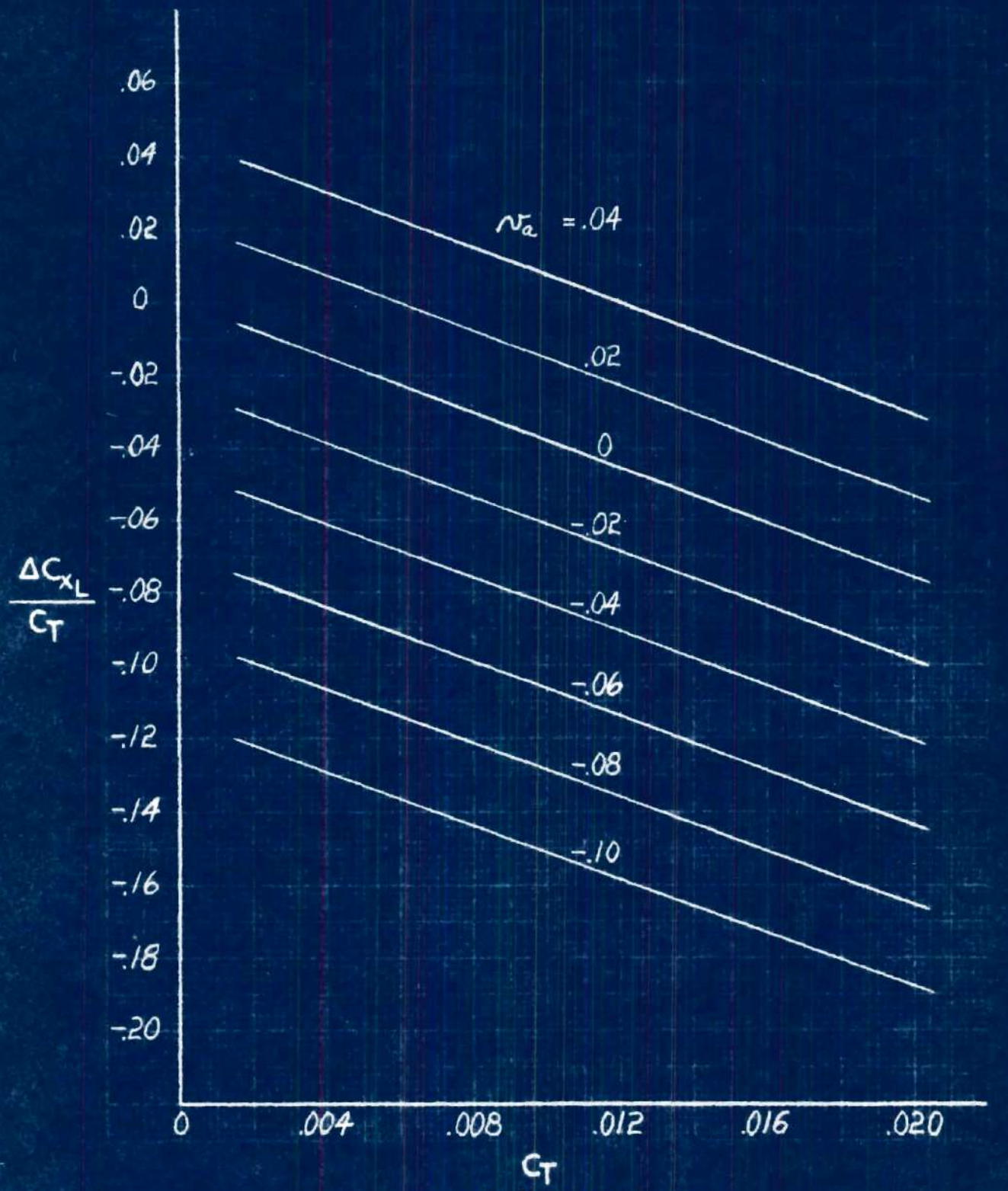

Figure 5 (h), $\mu_y = 0.50$

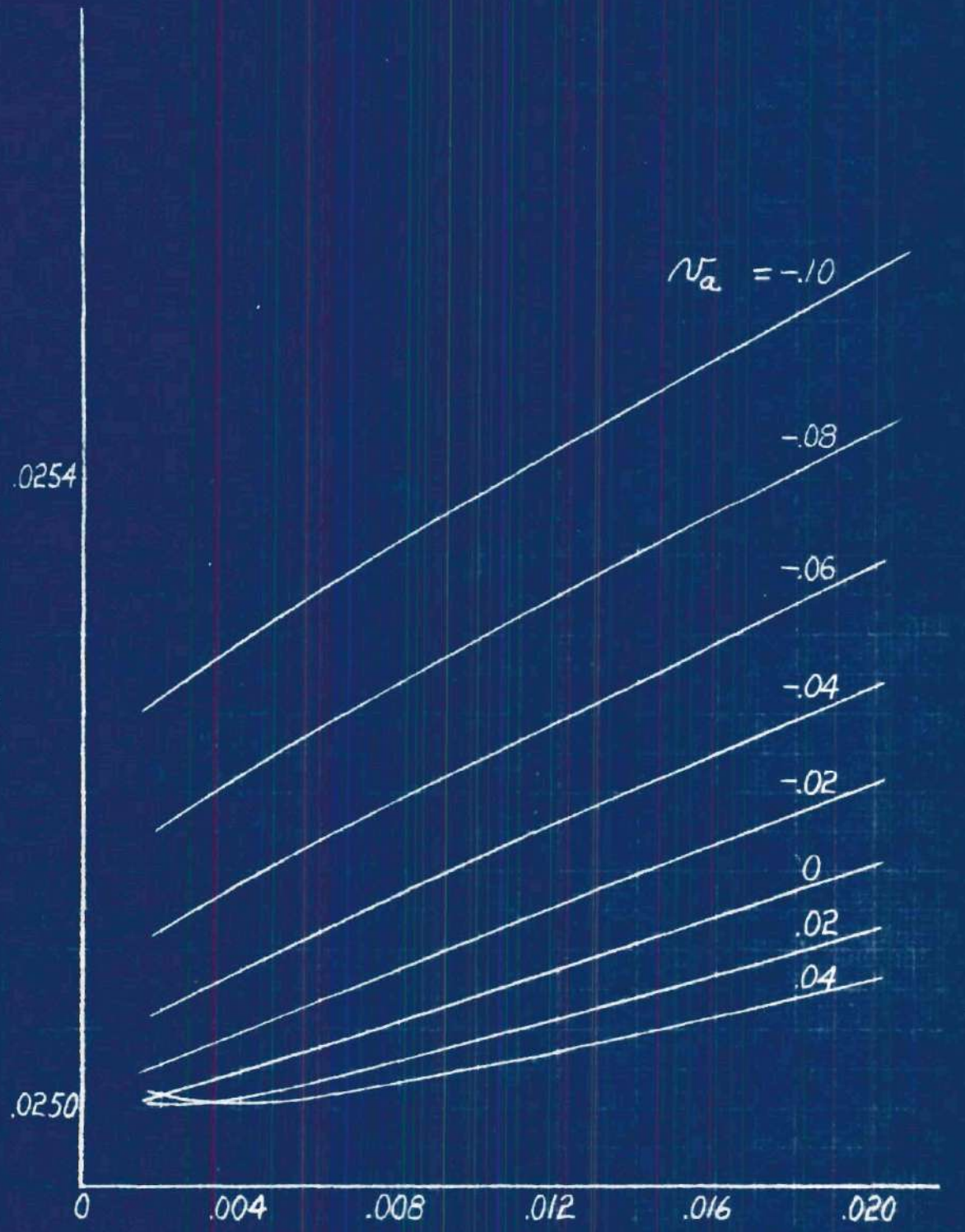

Figure 6 $\frac{C_T}{(a)}$, $\mu_v = 0.05$
Rotor X-Force Due to Constant Profile Drag

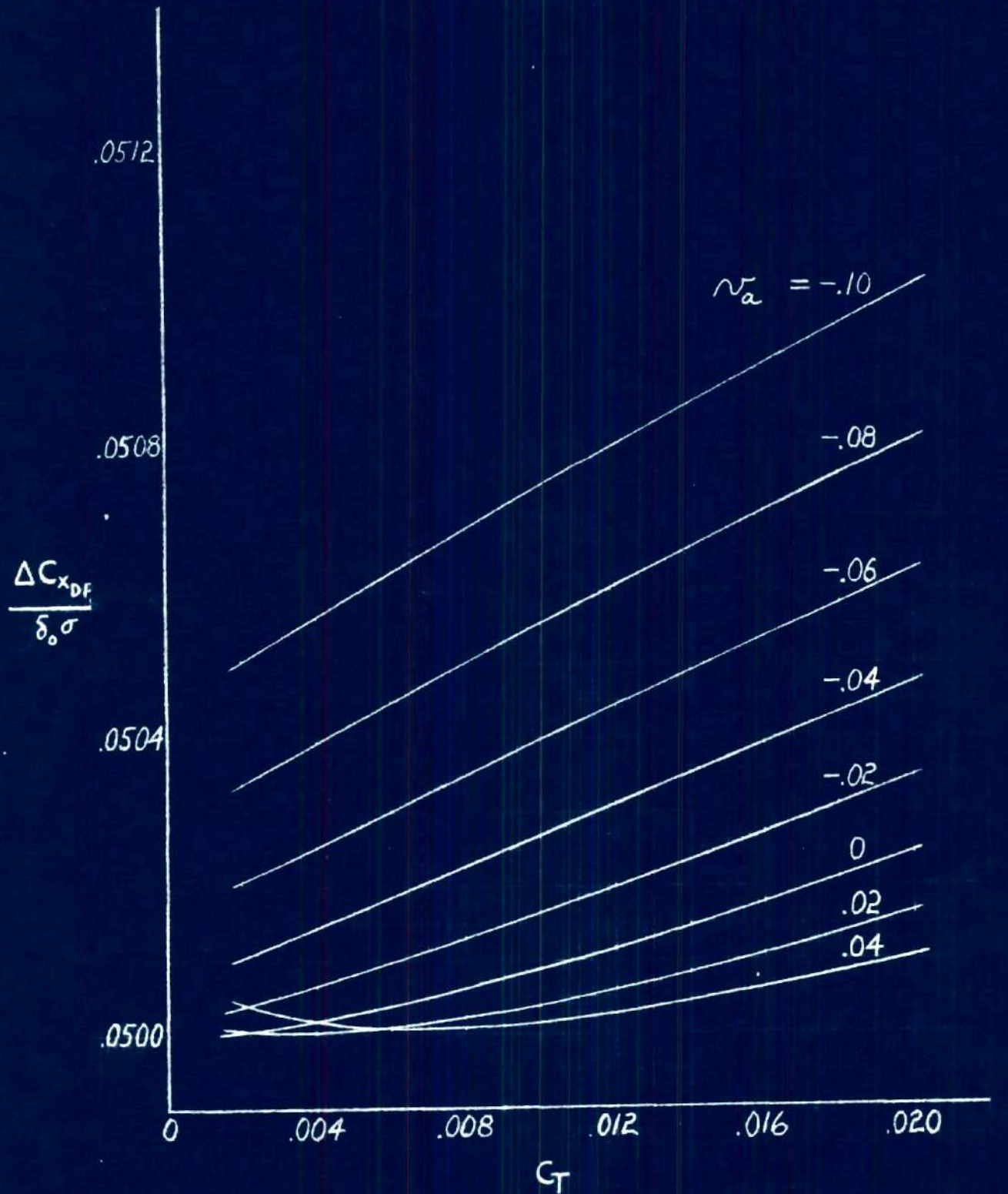

Figure 6 (b), $\mu_v = 0.10$

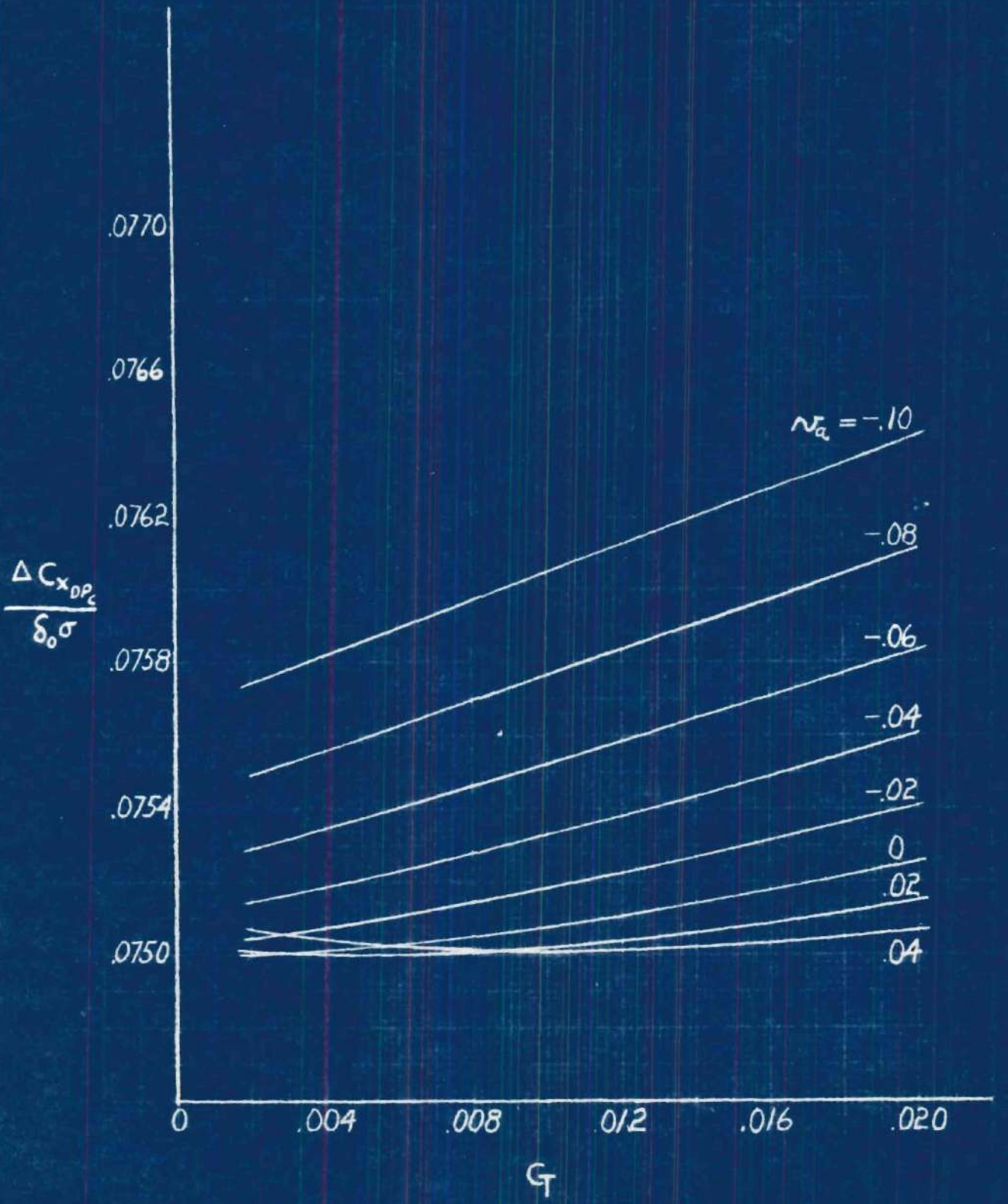

Figure 6 (c), $\mu_v = 0.15$

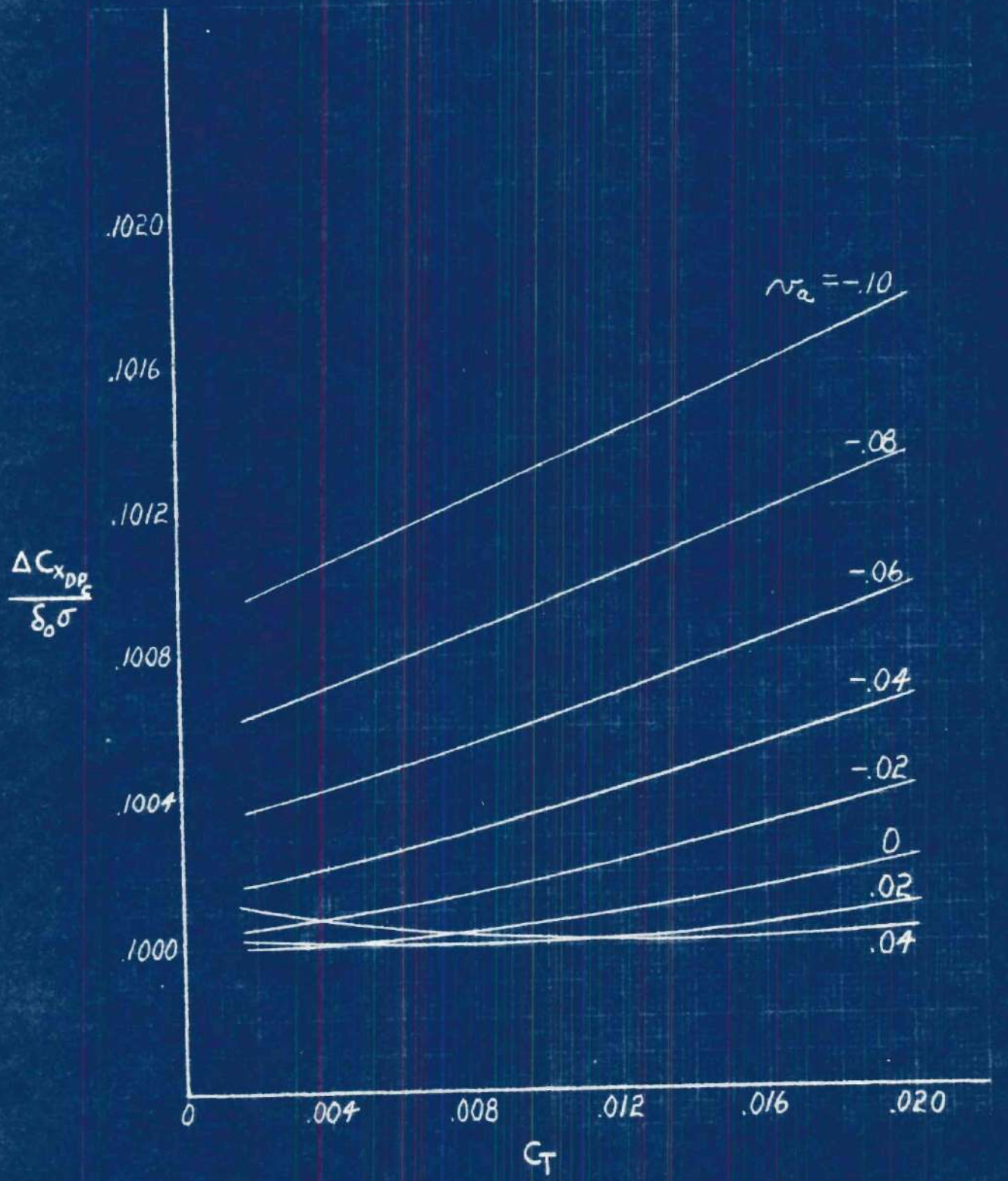

Figure 6 (d), $\mu_v = 0.20$

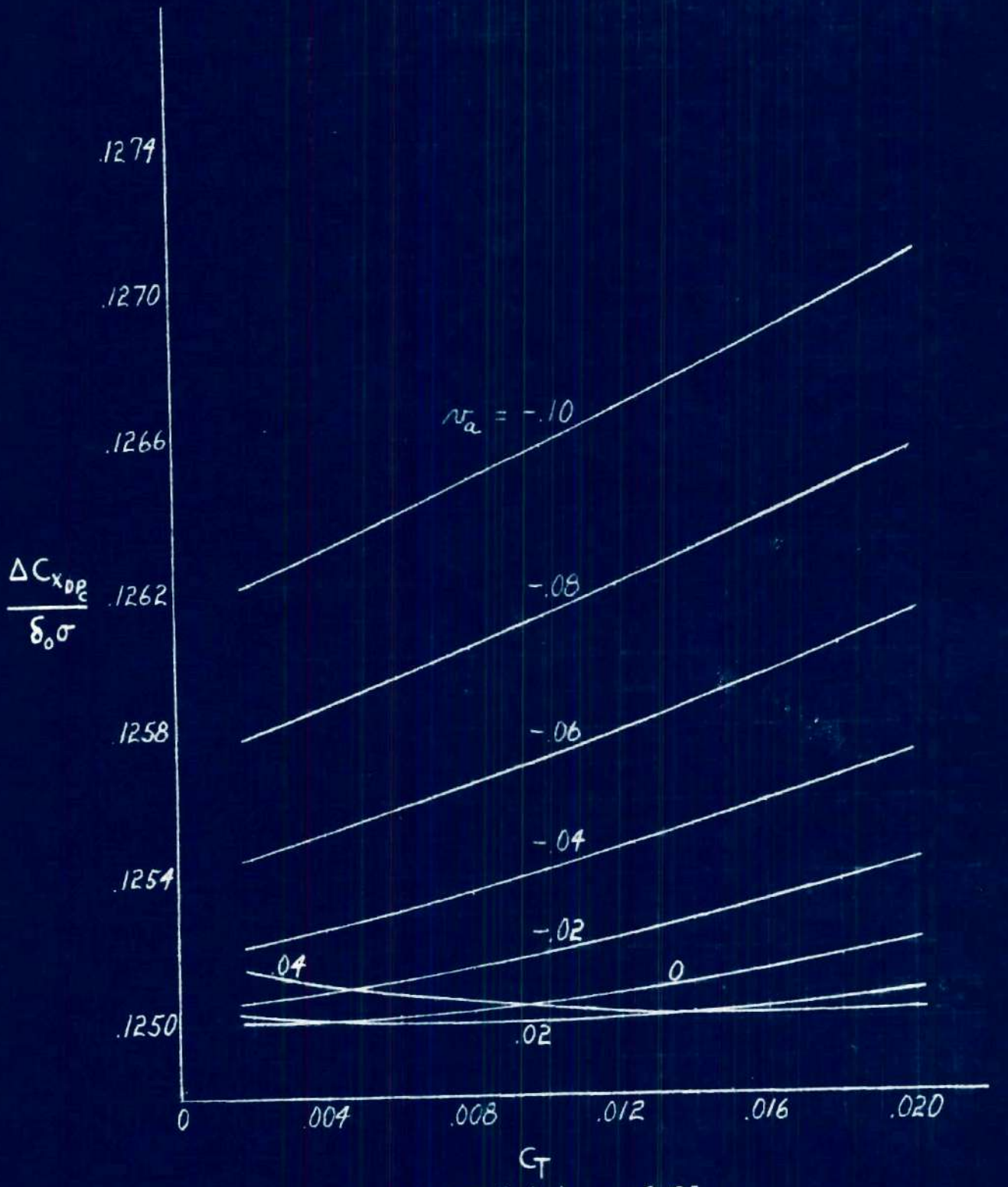

Figure 6 (e), $\mu_v = 0.25$

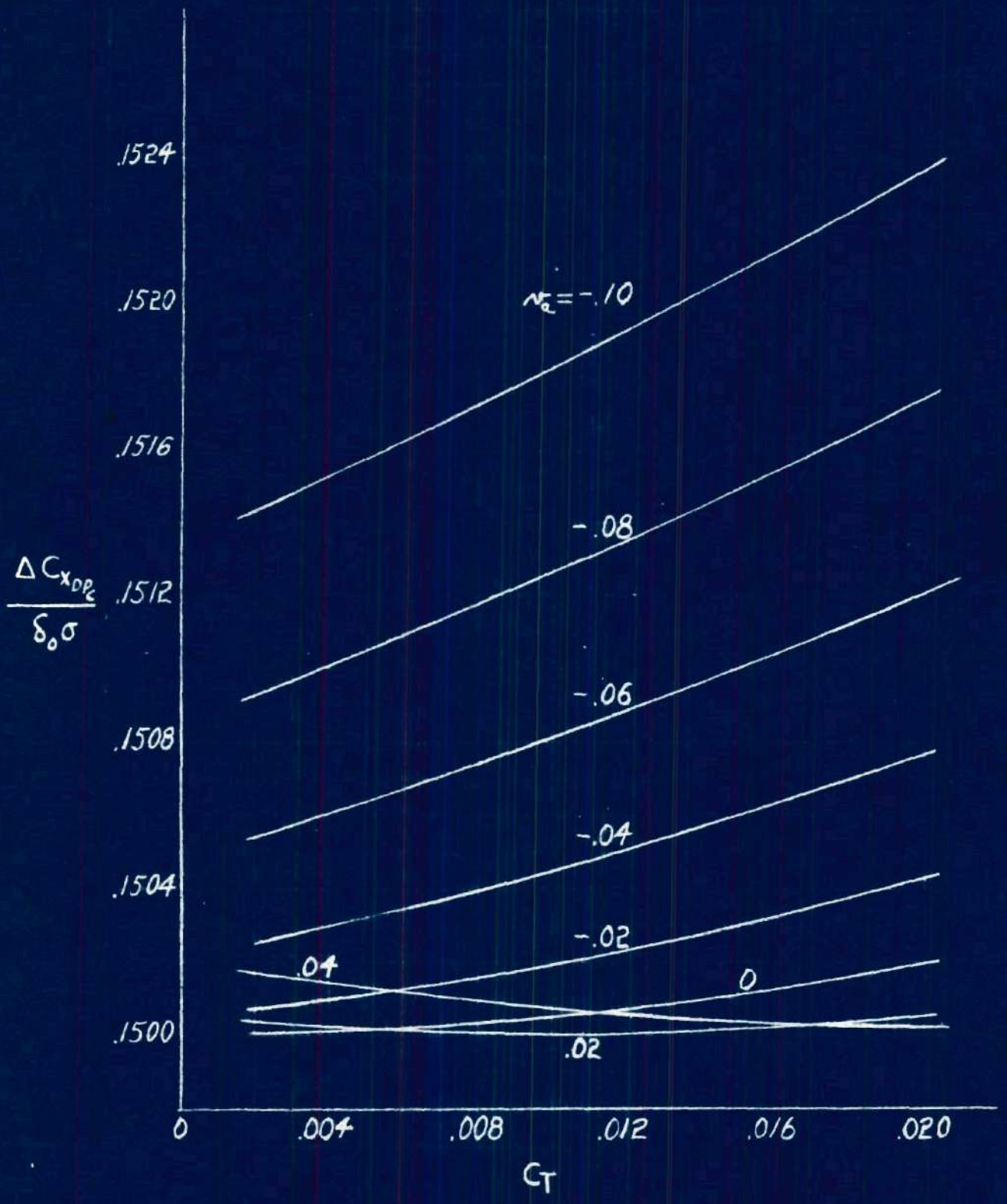

Figure 6 (f), $\mu_v = 0.30$

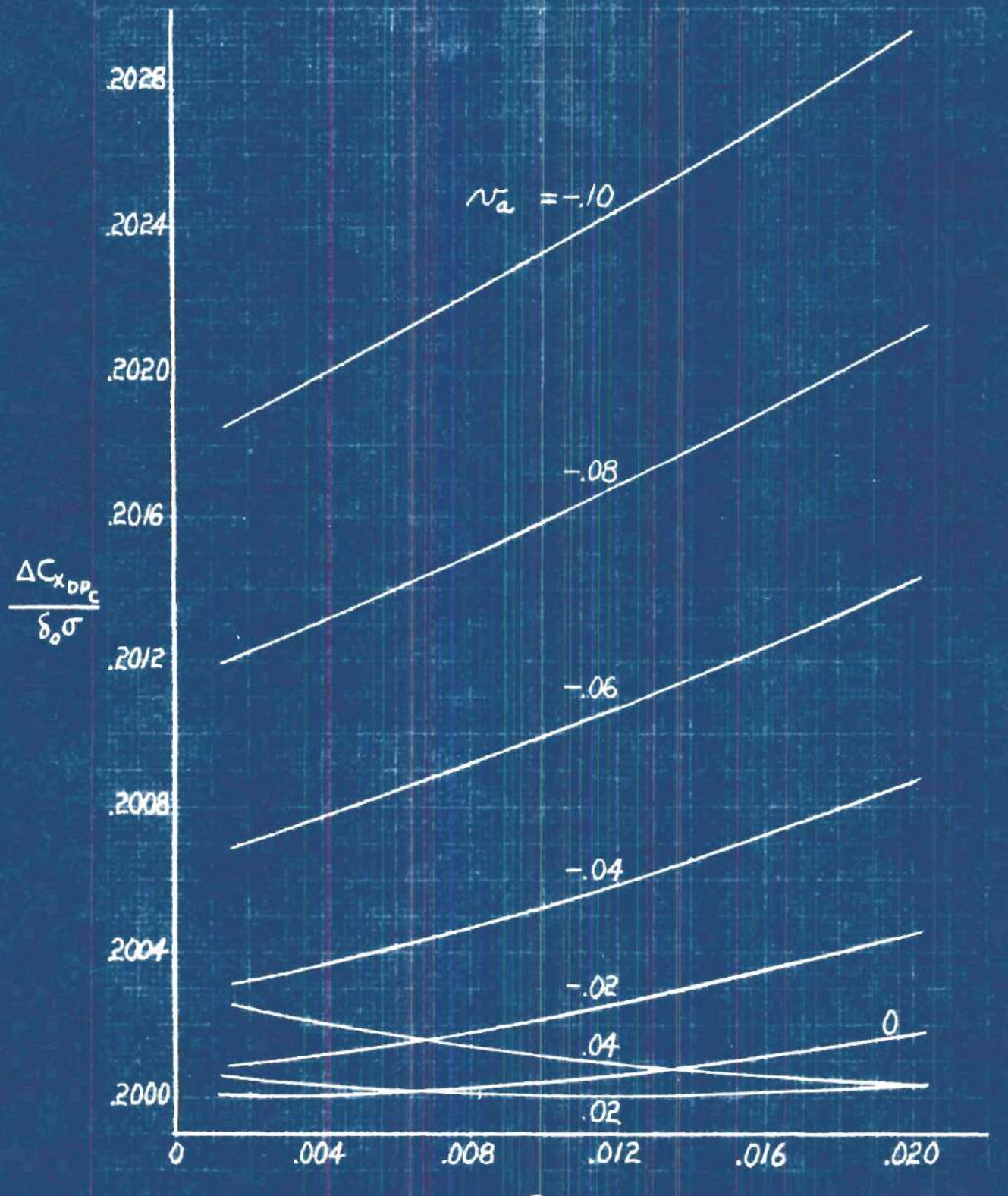

Figure 6 (g), $u_v = 0.40$

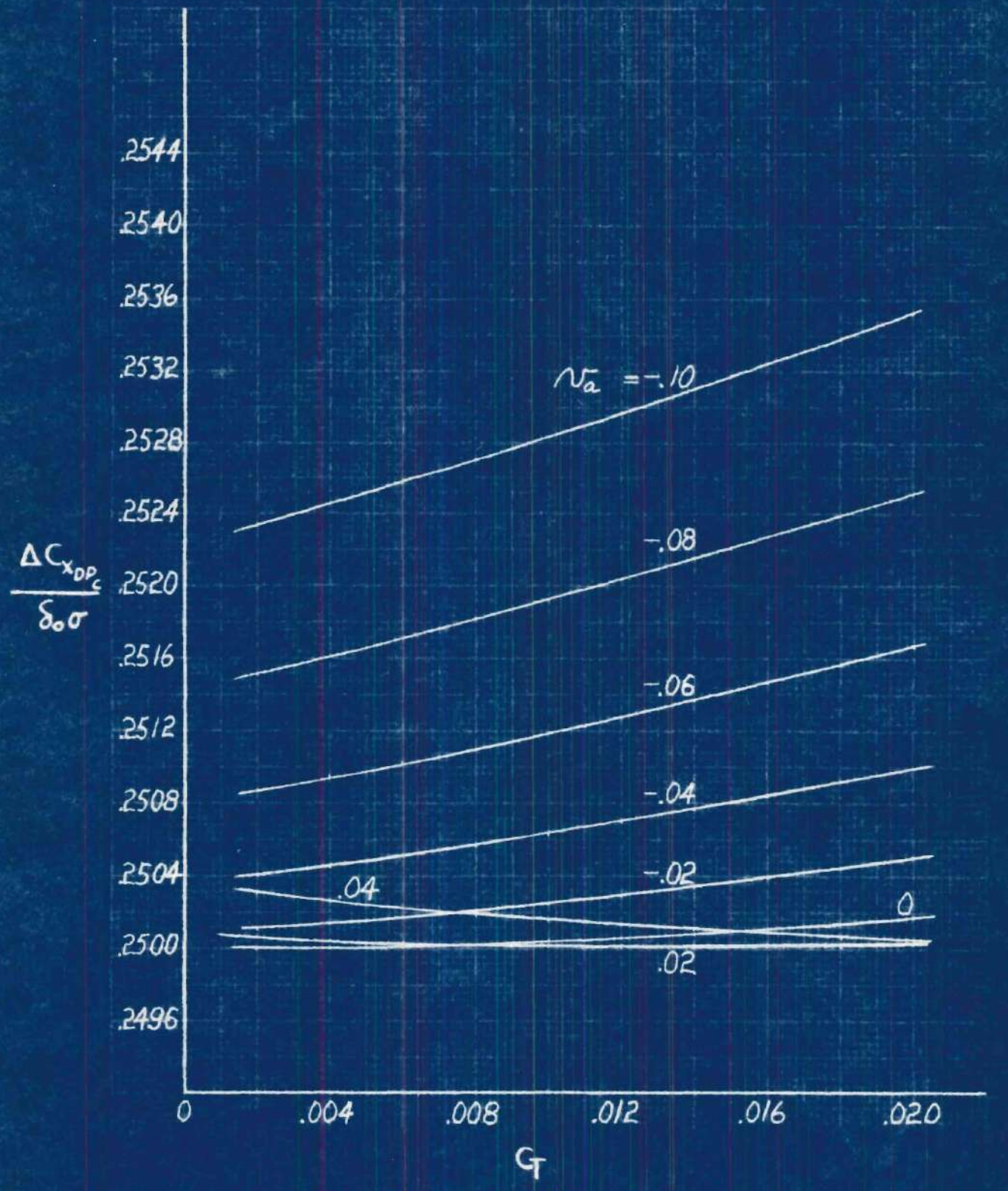

Figure 6 (h), $\mu_v = 0.50$

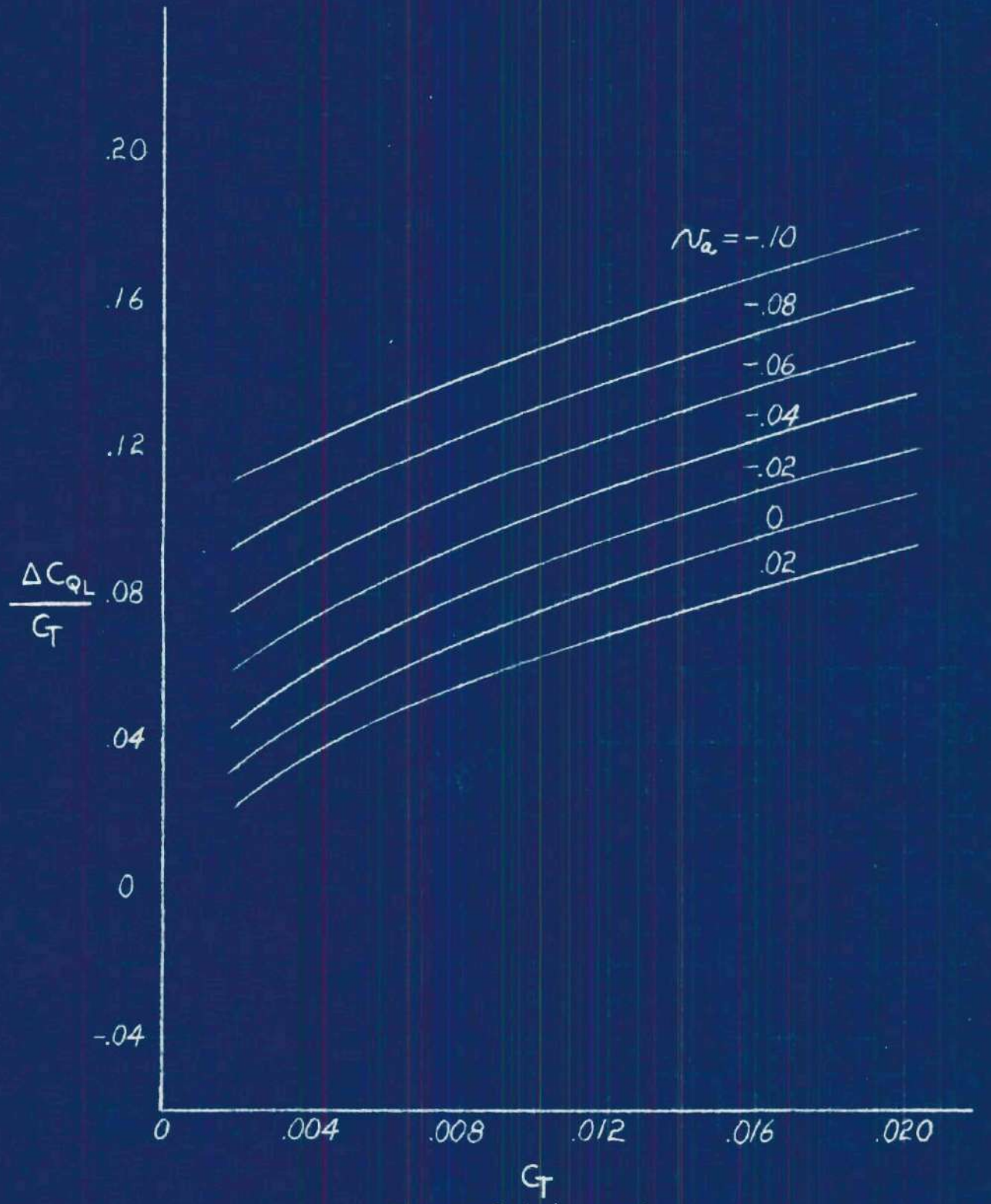

Figure 7 (a), $\mu_v = 0$.
Rotor Torque Due to Lift

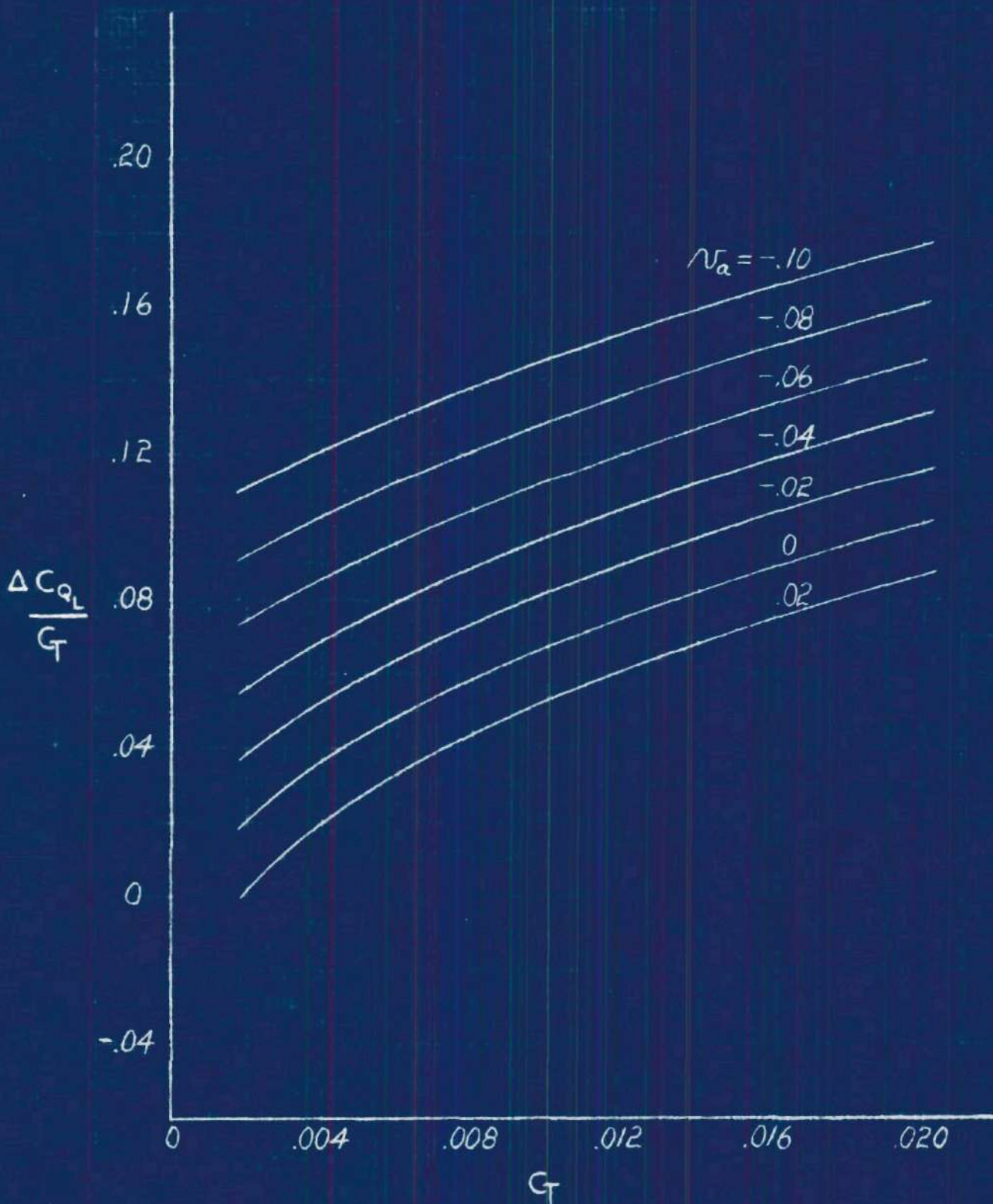

Figure 7 (b), $\mu_v = 0.05$

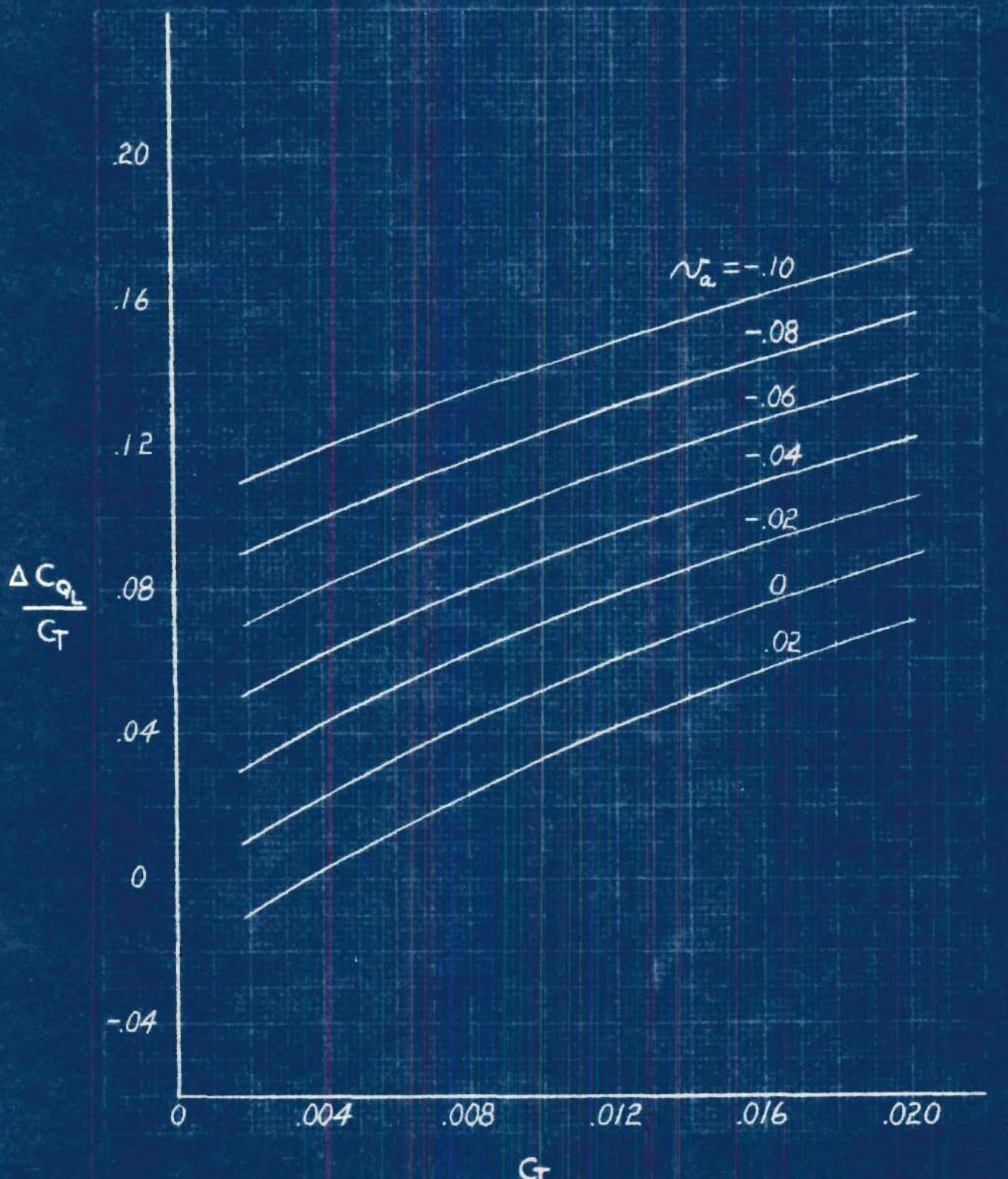

Figure 7 (c), $\mu_y = 0.10$

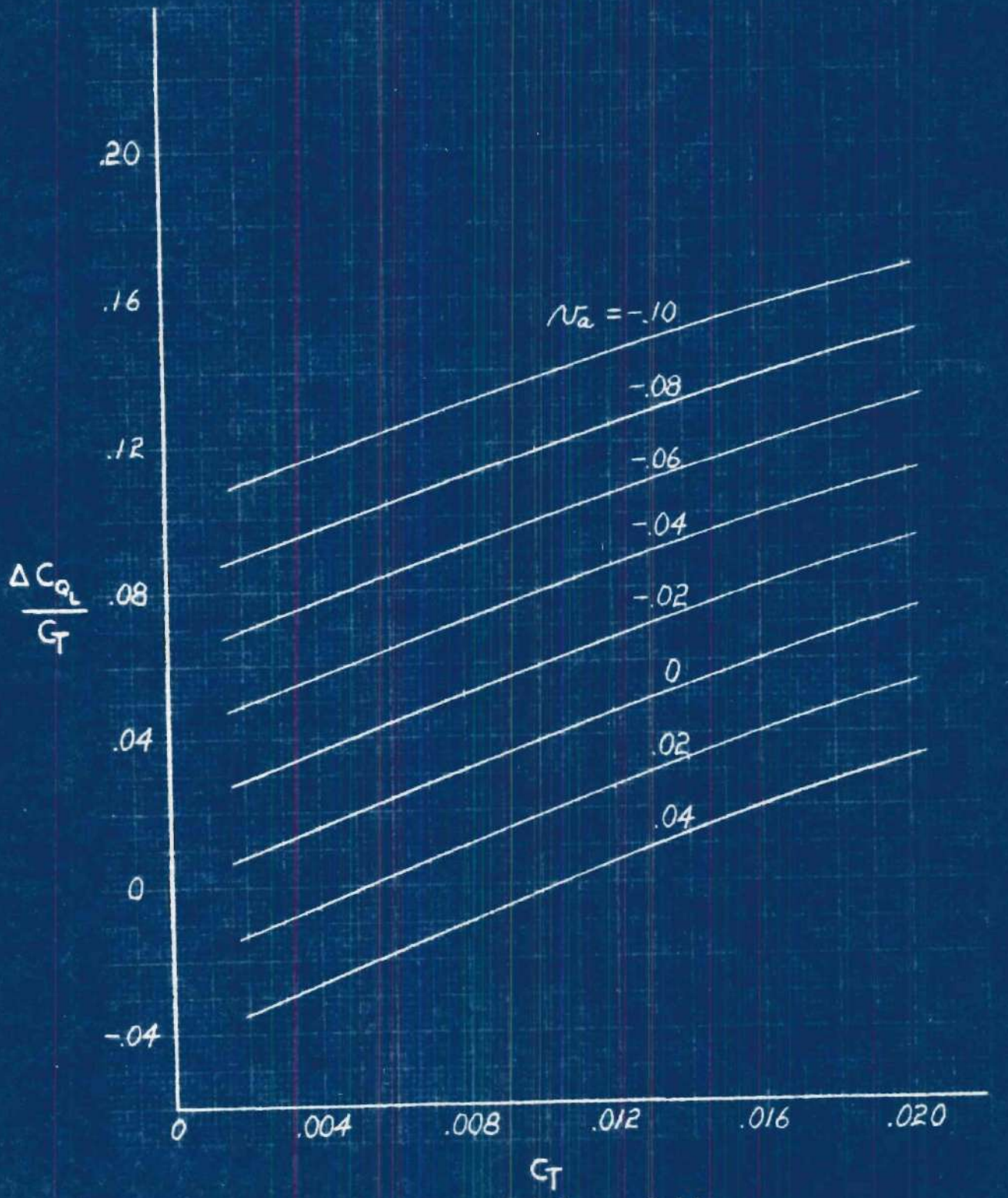

Figure 7 (d), $u_v = 0.15$

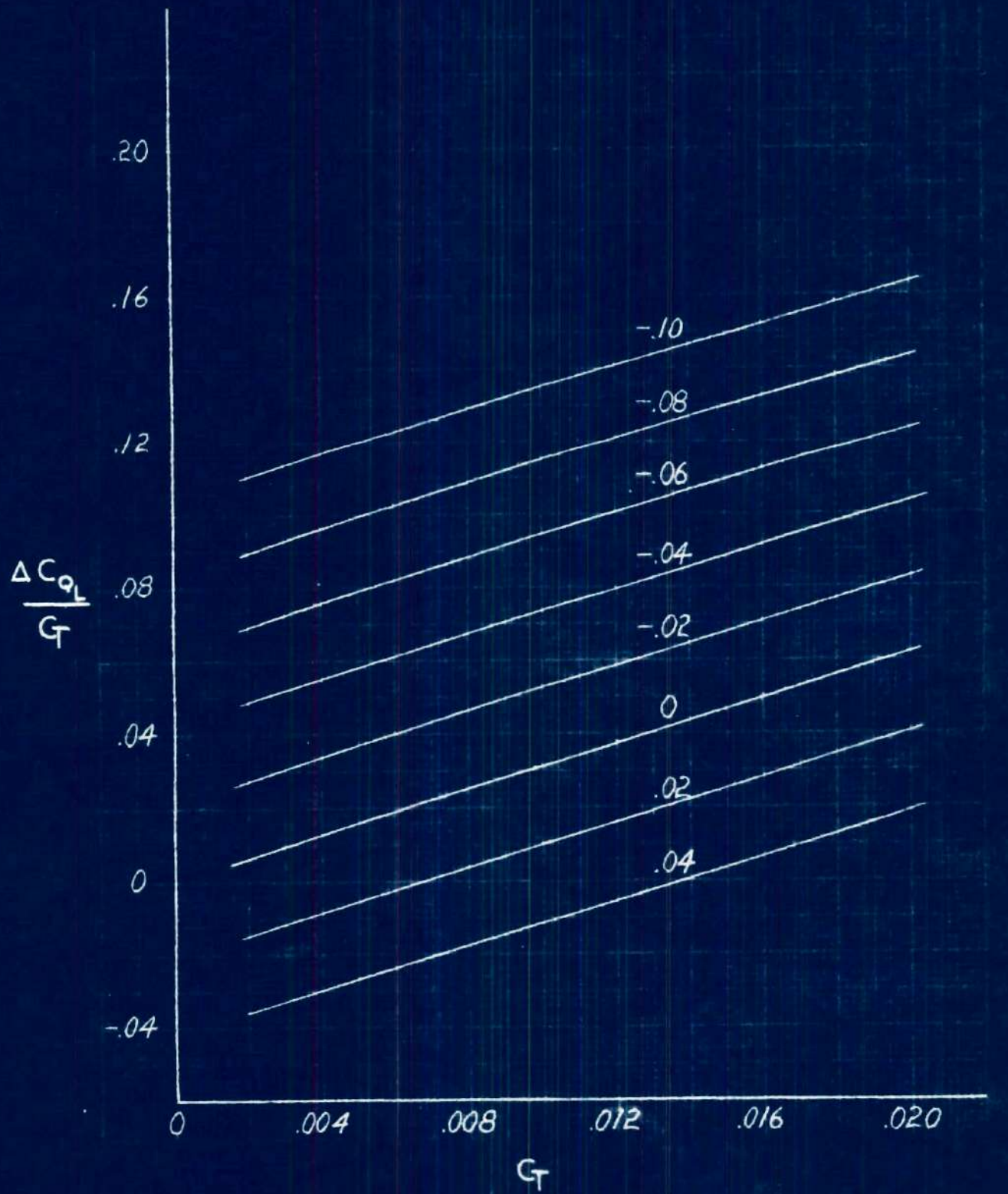

Figure 7 (e), $\mu_v = 0.20$

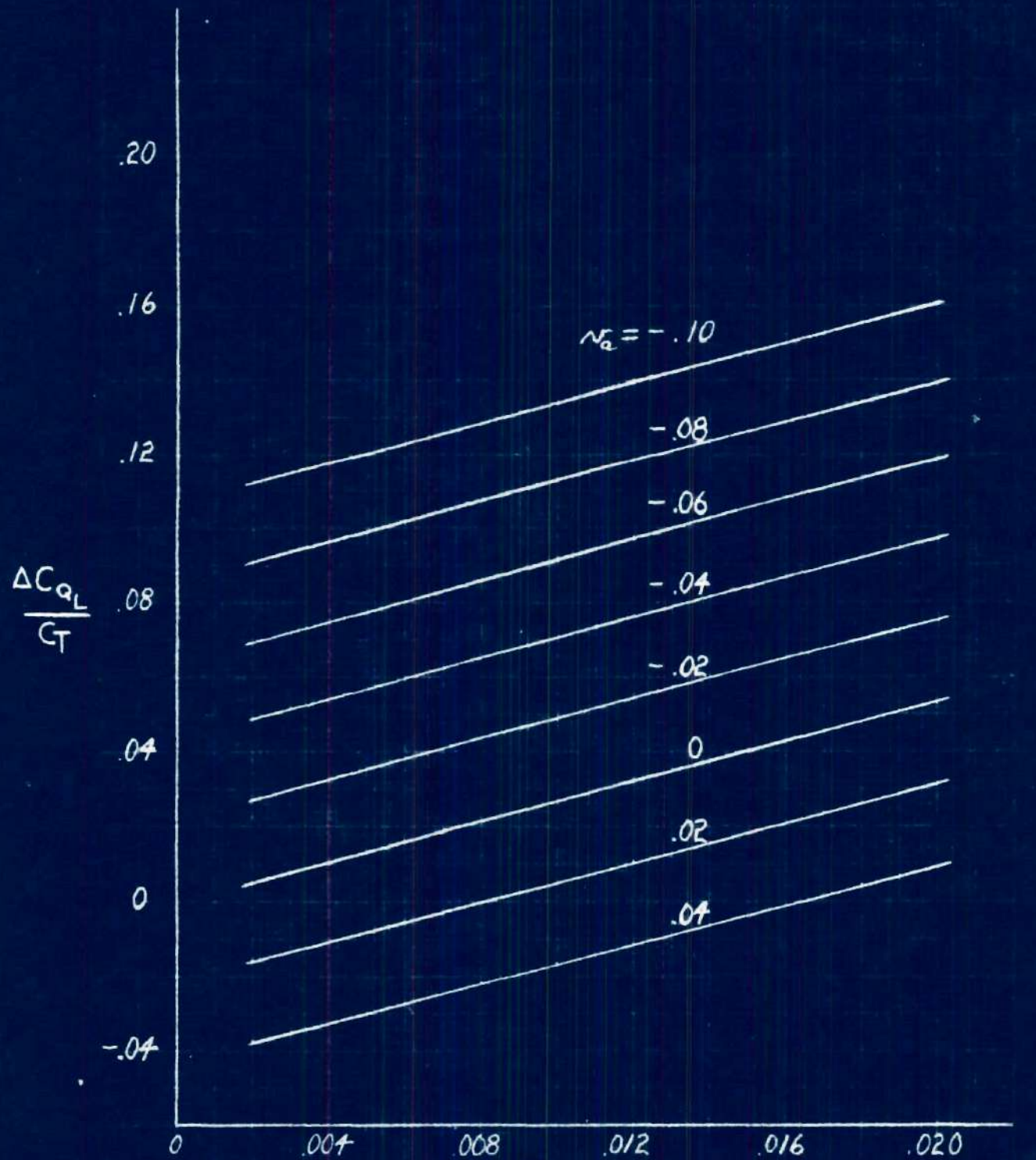

Figure 7 (f), μ_y=0.25

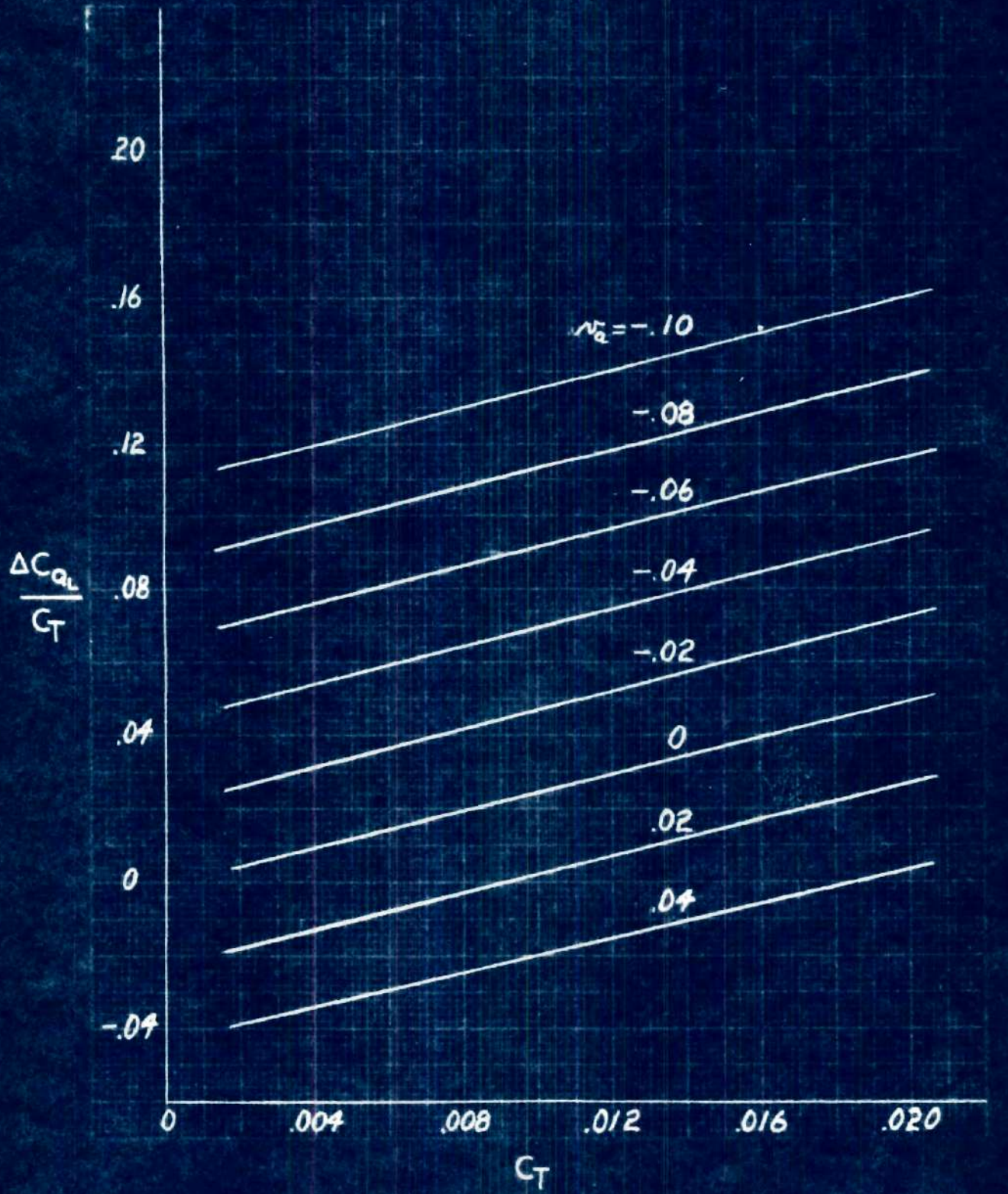

Figure 7 (g), $u_v = 0.30$

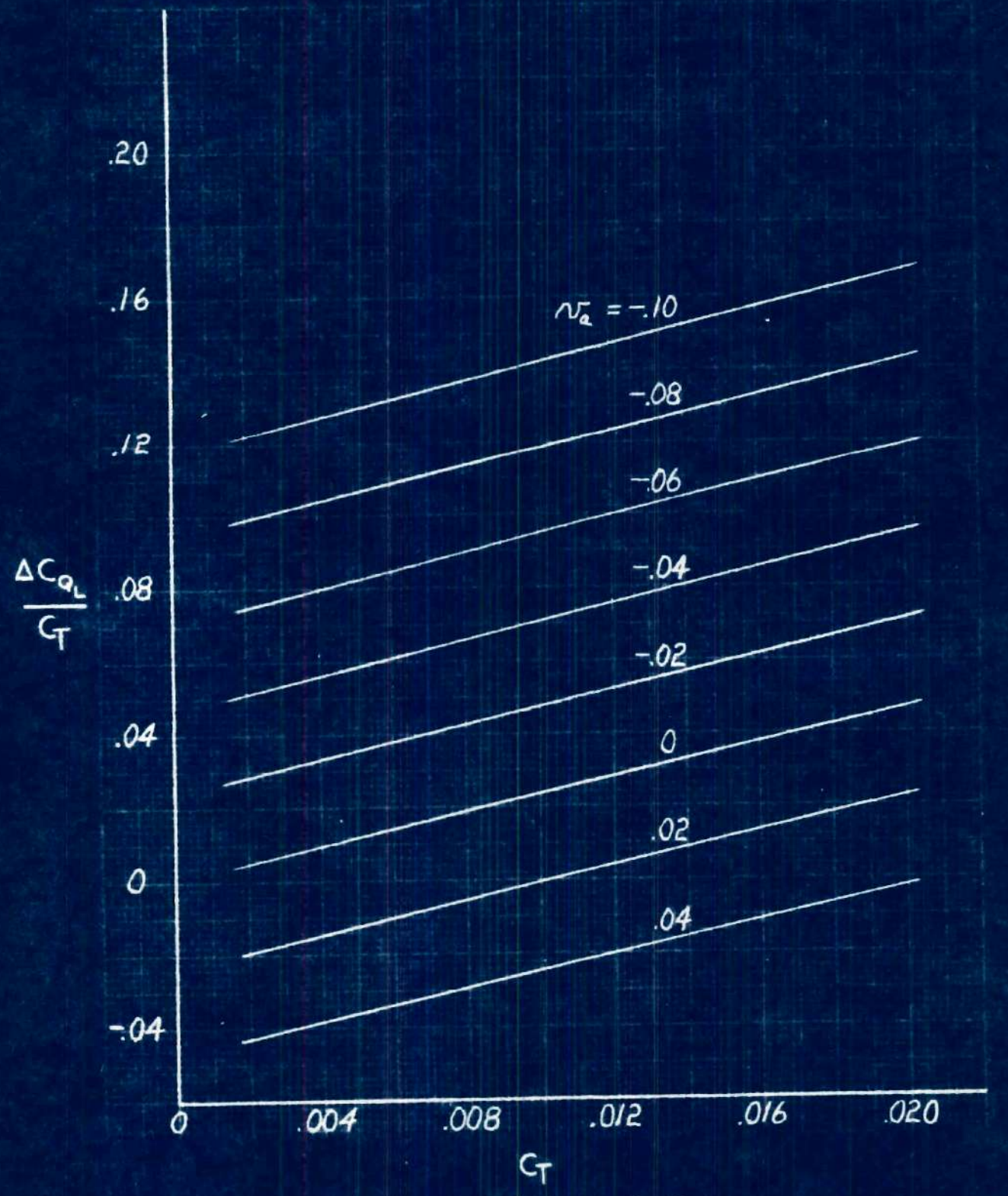

Figure 7 (h), $\mu_v = 0.40$

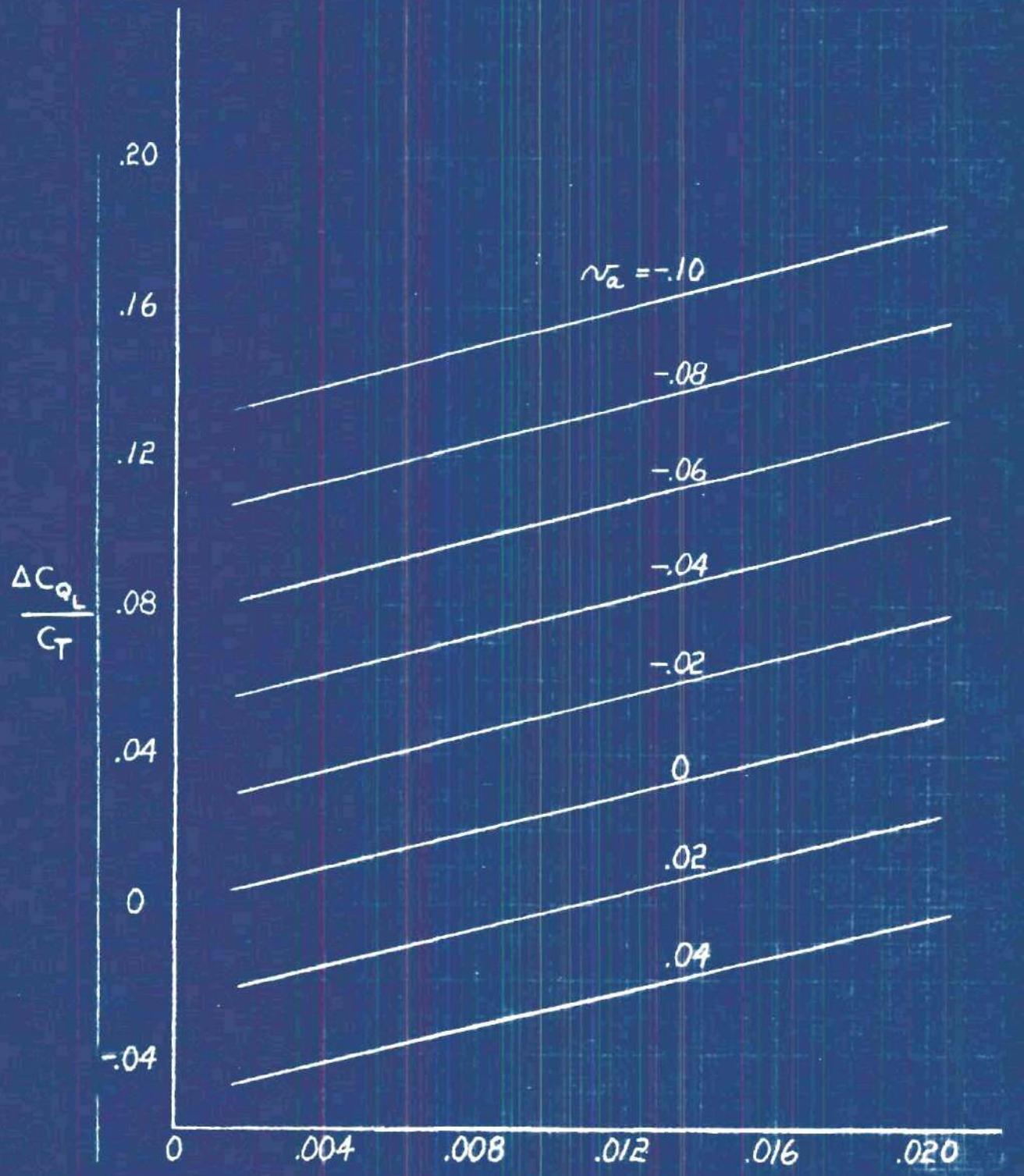

Figure 7 (i), μ=0.50

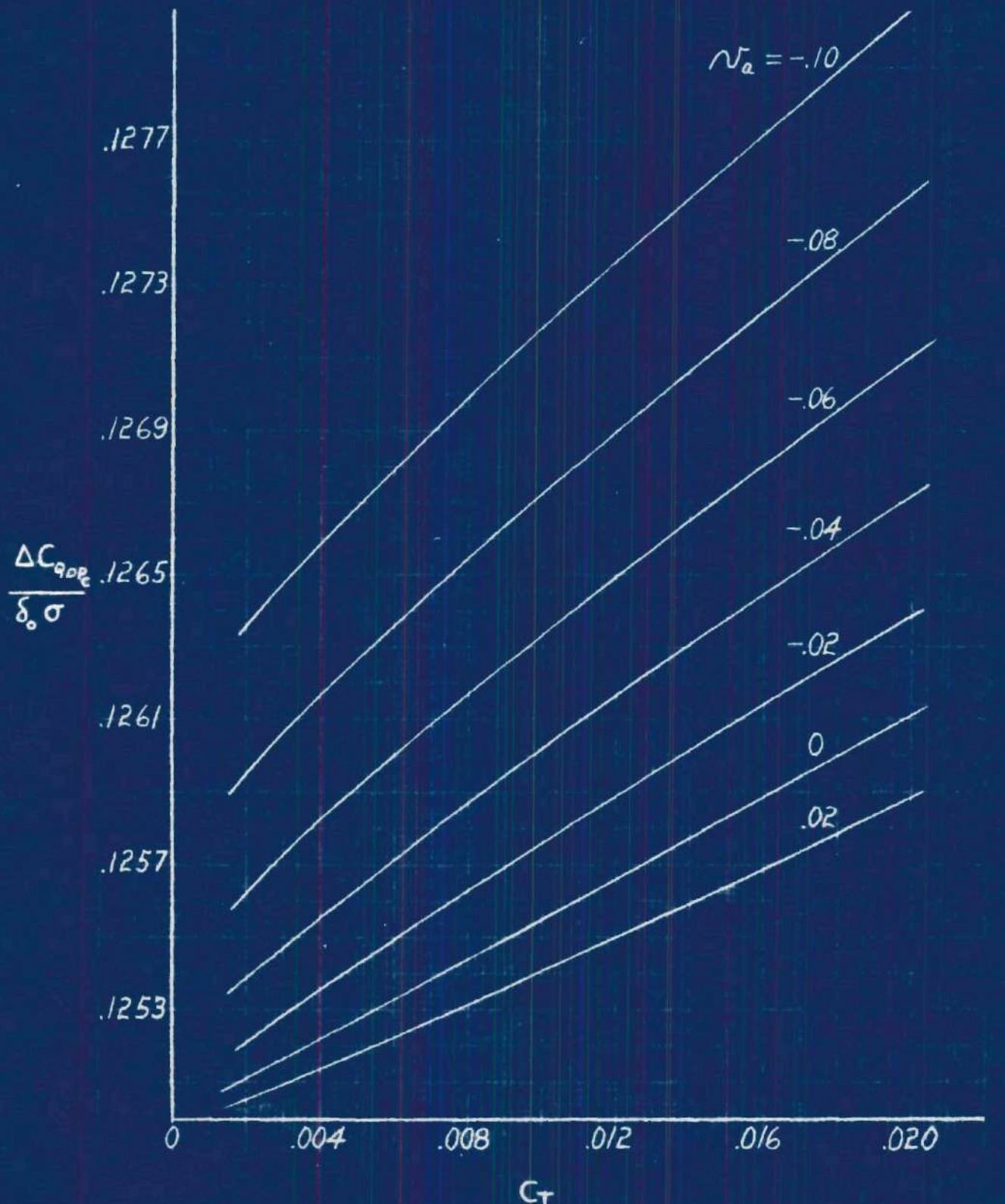

Figure 8 (a), $\mu_v = 0$.
Rotor Torque Due to Constant Profile Drag

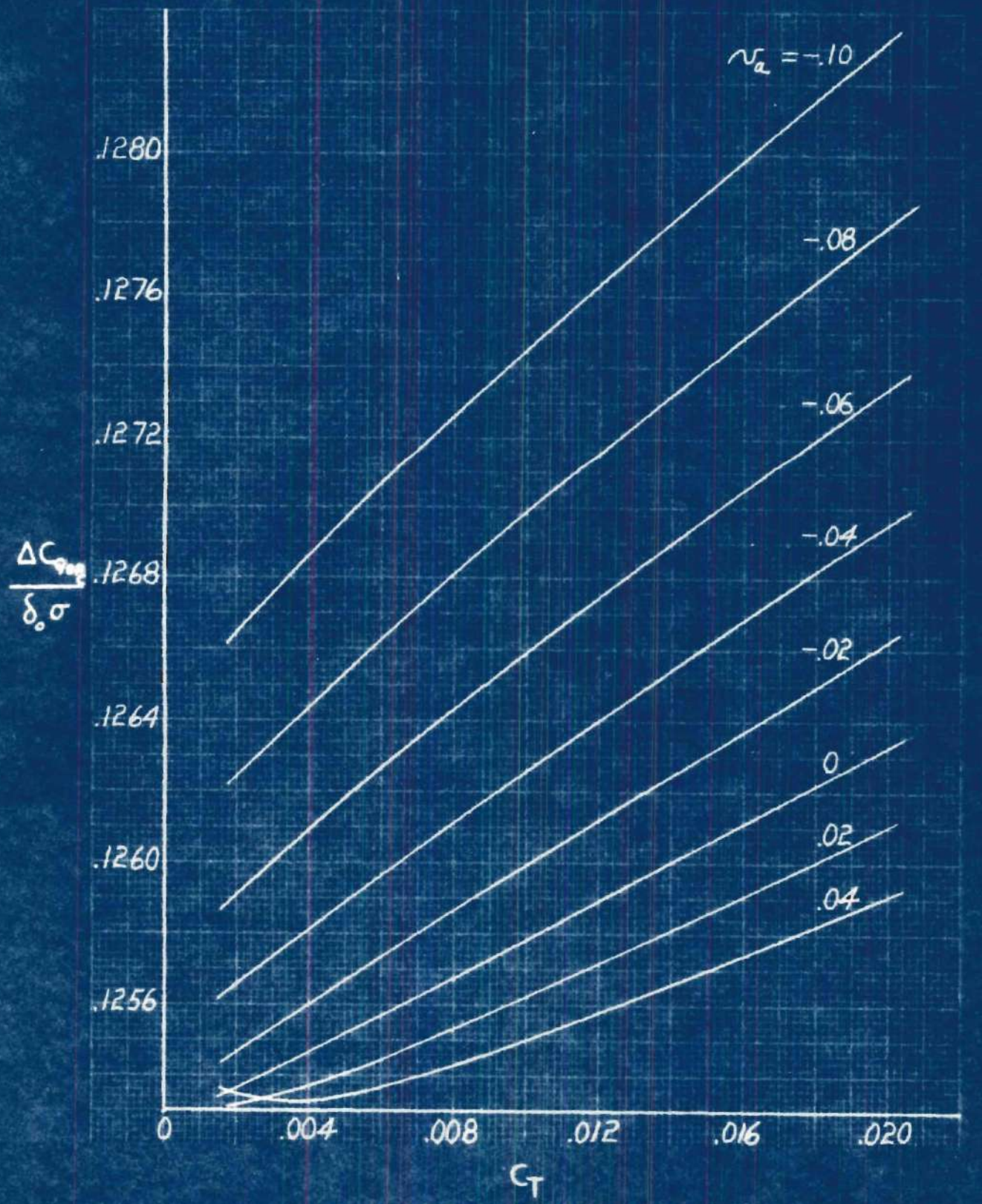

Figure 8 (b), $\mu_v = 0.05$

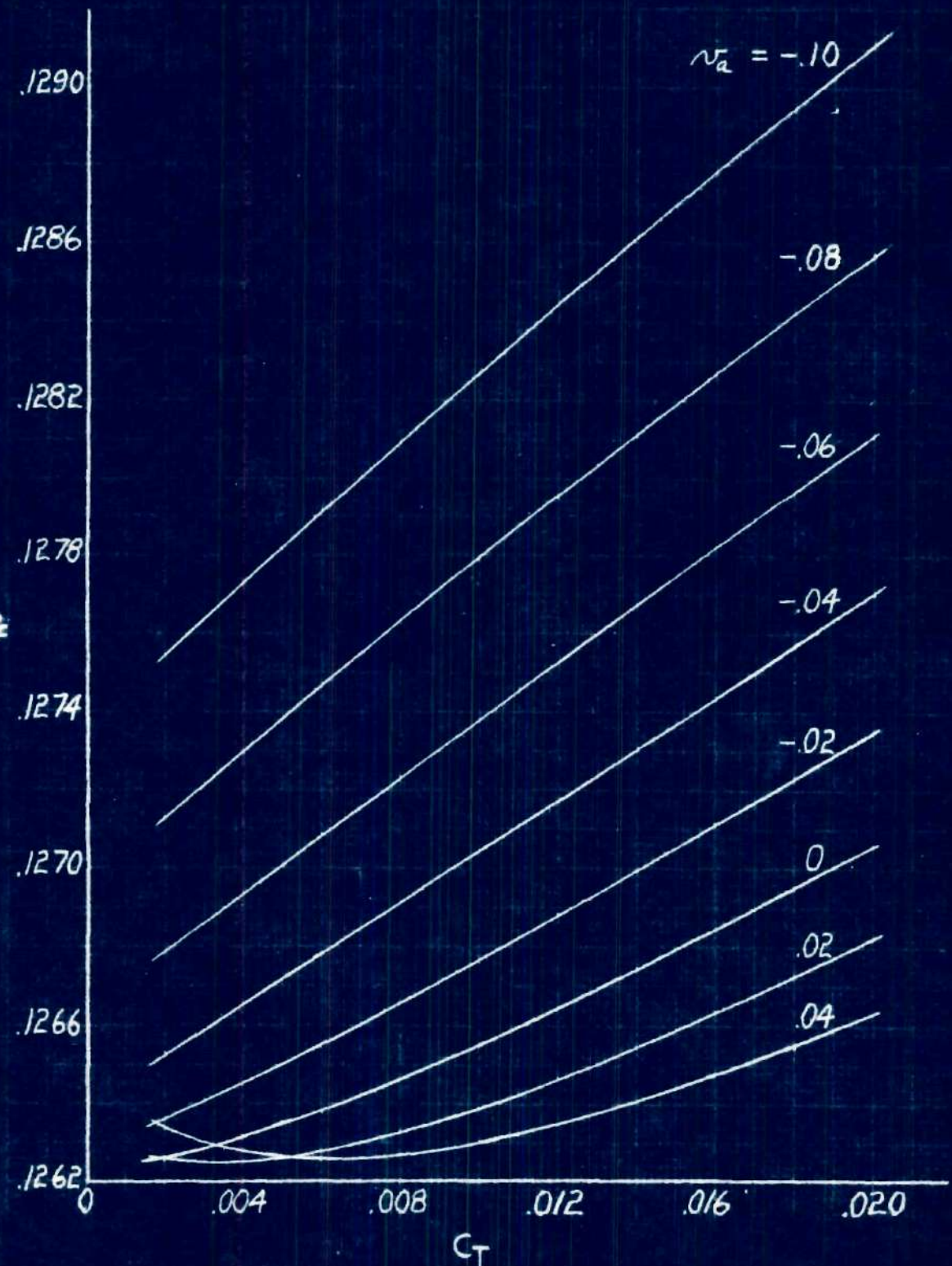

Figure 8 (c), $\mu_v = 0.10$

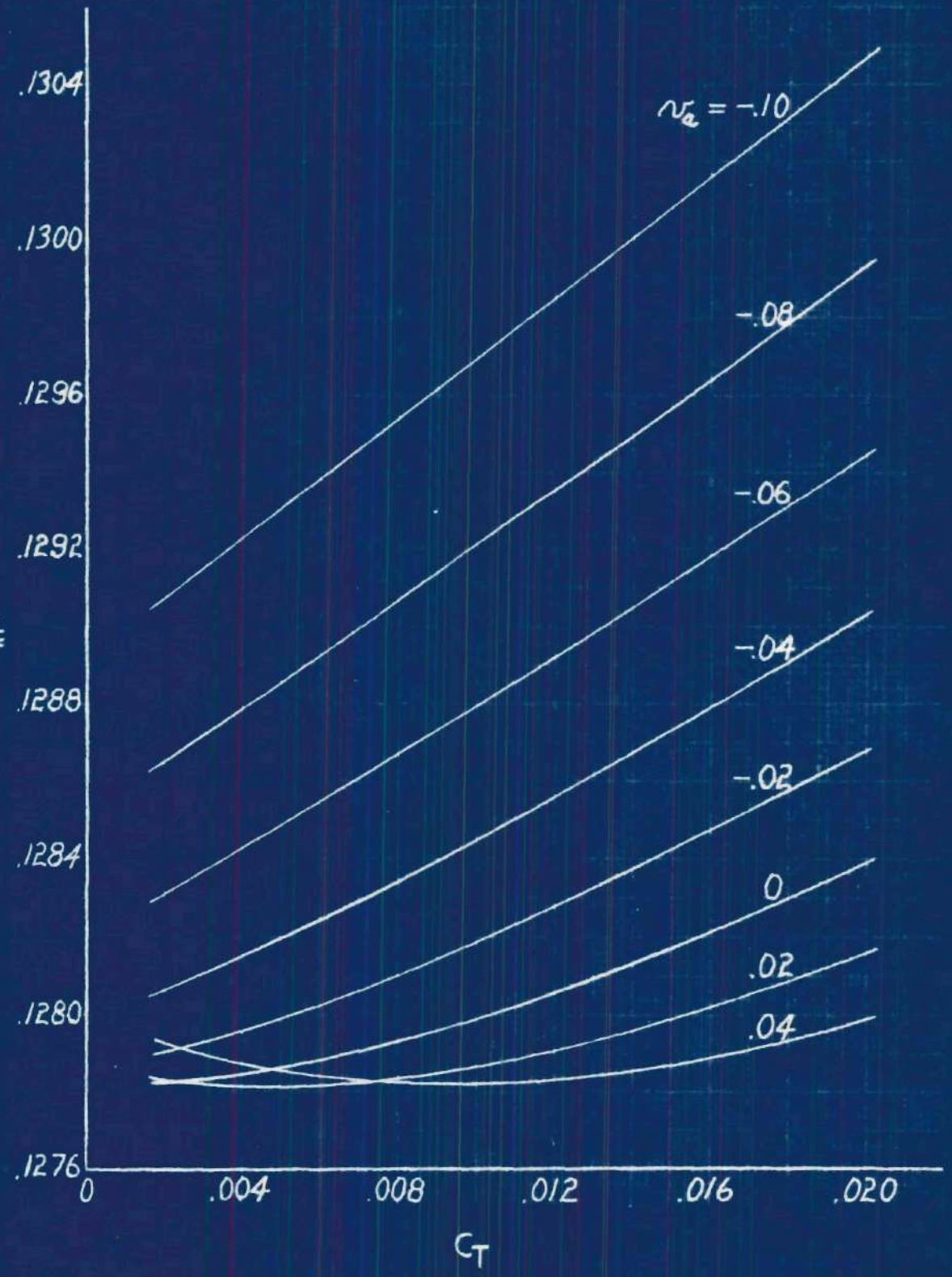

Figure 8 (d), $\mu_v = 0.15$

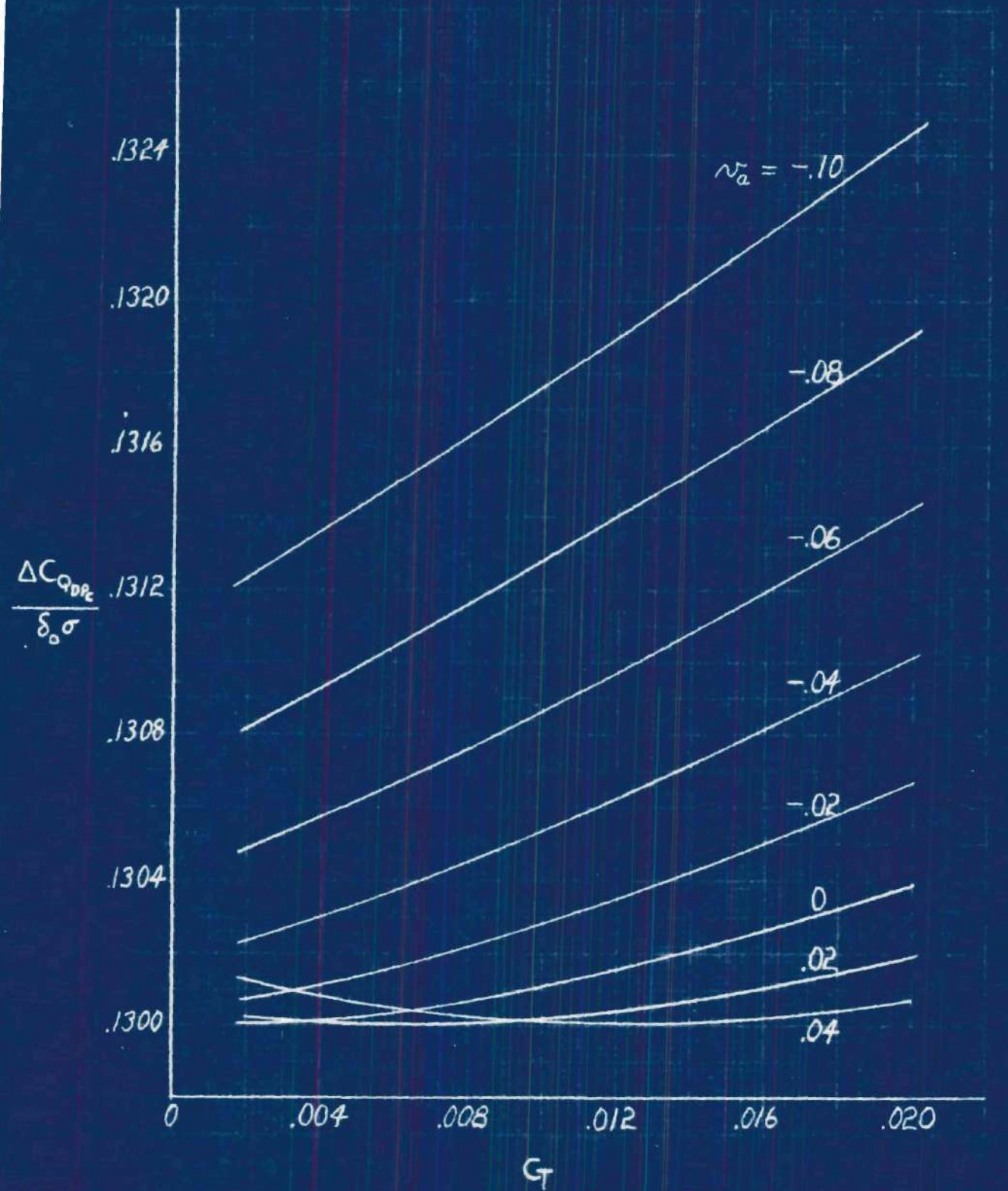

Figure 8 (e), $\mu_v = 0.20$

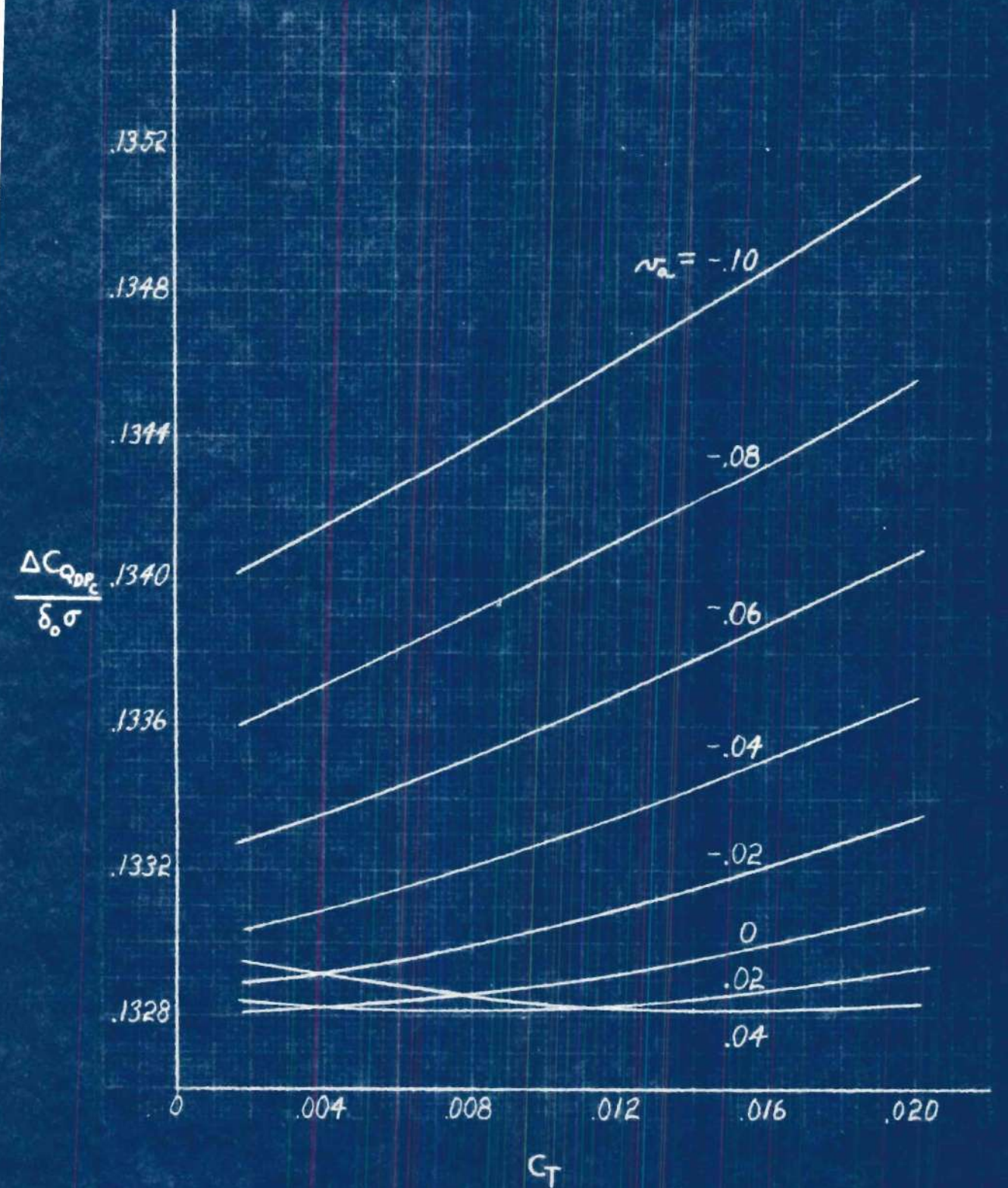

Figure 8 (f), $\mu_v = 0.25$

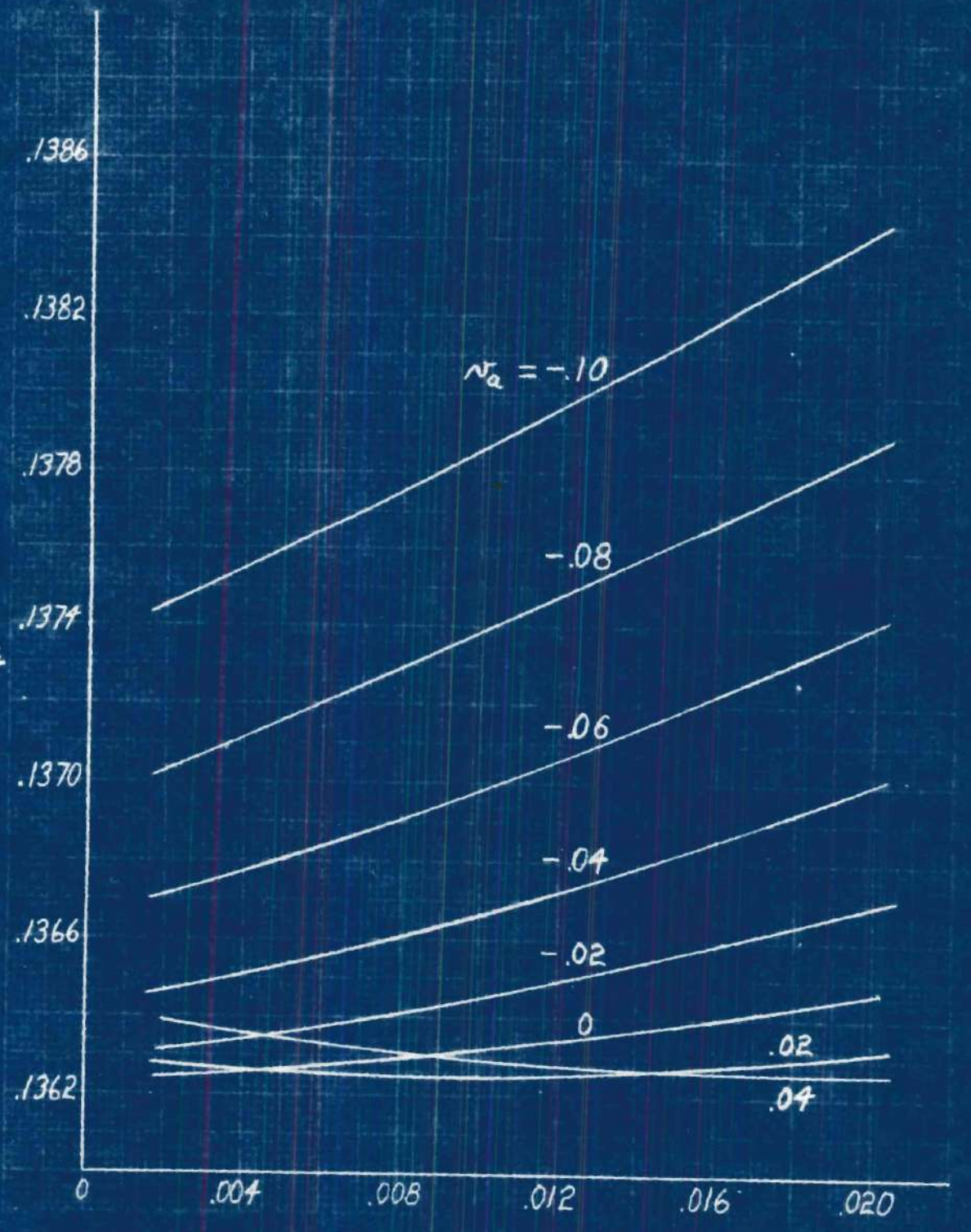

Figure 8 (g), $\mu_y = 0.30$

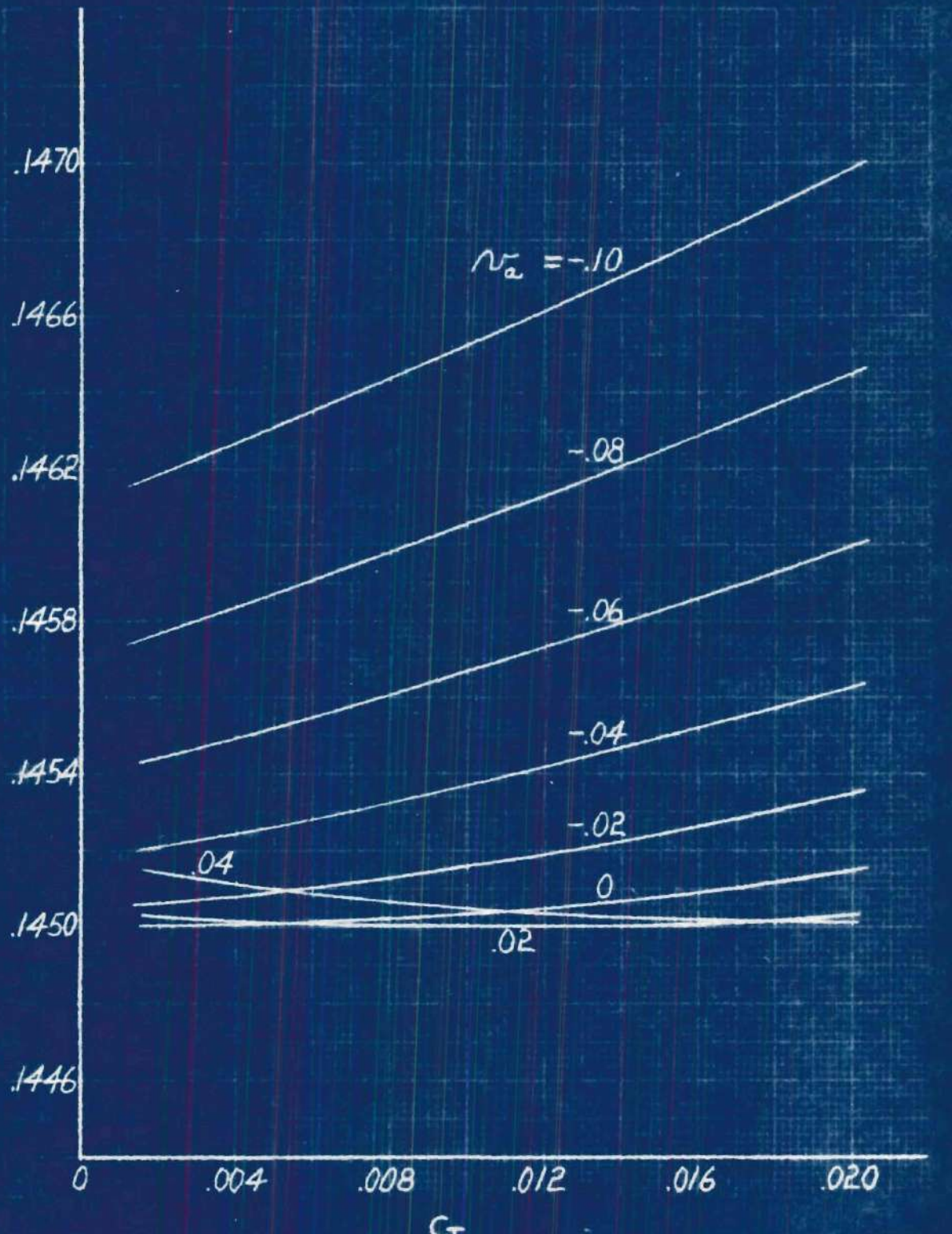

Figure 8 (h), $\mu_y = 0.40$

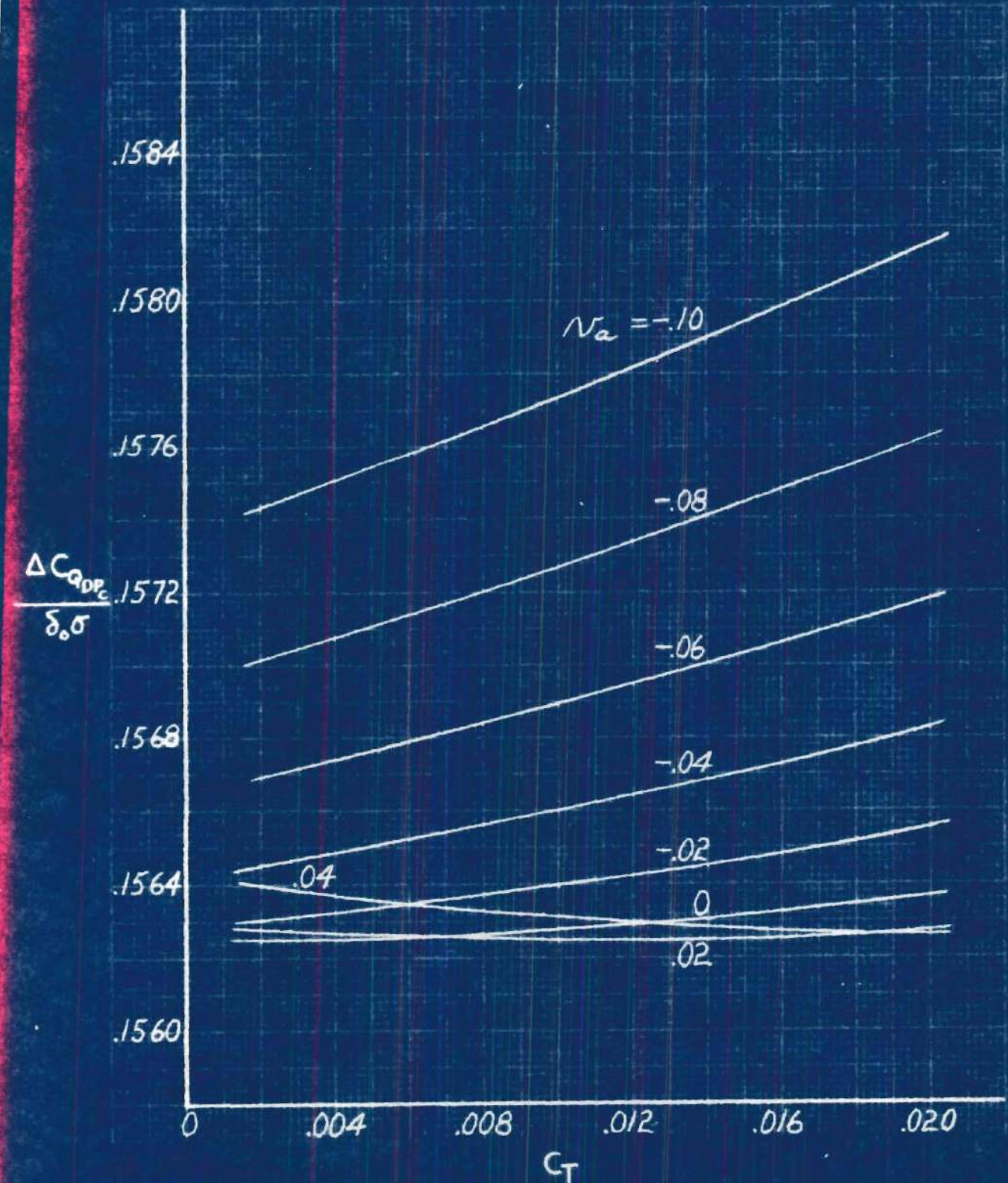

Figure 8 (i), $\mu_v = 0.50$

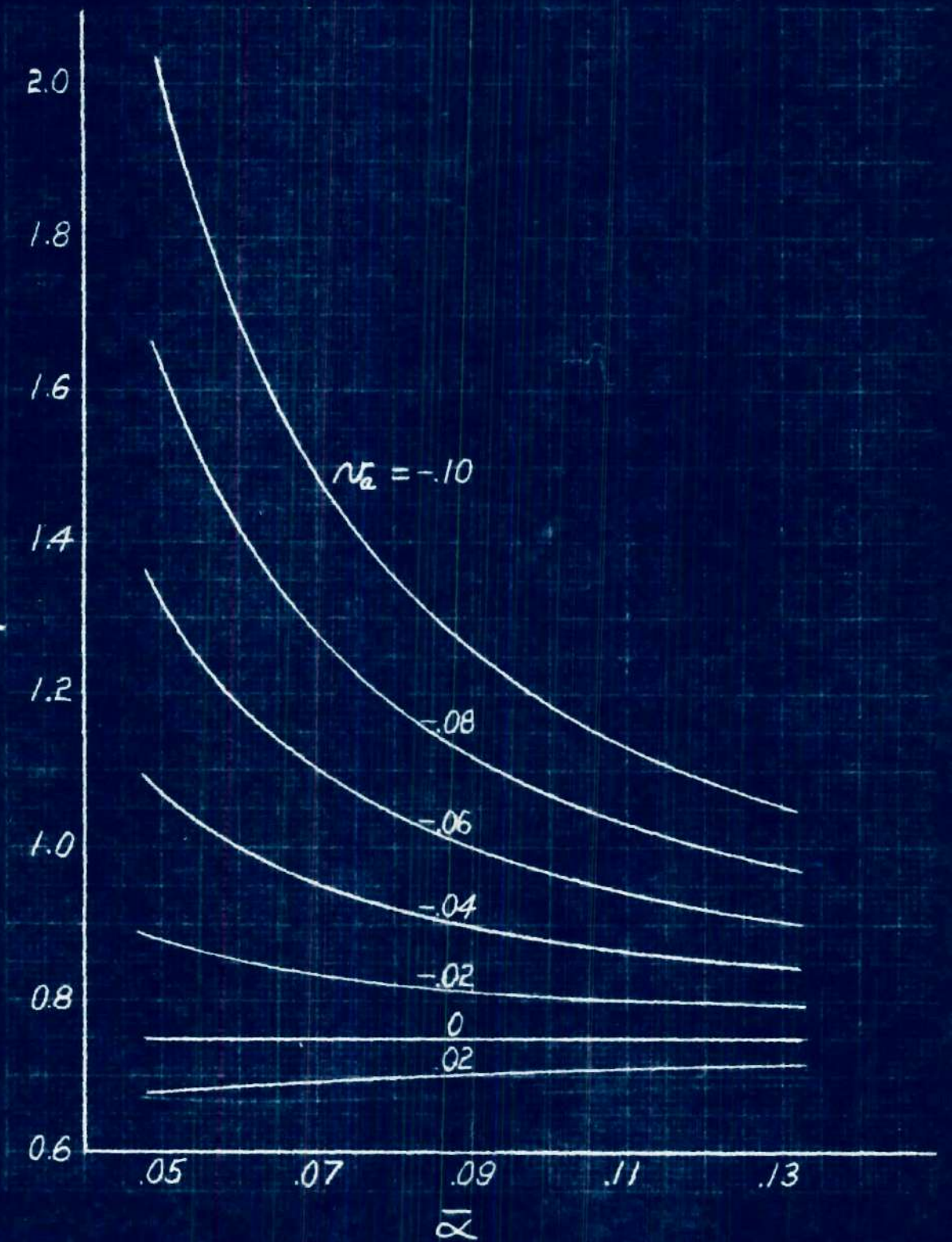

Figure 9 (a), $\mu_y = 0$.
Rotor Torque Due to Variable Profile Drag

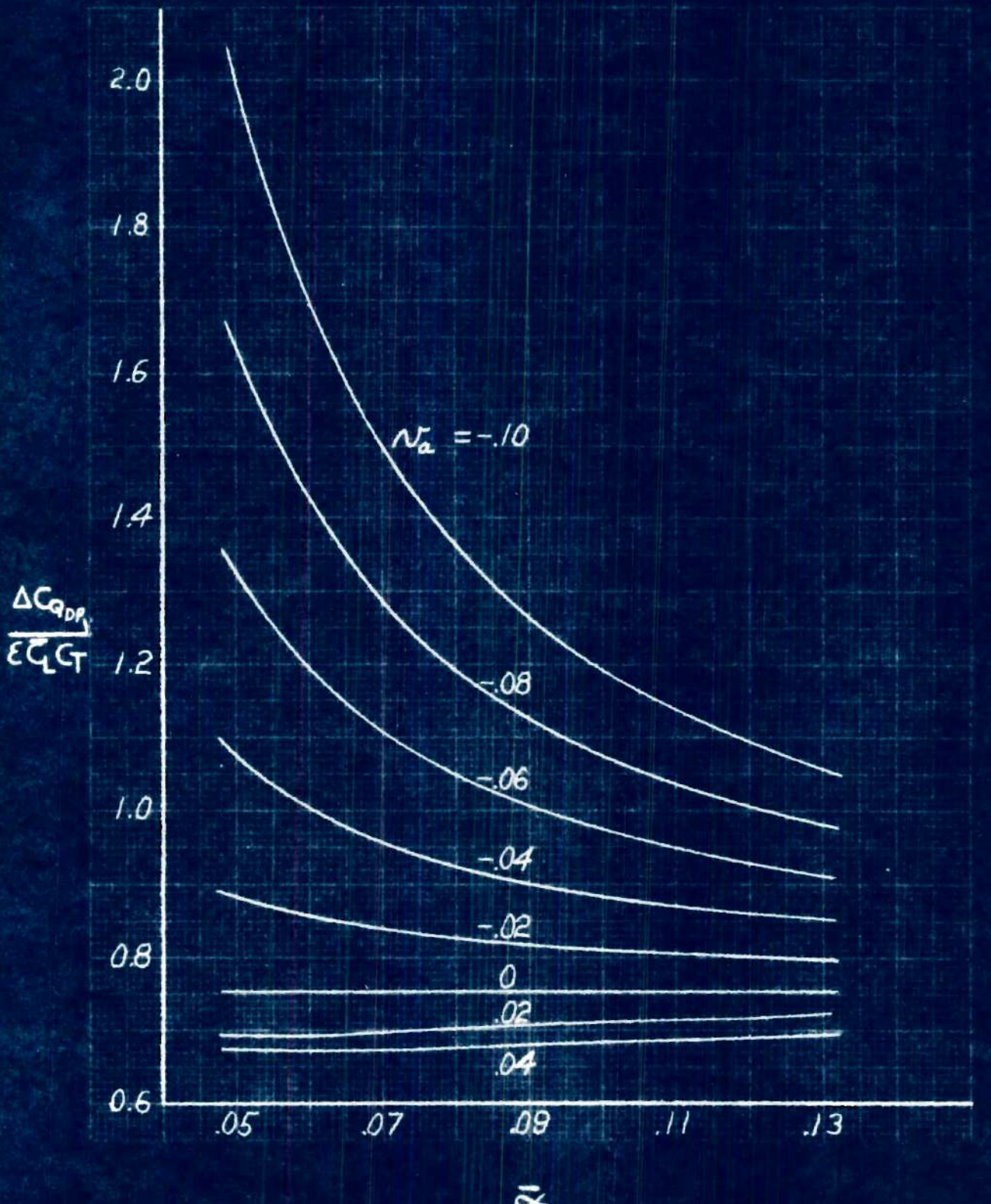

Figure 9 (b), $u_v = 0.05$

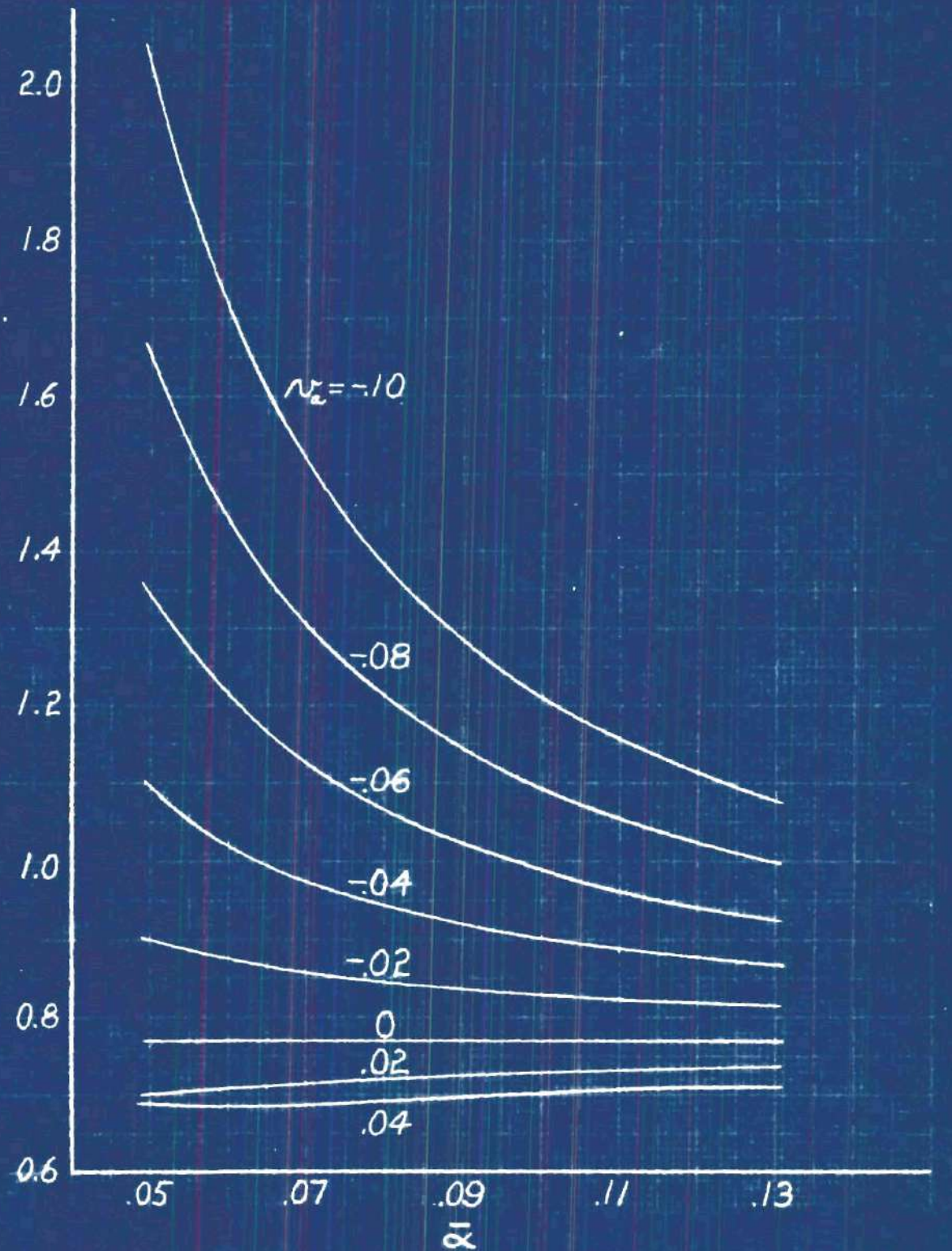

Figure 9 (c), $\mu_v = 0.10$

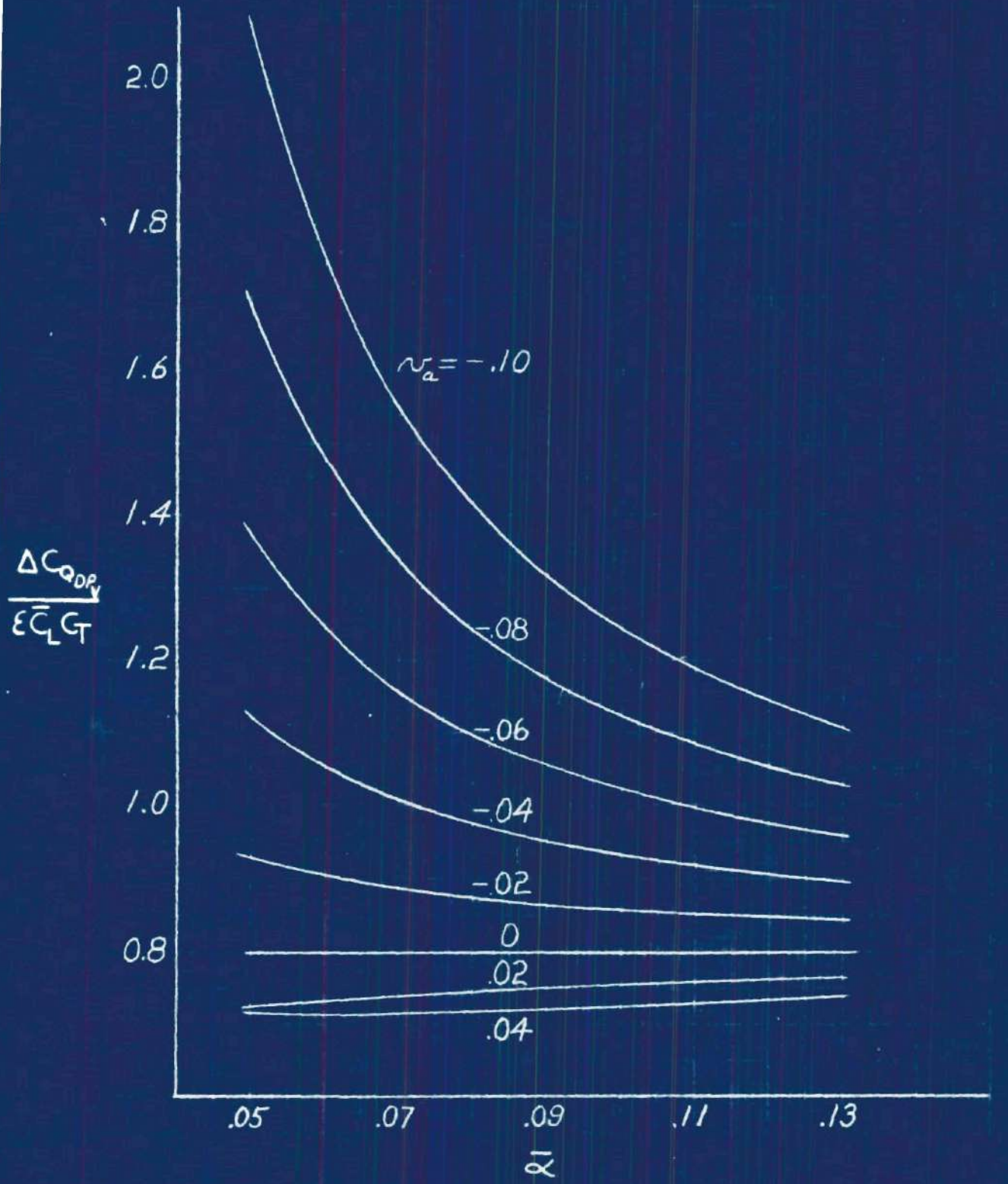

Figure 9 (d), $\mu_v = 0.15$

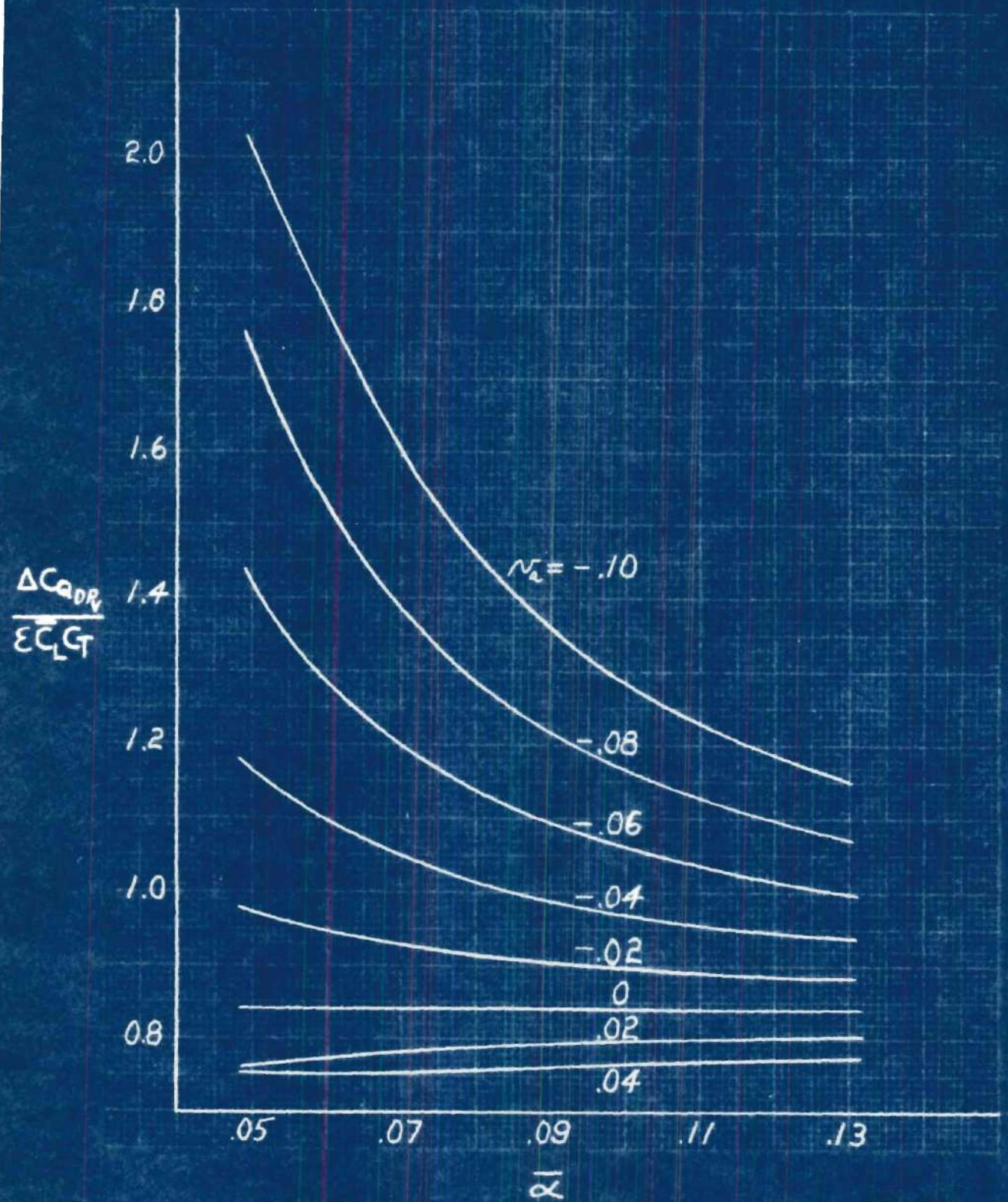

Figure 9 (e), $\mu_v = 0.20$

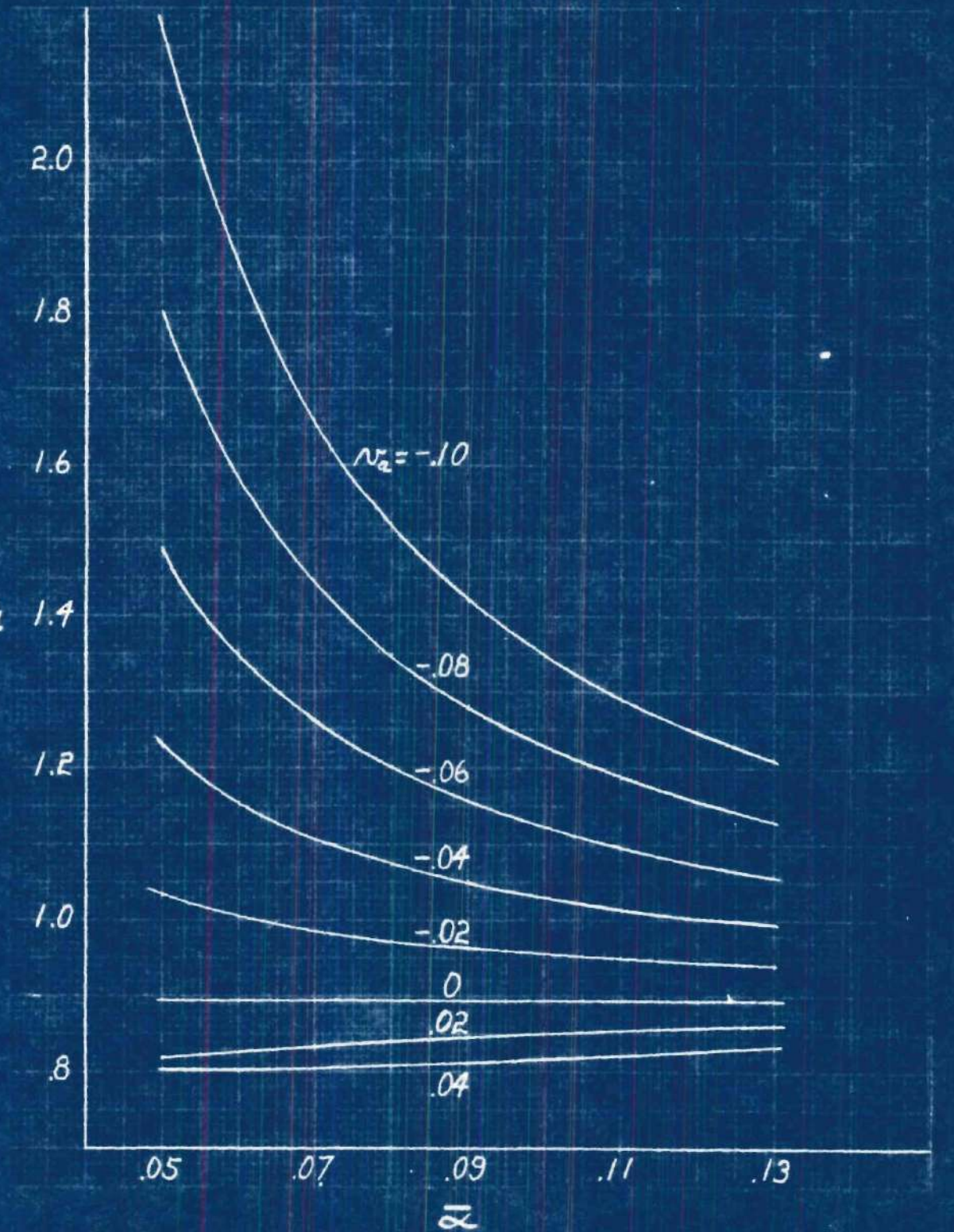

Figure 9 (f), $\mu_v = 0.25$

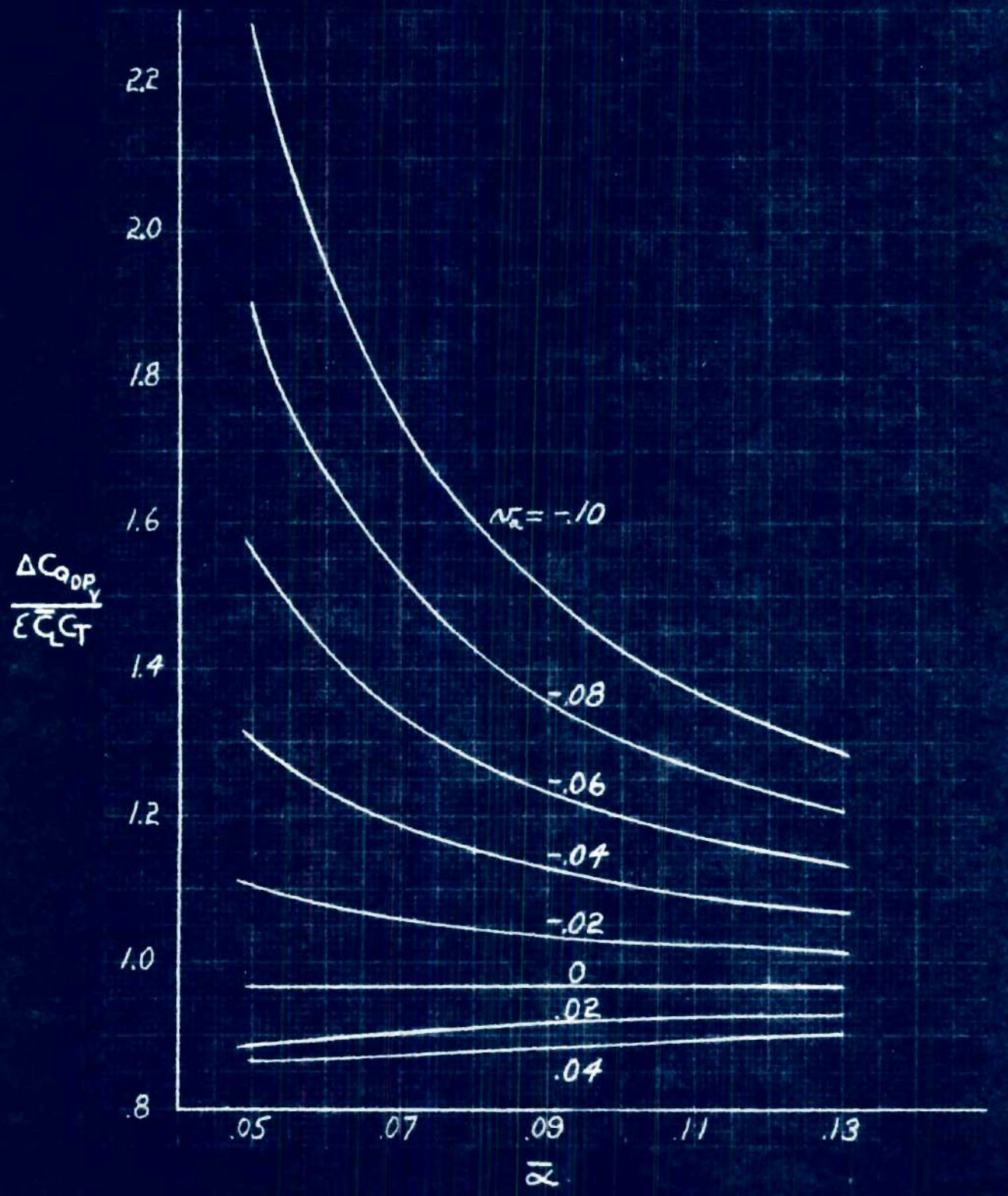

Figure 9 (g), $\mu_v = 0.30$

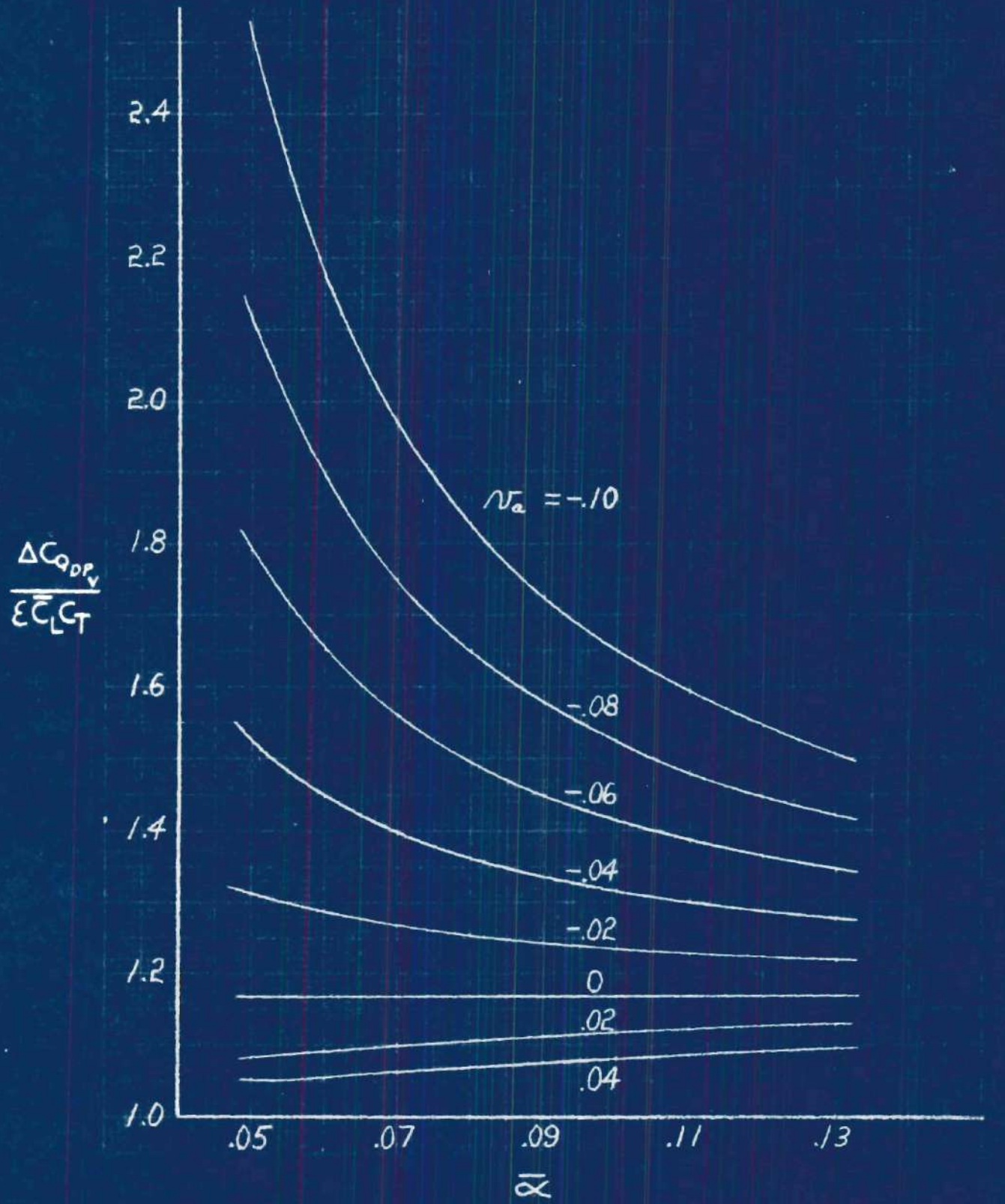

Figure 9 (h), $\mu_v = 0.40$

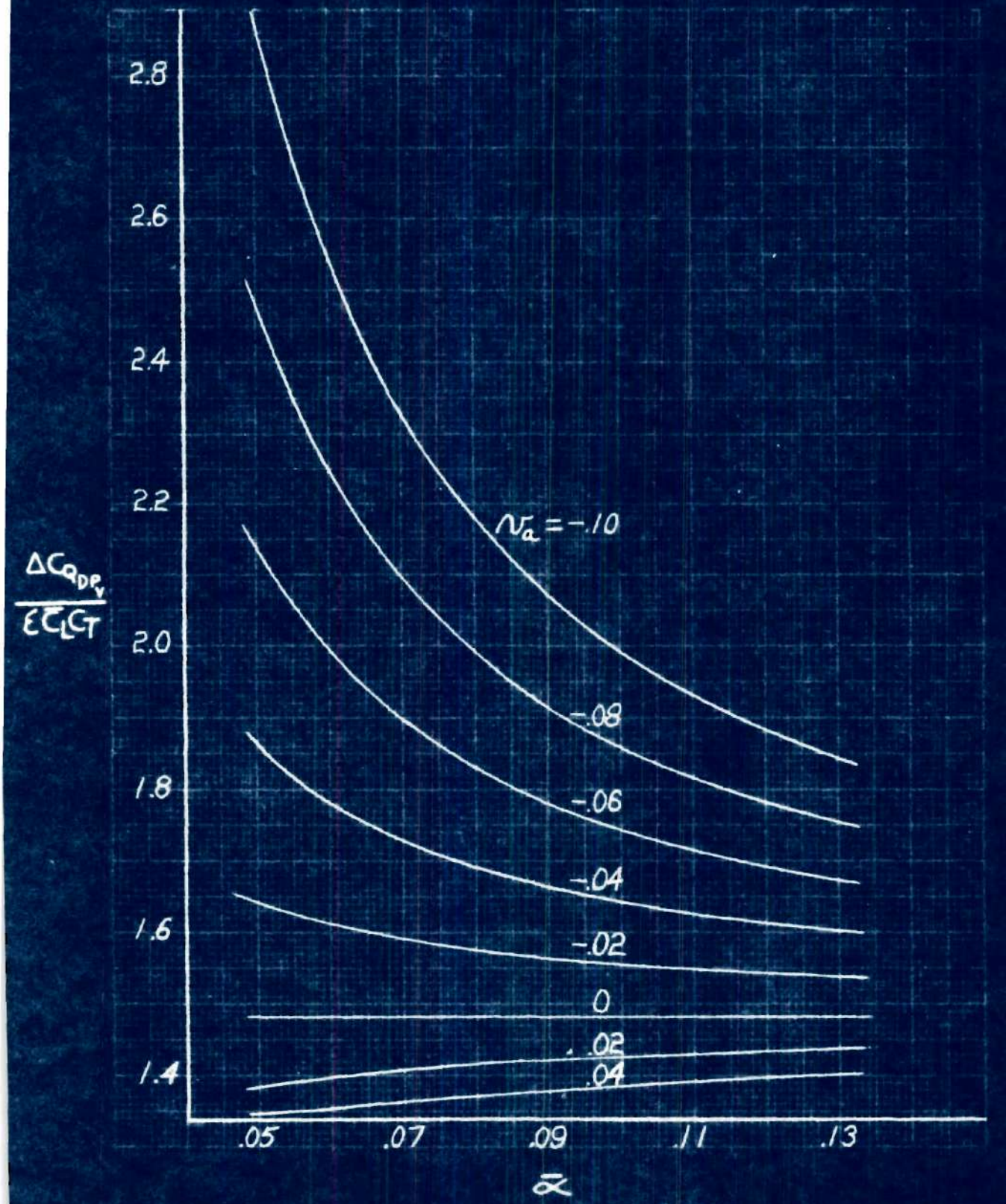

Figure 9 (i), $\mu_v = 0.50$

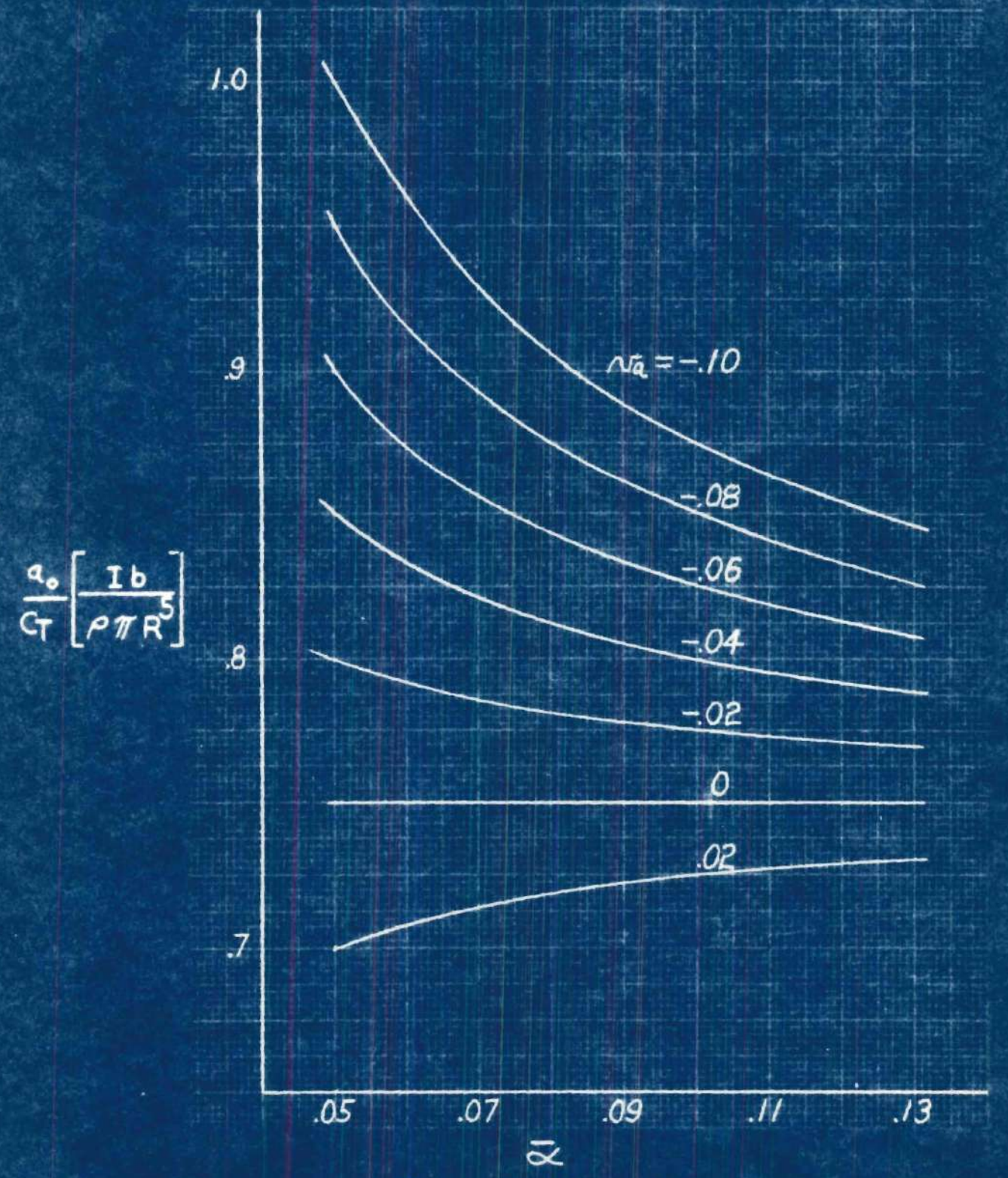

Figure 10 (a), $\mu_v = 0$.
Coning Angle

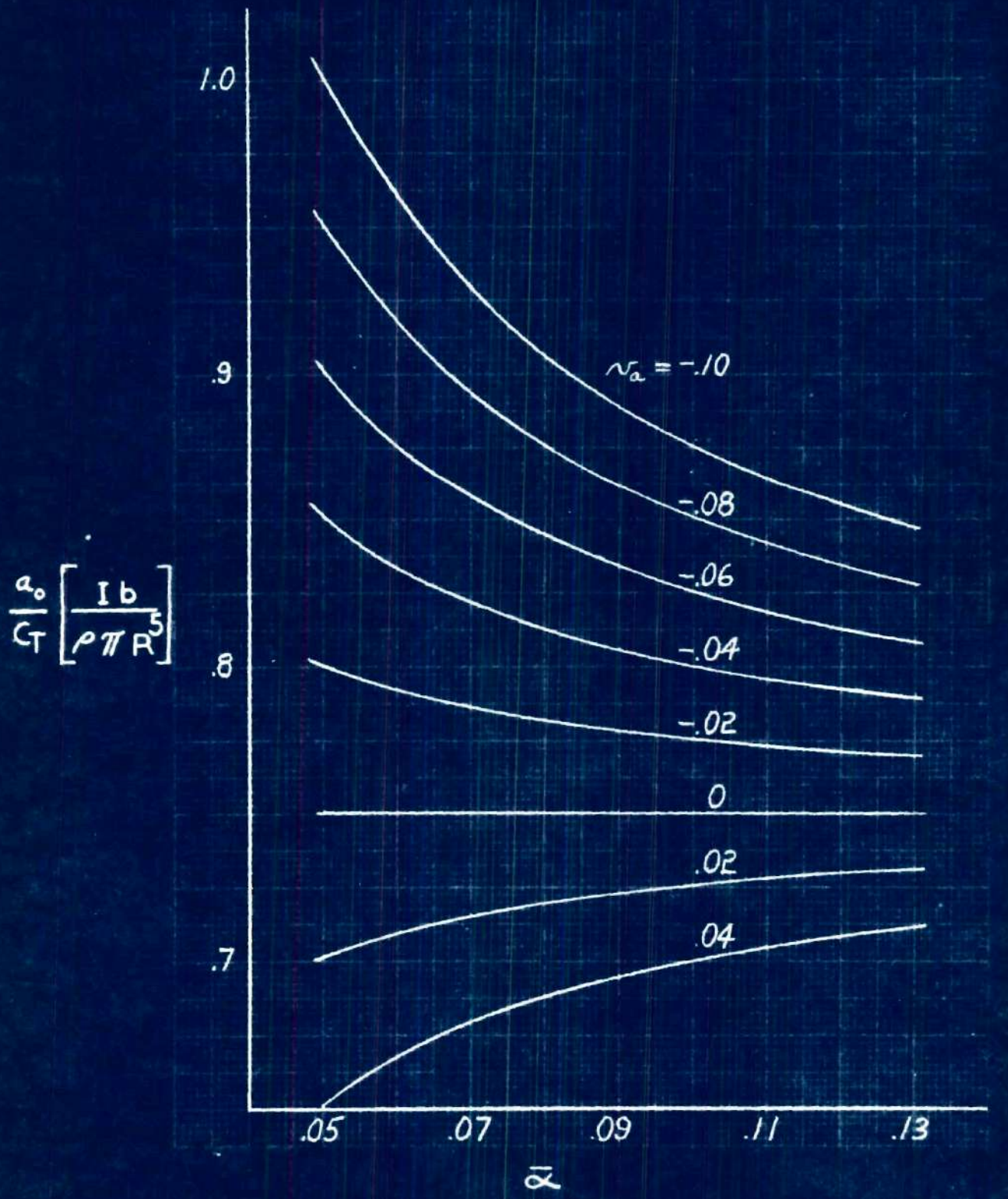

Figure 10 (b), $\mu_v = 0.10$

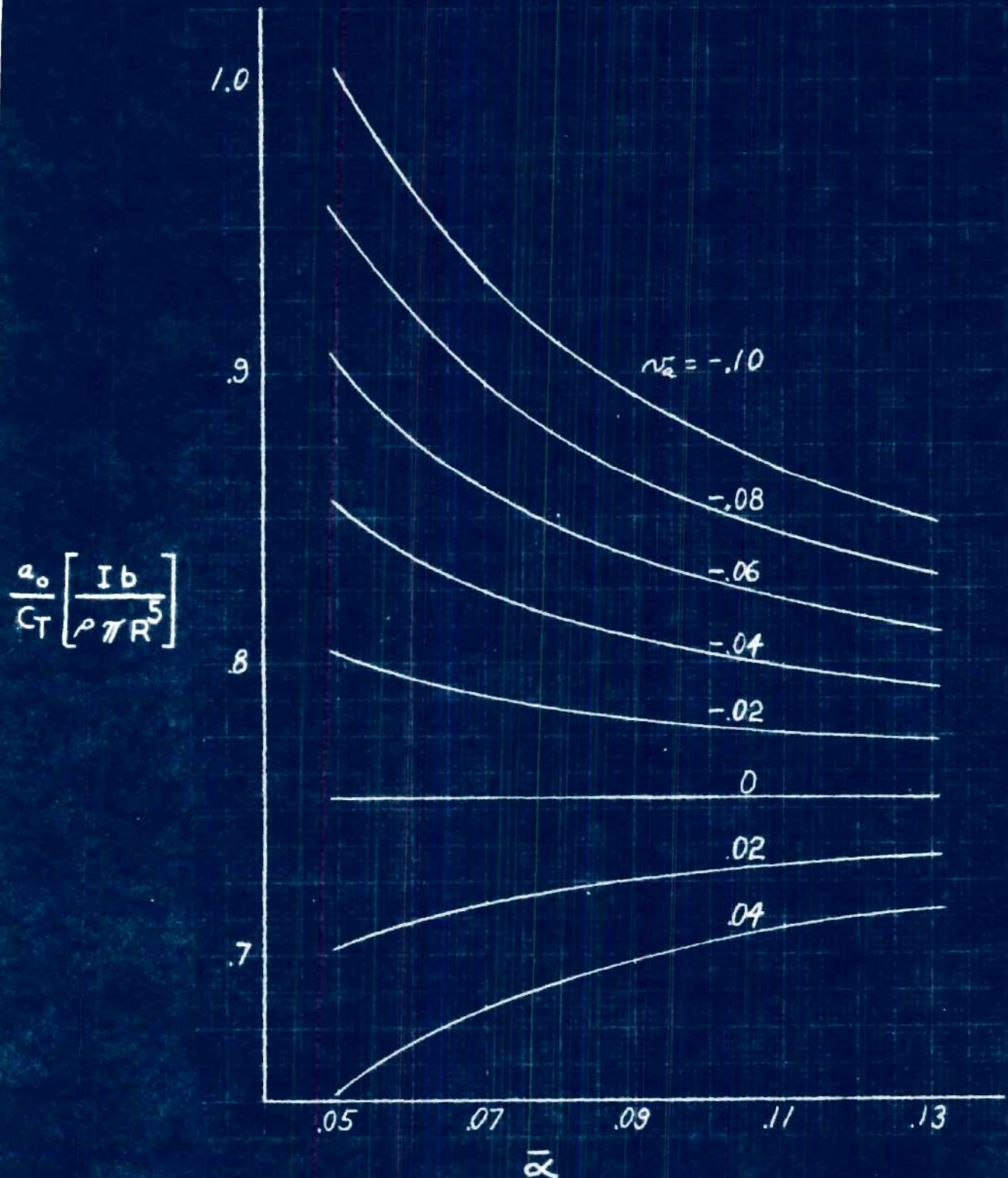

Figure 10 (c), $\mu_v = 0.20$

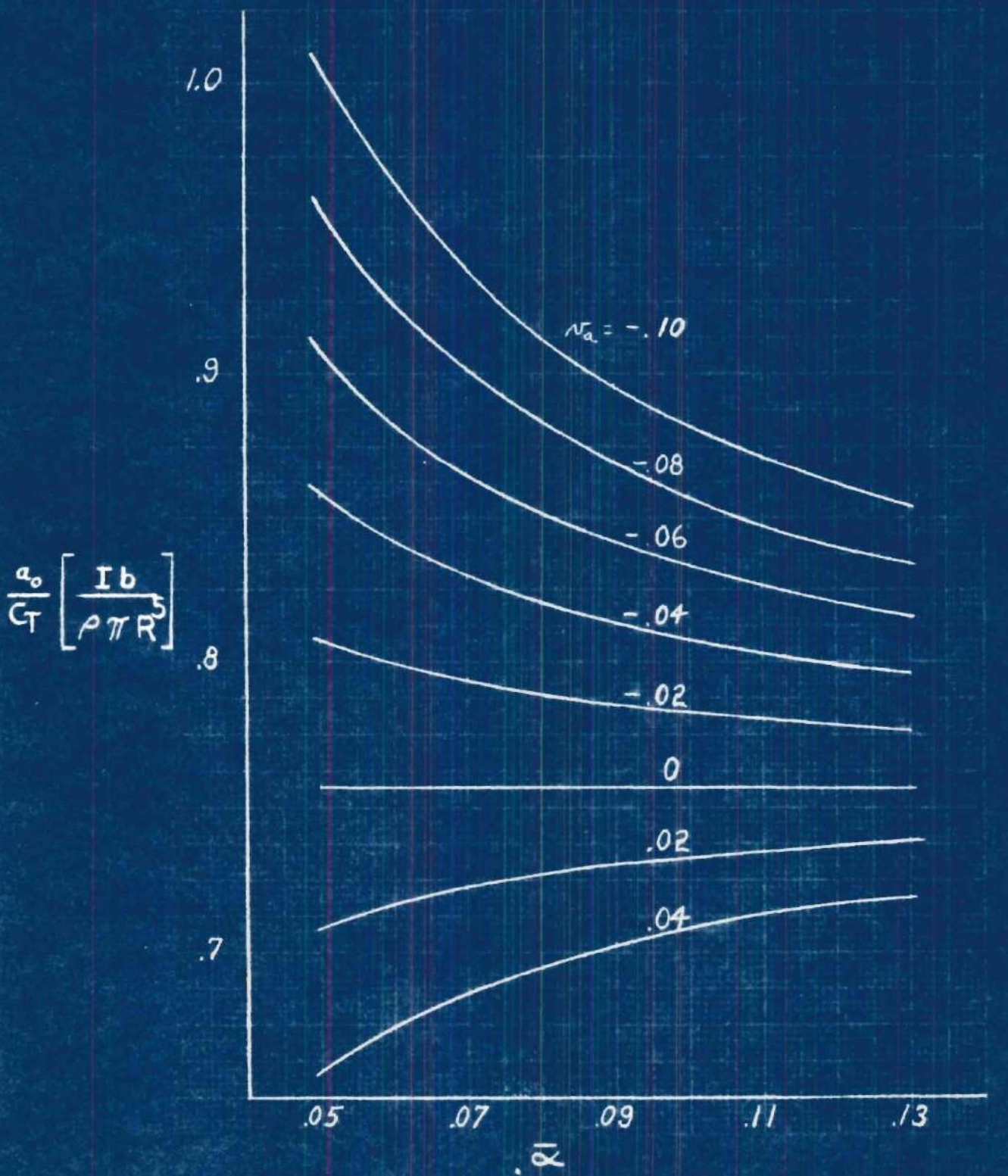

Figure 10 (d), $\mu_y = 0.30$

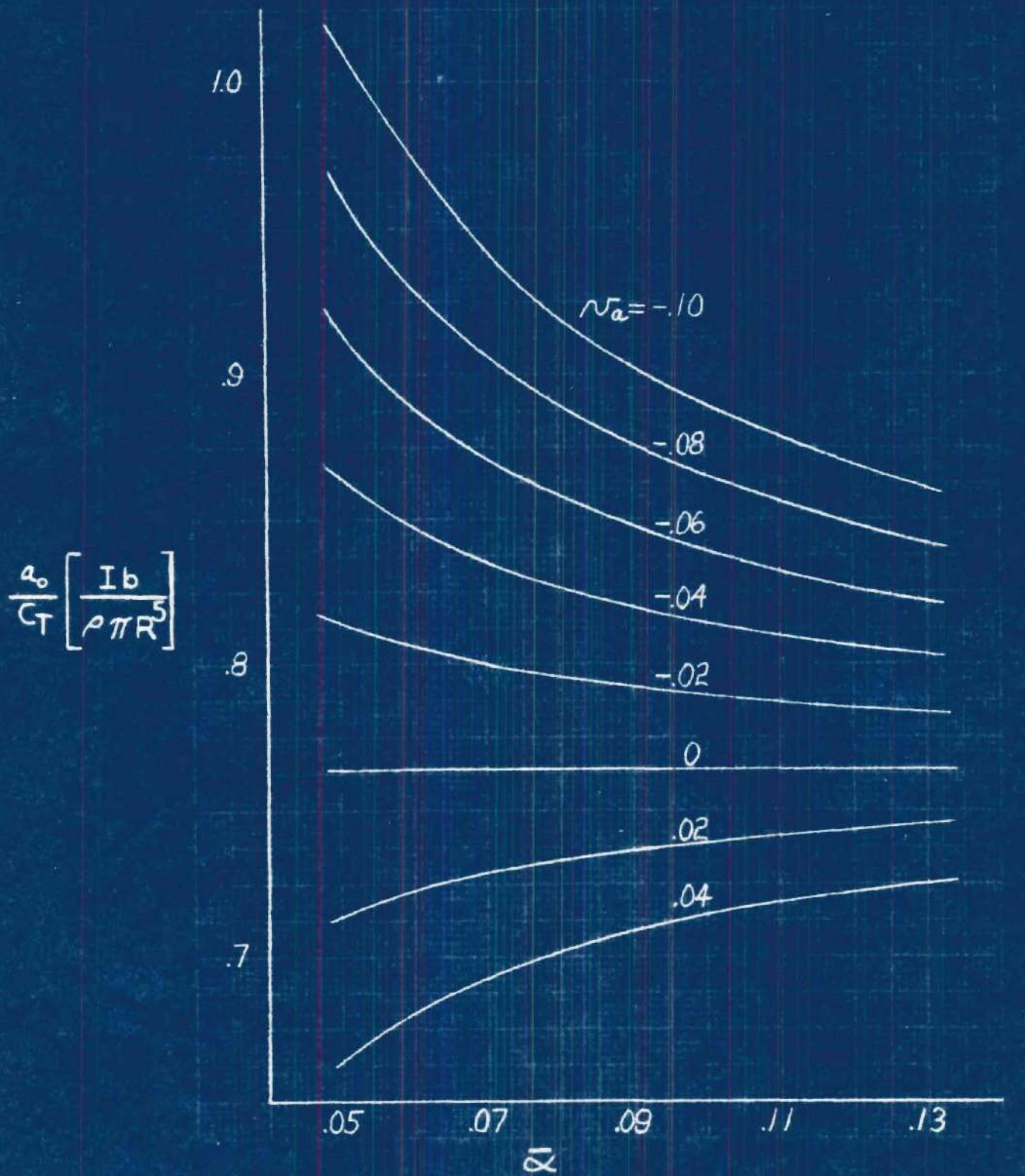

Figure 10 (e), $\mu_v = 0.40$

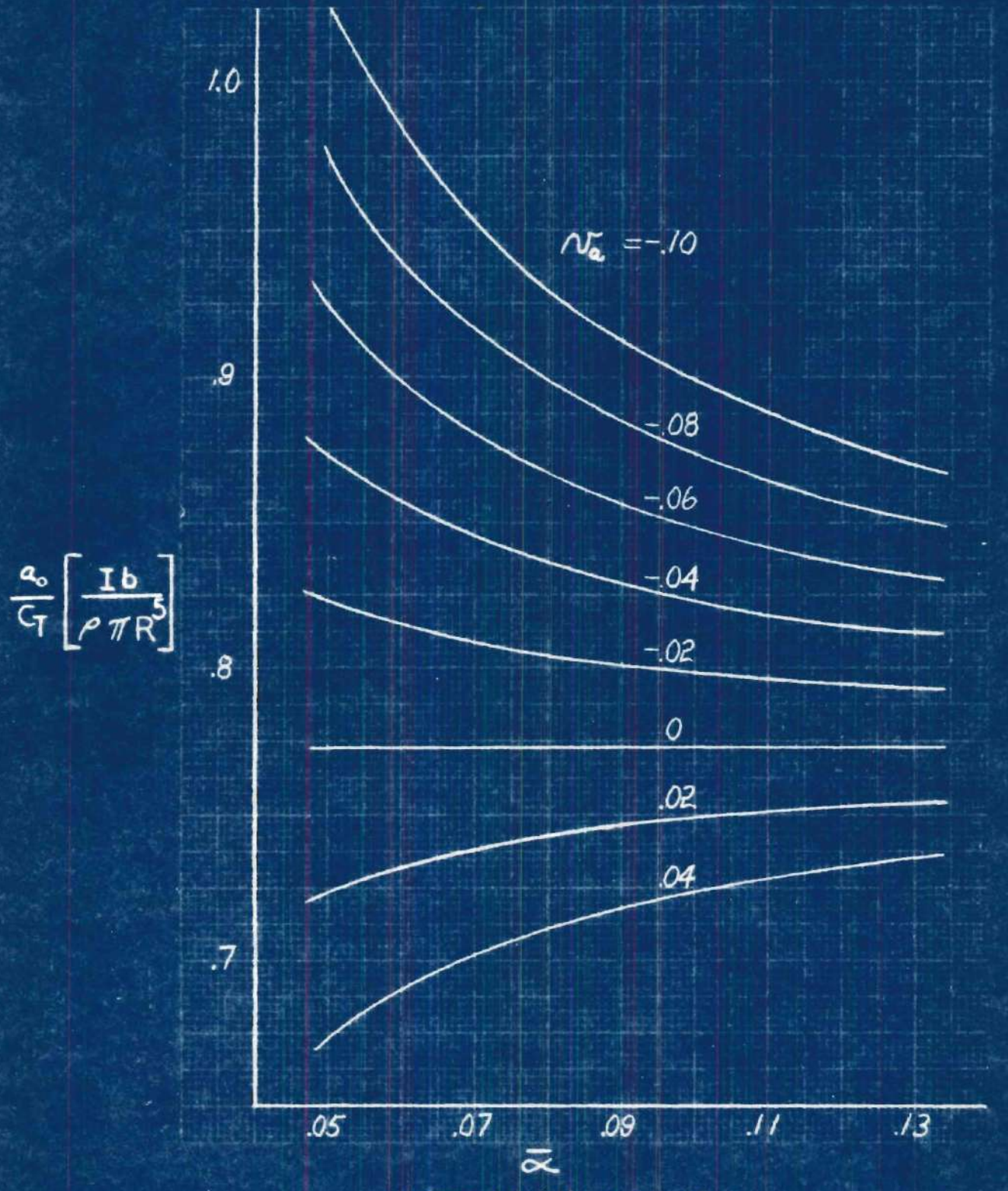

Figure 10 (f), $\mu_v = 0.50$

BIBLIOGRAPHY

BIBLIOGRAPHY

1. Castles, W., Jr. and New, N. C., A Blade-Element Analysis for Lifting Rotors That Is Applicable for Large Inflow and Blade Angles and Any Reasonable Blade Geometry, National Advisory Committee for Aeronautics, Technical Note No. 2556, 1952.

2. Gessow, A. and Tapscot, R. J., Charts for Estimating Performance of High-Performance Helicopters, National Advisory Committee for Aeronautics, Report No. 1266, 1956.

3. Gessow, A. and Crim, A. D., An Extension of Lifting Rotor Theory to Cover Operation at Large Angles of Attack and High Inflow Conditions, National Advisory Committee for Aeronautics, Technical Note No. 2665, 1952.

4. Bailey, F. J., Jr. and Gustafson, F. B., Charts for Estimation of the Characteristics of a Helicopter Rotor in Forward Flight. I-Profile Drag - Lift Ratio for Untwisted Rectangular Blades, National Advisory Committee for Aeronautics, Wartime Report L-110, 1944.

5. Heyson, H. H., Analysis and Comparison with Theory of Flow-field Measurements Near a Lifting Rotor in the Langley Field-scale Tunnel, National Advisory Committee for Aeronautics, Technical Note No. 3691, 1956.

6. Coleman, R. P. and Feingold, A. M., Evaluation of the Induced Velocity Field of an Idealized Helicopter Rotor, National Advisory Committee for Aeronautics, Wartime Report ARR No. L5E10, June 1945.

7. Castles, W., Jr. and Durham, H. L., Jr., Distribution of Normal Component of Induced Velocity in Lateral Plane of a Lifting Rotor, National Advisory Committee for Aeronautics, Technical Note No. 3841, 1956.

8. Pope, Alan, "Summary Report of the Forces and Moments Over an NACA 0015 Airfoil Through 180° Angle of Attack," Aero Digest, Vol. 58, April 1949, pp. 76-78, 100.

9. Hoerner, S. F., Aerodynamic Drag, Published by the Author, Printed by the Otterbein Press, Dayton, Ohio, 1951.

10. Myers, G. C., Jr., Flight Measurements of Helicopter Blade Motion with a Comparison Between Theoretical and Experimental Result, National Advisory Committee for Aeronautics, Technical Note No. 1266, 1947.

11. Gustafson, F. B. and Myers, G. C., Jr., Stalling of Helicopter Blades, National Advisory Committee for Aeronautics, Technical Note No. 1083, 1946.

12. Carpenter, P. J., Lift and Profile-Drag Characteristics of an NACA 0012 Airfoil Section as Derived from Measured Helicopter-Rotor Hovering Performance, National Advisory Committee for Aeronautics, Technical Note No. 4357, 1958.